Development of an assay to detect proteolytic activity in peptide arrays

Zur Erlangung des akademischen Grades eines
DOKTORS DER NATURWISSENSCHAFTEN
(Dr. rer. nat.)

Fakultät für Chemie und Biowissenschaften Karlsruher Institut für Technologie (KIT) – Universitätsbereich

Genehmigte
DISSERTATION
von
M.Sc. Anitha Golla
aus
Guntur

Dekan: Prof. Dr. Peter Roesky

Referent: PD Dr. Frank Breitling

Tag der mündlichen Prüfung: 16.07.2014

Table of Contents

Abstract 1

I. Introduction 5

  I.1. Peptide synthesis 5

  I.2. Microarrays 12

    I.2.1. High density peptide arrays - particle based peptide synthesis 15

  I.3. Proteases 19

    I.3.1. Catalytic triads 23

  I.4. Surface analytical techniques 25

    I.4.1. UV/Vis photospectrometry 25

    I.4.2. X-ray Photoelectron Spectroscopy 26

    I.4.3. Time of flight secondary ion mass spectrometry 28

II. Motivation and Objective of the work 33

III. Results and discussion 34

  III.1. First screening strategy 34

    III.1.1. Stability of the peptides under screening conditions 35

    III.1.2. Labelling of peptide arrays 39

    III.1.3. First screen 43

    III.1.4. Drawbacks of the first screening process 62

  III.2. Second screening strategy 63

    III.2.1. Design of a reporter peptide 65

    III.2.2. Design of a suitable surface for protease activity detection 75

    III.2.3. Sensitivity of the reporter surface 95

IV. Conclusion and outlook 105

V. Materials and Methods 108

  V.1. Materials 108

  V.2. Devices and measuring parameters 111

V.2.1. Fluorescence scans ... 111

V.3. Methods ... 113

V.3.1. Labelling of a peptide array with N-succinimidyl ester derivatives of dyes 113

V.3.2. Coupling of Fmoc-Lys(5/6-TAMRA)-OH ... 113

V.3.3. Deprotection of peptide side chain protecting groups ... 113

V.3.4. Digestion of PW and RP peptides in black 96-well plate ... 114

V.3.5. Digestion of PW and RP peptides in maleimide coated black 96-well plate 114

V.3.6. Cleaning and activation of glass slides ... 114

V.3.7. Cleaning and activation of silicon wafers ... 114

V.3.8. Silanization of glass slides and silicon wafers ... 114

V.3.9. Immobilization of the initiator for siATRP ... 115

V.3.10. Synthesis of 100% PEGMA films by siATRP ... 115

V.3.11. Synthesis of 10:90-PEGMA-co-PMMA films by siATRP ... 116

V.3.12. Coupling of Fmoc-β-alanine-OH ... 116

V.3.13. Cleaving Fmoc-protection group ... 117

V.3.14. Preparation of AEG_3 surfaces ... 117

V.3.15. Coupling of SMCC linker before spotting of peptides ... 117

V.3.16. Spotting of reporter peptides ... 117

V.3.17. Blocking the surfaces after spotting peptides ... 118

V.3.18. Coupling of Fmoc-pentafluoro-L-Phenylalanine-OH ... 118

V.3.19. Incubation of peptide array under dry ammonia vapor ... 118

V.3.20. Coupling of 5-hexenoic acid ... 118

V.3.21. Immunostaining of peptide array after transfer ... 119

VI. Abbreviations ... 120

VII. Bibliography ... 124

VIII. Appendix ... 130

Abstract

Proteases, the enzymes which catalyze the hydrolysis of peptide bonds, are not only responsible for various diseases such as cancer, Alzheimer's, rheumatoid arthritis etc., thus making them drug targets, but are also one of the largest group of industrially produced enzymes because of their use in washing powders. The catalytic ability of proteases is due to the spatial organization of the side chains of amino acids in the active site called the catalytic triad. In chymotrypsin, a subclass of serine protease, the catalytic triad is formed of aspartic acid, histidine and serine. Most proteases share this acid-base-nucleophile pattern, where different residues take up the roles of acids and bases. This pattern is conserved generally throughout evolution in various enzymes, signifying the importance of catalytic triad for enzyme activity. Synthesis of full length proteases is tedious and expensive; therefore, a peptide which mimics the catalytic triad and can be synthesized more easily would be desirable. However, in order to find a right sequence of amino acids which can mimic a catalytic triad, thousands of peptides should be screened, preferably in a high throughput manner. Therefore, there is a need for a screening system which can detect proteolytic activity in peptide arrays. This PhD thesis dealt with the development of an assay to detect proteolytic activity in the array format.

The first screen was developed based on the self-digestion property of the proteases. In a peptide array, peptides with proteolytic activity should cleave one another within the synthesis matrix, resulting in the loss of peptide fragments from a spot. The loss of peptides was monitored by attaching fluorescent dyes to peptide array and monitoring the fluorescence intensity over time. However, during the course of development of the screen, some major drawbacks such as intermolecular quenching of fluorophore were noticed; therefore a new screen was developed.

For the second screening method, a reporter surface which gains fluorescence on detection of proteolytic activity was developed. The reporter surface is a two dimensional monolayer covered with a reporter peptide, which consists of a fluorophore at the *C*-terminal, quencher at the *N*-terminal and protease cleavage site in the middle of the sequence. On the surface, the fluorophore is quenched by resonance energy transfer (RET). Upon contact with a proteolytic moiety, the quencher is cleaved off the peptide and a gain in fluorescence can be observed. The reporter surface was tested using trypsin as a model protease. A gain of 20 % fluorescence was recorded on detection of 429 pmol of trypsin/cm^2. This detection limit of reporter surface is well within the range of peptide concentration in the high density peptide arrays (1-4 nmol/cm^2). Hence, this assay provides a platform for screening peptide arrays to identify peptides with proteolytic activity without the drawbacks of direct labelling.

Kurzfassung

Proteasen katalysieren die Hydrolyse von Peptidbindungen. Ihre Rolle bei Krankheiten wie beispielsweise Alzheimer oder rheumatischer Arthritis macht sie für die Entwicklung von Medikamenten interessant. Außerdem werden sie industriell in großem Maßstab als Waschmittelzusatz hergestellt. Die katalytischen Eigenschaften von Proteasen sind auf die räumliche Anordnung von Aminosäureseitenketten im aktiven Zentrum zurückzuführen, der katalytischen Triade. In Serinproteasen, einer Unterklasse der Proteasen, handelt es sich dabei um Asparaginsäure, Histidin und Serin. Die meisten Proteasen verfügen über diese Kombination aus Säure, Base und Nucleophil im aktiven Zentrum. Dieses Muster wurde grundsätzlich durch die Evolution erhalten, was die Wichtigkeit der katalytischen Triade für die Enzymaktivität unterstreicht. Die vollständige Synthese von Proteasen ist komplex und teuer. Daher wäre ein einfacher herzustellendes Peptid, das die katalytische Triade modelliert, eine Alternative. Allerdings müssten zur Identifikation eines solchen Peptides tausende von potentiellen Kandidaten möglichst in einem Hochdurchsatzverfahren untersucht werden. Es besteht daher Bedarf an einem Nachweissystem zur Detektion proteolytischer Aktivität auf Peptidarrays. In dieser Arbeit sollte ein solches Nachweissystem entwickelt werden.

Das erste Nachweissystem basierte auf der Eigenschaft der Proteasen, sich selbst zu hydrolysieren. In einem Peptidarray sollten Peptide mit proteolytischen Eigenschaften in der Lage sein, sich gegenseitig innerhalb der Synthesematrix zu hydrolysieren. Der Verlust an Peptiden wurde durch Anbringen eines Fluorphors und der Betrachtung der Fluoreszenzintensität im zeitlichen Verlauf detektiert. Allerdings konnten während der Untersuchungen einige gravierende Nachteile des Systems wie intermolekulare Fluoreszenzauslöschung beobachtet werden. Daher wurde ein weiteres Nachweissystem entwickelt.

Für das zweite Nachweissystem wurde eine Oberfläche entwickelt, deren Fluoreszenz sich in Gegenwart proteolytischer Substanzen erhöht. Sie besteht aus einer zweidimensionalen Monolage, auf der sich ein Nachweispeptid befindet. Dieses verfügt über ein Fluorophor am C Terminus, einen Quencher am N Terminus sowie eine Aminosäure, die Proteasen die

Spaltung ermöglicht, in der Mitte der Sequenz. Auf der Oberfläche wird das Fluorophor durch Resononzenergietransfer ausgelöscht. Wird das Peptid proteolytisch aktiven Substanzen ausgesetzt, wird der Quencher abgespalten und ein Anstieg der Fluoreszenz kann beobachtet werden. Die Oberfläche wurde mit Trypsin getestet. Dabei induzierten 429 pmol/cm^2 Trypsin eine Zunahme der Fluoreszenz um 20%. Die Nachweisgrenze der Oberfläche liegt damit weit unter den für Peptidarrays üblichen Konzentrationsbereichen (1-4 nmol/cm^2). Daher kann das Nachweissystem zur Identifikation von Peptiden mit proteolytischer Aktivität im Arrayformat verwendet werden.

I. Introduction

I.1. Peptide synthesis

The early work of Emil Fischer led to the first methods to form peptide bonds (amide linkages between alpha-amino acids).[1] The first reversible protecting group led to the synthesis of variety of small peptide substrates.[2] In general, synthesis of peptides constitutes of stepwise addition of amino acids. In solution, peptides can be assembled either by step by step or by fragment coupling.[3] The synthesis of oxytocin by Du Vingenaud *et al*. is the beginning of this remarkable field.[4] The past five decades can be defined as the golden era of peptide synthesis; during this period extraordinary progress has been made in the chemical synthesis of peptides and proteins.

Solid phase peptide synthesis

In 1960 Merrifield introduced the concept of solid phase peptide synthesis (SPPS) revolutionizing the field.[5] The basic Merrifield synthesis concept has two key features, one being the solid support on which the synthesis is done and the other is the orthogonal protection of the amino acids. The α-amino group in the amino acids is protected by a temporary protecting group and the side chains are protected by permanent protecting groups. The permanent protecting groups are stable under the conditions used for the removal of temporary protection of the α-amino group. The synthesis is started by anchoring the *C*-terminal end of an amino acid to a solid support via a linker. A characteristic linker is chosen in a way that both the permanent protecting groups of the amino acid side chains and the linkage between the peptide and the solid support can be cleaved under similar conditions. During the synthesis, after coupling of each amino acid the α-amino group’s temporary protecting group is deprotected so that the next amino acid can be coupled. During each coupling step excess amount of amino acid is used in order to help drive the reaction to completion. The excess reagents can be filtered and washed off from the support. In this manner the peptide chain is elongated until desired peptide length is achieved. In the final step, the peptide is released from the solid support along with deprotection of side chains (Figure I.1).

Merrifield employed protecting groups based on t-butyl and benzyl-derivatives which can be removed by graduated acidolysis. Tert-Butoxycarbonyl (Boc) which is trifluoroacetic acid (TFA) labile was used as the temporary protecting group for the α-amino group. Both this temporary Boc-group and the permanent benzyl-derivatives used for side chain protection are acid labile. The benzyl-derivatives require stronger acidic conditions (liquid hydrogen fluoride - HF) for cleavage when compared to the TFA used for the Boc-deprotection. Nevertheless, absolute selectivity during the cleavage was not possible resulting in loss of product and other side reactions. This problem was circumvented by the introduction of base-labile 9-fluorenylmethoxycarbonyl (Fmoc)-protecting group for the α-amino group.[6] In this approach the amino acid side chains are protected by mild acid labile protecting groups (t-Butyl) which are unaffected by the removal of the Fmoc-group using a base (piperidine). The linker which binds the peptide to the solid support is chosen in a way that the peptide can be released form the solid support when the side chains are deprotected under mild acidic conditions. With the introduction of the Fmoc-group, the use of highly dangerous HF used for deprotection of benzyl derivatives is completely replaced by TFA, which is an excellent solvent for peptides and can be removed by evaporation due to its volatile nature.

Solid phase synthesis has some definite advantages over the solution phase. In solid phase the final product is attached to a solid support, therefore the loss of product during every step of the reaction is minimal. Reagents can be used in excess amounts to drive the reaction to completion in the solid phase synthesis as the remaining reagents can be easily washed off and filtered from the solid support; whereas in solution phase, the excess reagents needs to be separated by a tedious purification process.[7] Typically, in solid phase the reaction completion is monitored via a colored test; whereas in the solution phase, after every step of the reaction, the product is purified and characterized.[8]

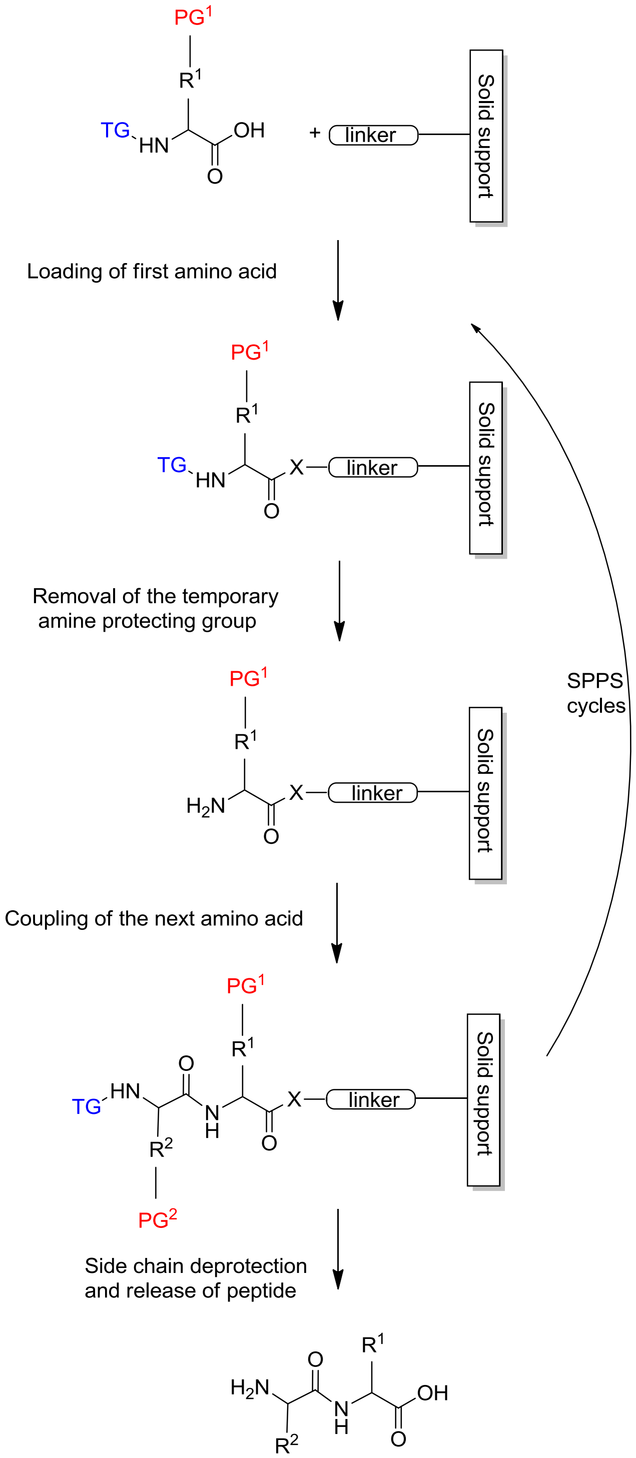
PG1
R1
TG
HN
OH
O
+
linker
Solid support
Loading of first amino acid
X
Removal of the temporary amine protecting group
H2N
Coupling of the next amino acid
R2
PG2
N
H
Side chain deprotection and release of peptide
SPPS cycles

Figure I.1. Schematic representation of solid phase peptide synthesis (SPPS). PG – Permanent protecting group, TG – temporary protecting group.[7]

Amino acids and their side chains

More than half of the 20 proteogenic amino acids contain reactive side chain functional groups. During the solid phase peptide synthesis it is essential that these side chains are protected before coupling the amino acids to the growing peptide chain. The protecting groups should be able to withstand the harsh conditions used during the synthesis. Various protecting groups have been developed and reported overtime which can be employed.[9] Protecting groups which enable selective modification of side chains of individual residues within peptide chains help in synthesis of cyclic peptides, phosphopeptides etc.[10-12]

Activation of amino acids

During the peptide synthesis the incoming amino acid requires carboxy activation. Different kinds of coupling agents are available which can activate the carboxy group in situ. The other alternative is to use pre-activated amino acid derivatives. Typically 2-10 times excess amino acid is added to drive the coupling reaction to completion. The efficiency of the methods of amino acids activation is as follows OPfp ester/HOBt<DIC/HOBt<HBTU~PyBOP<HATU.[13]

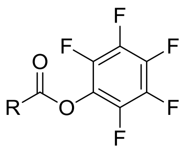

Pentafluorophenyl ester (OPfp ester)

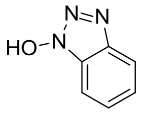

1-hydroxybenzotriazole (HOBt)

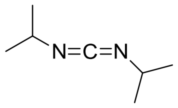

Diisopropyl carbodiimide (DIC)

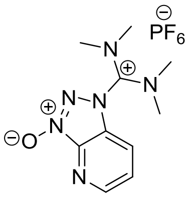

2-(7-Aza-1H-benzotriazole-1-yl)-1,1,3,3-tetramethyluronium hexafluorophosphate (HATU)

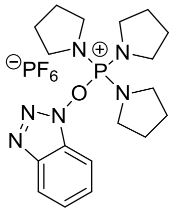

Benzotriazole-1-yl-oxy-tripyrrolidinophosphonium hexafluorophosphate (PyBOP)

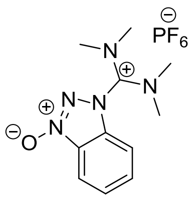

2-(1H-benzotriazole-1-yl)-1,1,3,3-tetramethyluronium hexafluorophosphate (HBTU)

Coupling of first amino acid

Coupling of first amino acid to the solid support is crucial as the extent of this reaction determines the final yield of the product. In case of surfaces with hydroxyl groups this first coupling is often accompanied by enantiomerization due to the harshness of the conditions applied to form the ester bond. The enantiomerization is more pronounced if the first residues to be coupled are either histidine or cysteine. If the first residues are either proline or N-alkylated amino acids, then there is possibility of the cyclization of dipeptides giving the corresponding diketopiperazine. This side reaction is particularly favored in Fmoc-SPPS due a free NH_2 group formed by base-induced deprotection of Fmoc group. This results in reduction of yield and truncated sequences. This can be avoided by attaching the amino acid to the solid support via a more hindered trityl ester.[13] The cyclization resulting in formation of diketopiperazine is demonstrated in Figure I.2.

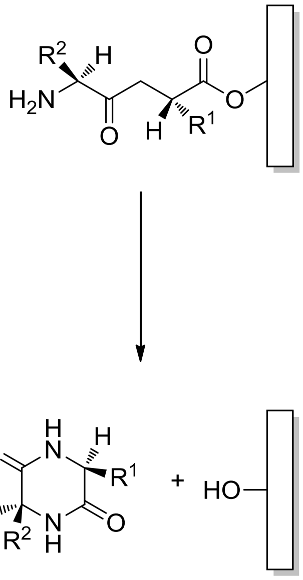

Figure I.2. Formation of diketopiperazine during peptide synthesis.

Removal of Fmoc-protecting group:

The Fmoc-protecting group which is used as a temporary protecting group for the α-amino group is removed by using 20-50% piperidine in N, N-dimethylformamide (DMF).[6] The dibenzofulvene formed during the reaction is scavenged by piperidine forming an adduct. This adduct have a strong absorption in the ultraviolet (UV) region offering a potential way to monitor the reaction completion. In peptide synthesizers, the machines which are automated to perform the coupling and washing steps of the peptide synthesis, the reaction completion is monitored by following the absorption values of the Fmoc-deprotection solution.

Enantiomerization

With the exception of glycine all the other amino acids found in proteins have chiral center of L-configuration at their α-carbon. The configuration of the chiral centers in the backbone of proteins and peptides plays a crucial role in their biological properties. Enantiomerization of an amino acid where the acidic hydrogen atom at the chiral center is removed and subsequently replaced might destroy the chirality. Enantiomerization via oxazolone formation is mainly associated with condensation of peptide fragments which involves carboxy group activation (Figure I.3).[7]

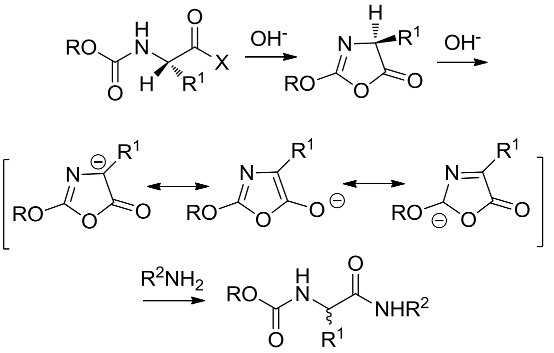

Figure I.3. Enantiomerization via oxazolone formation.[7]

Protein synthesis

Ribosomal protein synthesis

Proteins take part in most of the functional roles in a living cell. These proteins are encoded by the genetic material deoxyribonucleic acid (DNA). The process of translation of information in the DNA into proteins is a very complex process.[14] At the core of this complex translation process is the ribosome, a large molecular machine. A large number of co-factors including the transfer ribonucleic acid (tRNA) and messenger ribonucleic acid (mRNA) take part in this process. With all this machinery, synthesis of proteins longer than

30,000 amino acids is feasible. The synthesis takes place at a very rapid speed and is very accurate, the frequency of inserting an incorrect amino acid is less than 10^{-4}.[15] The protein is synthesized from Amino to Carboxyl direction by the addition of incoming amino acid to the carboxyl end of the growing peptide chain.

Chemical protein synthesis

Before the proposal of SPPS by Merrifield, synthesis of peptides chemically was tedious with several concerns. It is estimated that SPPS is ~50 fold less arduous than a solution phase synthesis of a protein.[16] However, SPPS had no impact on the maximum size of polypeptides that could be chemically synthesized. Due to incomplete reactions and accumulation of byproducts a peptide of ~50 amino acids length was the maximum that could be synthesized in a reliably good yield using SPPS. A new principle called as native chemical ligation was introduced by B.H.Kent, which propelled the chemical synthesis of proteins at exponential rate (Figure I.4).[17] In chemical ligation two unprotected peptide segments are covalently joined by a chemoselective reaction of unique and mutually reactive functional groups, one on each peptide segment.

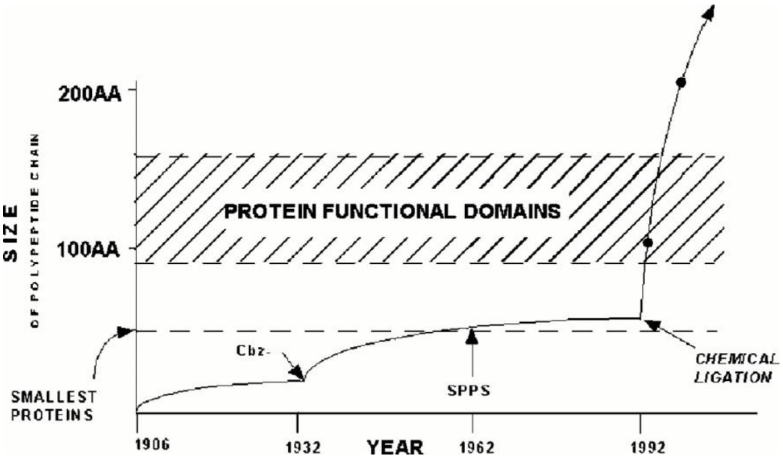

Figure I.4. Historical progress in the size of synthetically accessible polypeptides.[18] AA-amino acids

I.2. Microarrays

Typically a molecular array consists of a collection of distinct molecules attached to a solid substrate at predefined locations within a grid pattern. Each spot of the array consists of a specific type of molecule thus providing the means of parallel processing in a high throughput manner saving time and costs of raw materials. The elegant approach of using arrays to study binding events in immunoassays was put forward by Ekins.[19] Tse Wen Chang spotted antibodies on a glass cover slip forming matrix-like arrays and then screened them for specific cell surface antigens in a single run.[20] Based on the concept of oligonucleotide hybridizations on glass supports put forward by Maskos and Southern[21], Ron Davis and Pat Brown[22] put forward the idea of high-speed robotic printing of complementary deoxyribonucleic acid (cDNA) on a glass slide followed by screening, bringing into light the potential of using arrays to screen for thousands of spatially addressed molecules in a single run. The benefit of using arrays (systematic arrangement) have been identified and exploited by biologists, which enables them to screen for biochemical interactions in a high throughput manner by using thousands of moieties (nucleotide microarrays, peptide arrays, protein arrays, carbohydrate arrays etc.) in a single run.[23-25] Various technologies developed over the years have enabled scientists in creating high density arrays with thousands of biochemical or biological compounds on small areas. By incorporating internal standards in the array, the overall quality of the assay can be increased. Application of microarrays for various screenings has revolutionized the fields of genomics and transcriptomics.[15, 23] Developments in the field of technology are resulting in significant improvements in the high throughput screenings of various microarrays.

Nucleotide and peptide arrays have come a long way since their introduction. When compared, nucleotide microarray synthesis is relatively easier than the synthesis of peptide arrays due to the number of building blocks employed respectively. There are 20 proteogenic amino acids but only four natural nucleotides making the peptide array synthesis a challenge to the chemists. However, the chemistry of peptide arrays was and is being developed by researchers around the world, making them commercially cost effective.

SPOT synthesis

Spot synthesis was first reported by Frank in 1992.[26-27] The chemistry employed for the peptide synthesis is the standard Fmoc-chemistry. With this approach peptides are synthesized by spotting small volumes of activated amino acids on a modified cellulose sheet (Figure I.5). The amino acids react with the functional groups of the modified cellulose sheet forming the first layer of amino acids. The next layers of amino acids are spotted successively on the previous layer making sure that the adjacent spots do not merge. With this method parallel synthesis of large number of addressable peptides in small amounts is possible. The cost per peptide synthesized by SPOT synthesis method is significantly less than that of a peptide synthesized on a resin (less than 1%).[25]The convenience of this method is that it can be undertaken without any special equipment. The arrays produced via SPOT synthesis have been employed in various screens and studies.[28-30] After the synthesis the peptides can be cleaved from the cellulose support by dry aminolysis.[29] Each peptide spot can be stamped out and can be purified by HPLC. The purified peptides can be re-spotted on glass supports. However, this purification process is tedious and expensive when it has to be done for thousands of peptides.

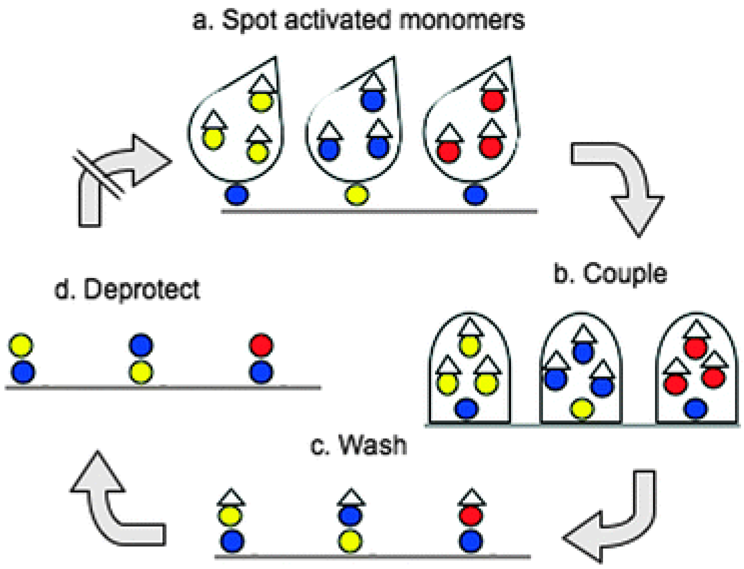

Figure I.5. Diagrammatic representation of spot synthesis. a) Activated amino acids in solution are spotted on a modified cellulose support b) the amino acids couple to the functional groups on the modified cellulose c) the excess amino acids are washed away d) the temporary α-amino protecting group is deprotected for further coupling steps.[25]

Peptide arrays of density 25 peptide spots per cm^2 can be synthesized with SPOT synthesis. It is difficult to increase the density of the spots further due to evaporation and spreading of the liquid amino acid droplets.[27, 29]

Photolithographic synthesis

Synthesis of peptide arrays by photolithographic approach is a modified version of the solid phase peptide synthesis, where, the protecting groups employed are photolabile.[31] A lithographic mask is used to define a specific 2D pattern of light. When the surface with photolabile protecting groups is exposed to this 2D patterned light, only the protecting groups which are in the illuminated areas are removed and the protecting groups in the dark areas remain intact. The whole surface is incubated with an activated amino acid solution enabling the coupling at the deprotected sites. The unreacted amino acid solution is washed away followed by exposing the surface again to a patterned light which gives a chance for the coupling of the next amino acid (Figure I.6).

Using this method, truly high-density arrays of oligonucleotides were produced. Fodor *et al.* showed that peptide arrays can be synthesized with the lithographic method.[31] This method is a milestone in the field of oligonucleotide arrays. However in the field of peptide arrays, even though this method is promising in terms of achieving high-density, it has some practical limitations.

For every layer of amino acids that should be deposited on the surface, the deprotection and coupling step should be done 20 times. For example, in order to synthesize an array of 10meric peptides, the number of coupling steps will be 20x10. With the increase in the number of coupling steps, the number of side reactions increases resulting in the poor quality of the arrays. However, with oligonucleotides, which have only 4 monomers, the number of repetitive cycles decrease, making this method a commercial success for the production of high density oligonucleotide arrays.[32]

Another drawback with this method is that, the photo-labile protecting groups perform poorly in terms of repetitive coupling yield when compared to the conventionally used Fmoc or Boc protecting groups. This drawback was overcome by Pellois *et al.* by using a photoacid. Nevertheless, the cost of production is high due to the photo-labile protecting groups.

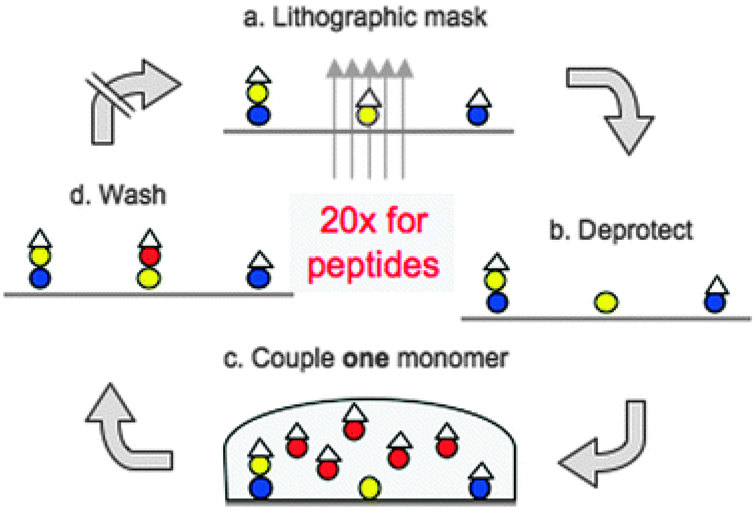

Figure I.6. Diagrammatic representation of photolithographic synthesis of peptide arrays. a) Surface with photolabile protecting groups is exposed to a pattern of light via photolithographic mask b) on illumination the photolabile protecting group is removed c) the entire surface is covered with solution of activated amino acid enabling coupling at the illuminated regions d) after coupling excess amino acids are washed away.[25]

I.2.1. High density peptide arrays - particle based peptide synthesis

The peptide arrays used in this work were supplied by a collaboration partner *PEPperPRINT GmbH* (Heidelberg, Germany). The method used by the company for the production of high-density peptide arrays is particle based peptide synthesis. In this method, solid amino acid toner particles are addressed onto a solid support by a laser printer (Figure I.8). Unlike SPOT synthesis, where the resolution is limited due to spreading of the solvent, the particle based peptide synthesis using laser printer allows for a good spatial resolution resulting in 700-800 different peptides per cm^2.

The key to the particle based peptide synthesis are the amino acid toner particles. Twenty amino acid toner particles are used in the printing process corresponding to the twenty natural amino acids found in proteins. The amino acid toner consists of 10% (m/m) of Fmoc-protected and OPfp-activated amino acids along with commercial styrene acrylic copolymer (e.g. SLEC PLT 7552, *Sekisui Chemical GmbH*, Dusseldorf/Germany).[33] The amino acids embedded in the toner particles are reported to have low decay rates of <1% per month (except for arginine with 5% per month). The coupling efficiencies obtained with these amino acid toner particles are similar to standard SPPS.[33-34]

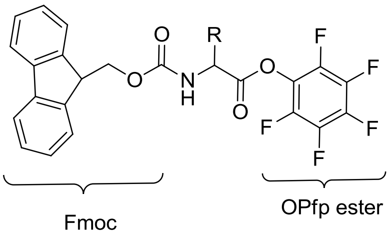

Figure I.7. Amino acid OPfp ester

The amino acid toner particles are deposited on a surface by employing the laser printing method. The working principle of the peptide laser printer is similar to a standard color laser printer. The standard color laser printer contain 4 cartridges (CMYK: cyan, magenta, yellow, black) whereas the peptide laser printer contains 20 cartridges, each one for a specific proteogenic amino acid. The 20 cartridges are precisely positioned in the laser printer and only the currently active cartridge comes in contact with the solid support by moving in the z-direction. With the use of driver software and positioning mechanism, which allows for micrometer precision, a peptide array density of 700-800 spots per cm^2 can be printed using the laser printer.[33]

The central component of the laser printer is the organic photoconductor (OPC) drum. Organic photoconductor materials acts as insulators in the dark and when exposed to light becomes conductive. The OPC drum in the laser printer consists of a metal drum, which is covered with a thin layer of organic photoconductor by a charging unit resulting in a uniform charge on the OPC drum. A light-emitting diode (LED) selectively illuminates the uniformly charged OPC drum, creating a charge pattern on the drum surface. The amino acid toner particles develop charge due to the friction between the charging drum and the transfer drum. These charged particles on the transfer drum are selectively transferred to the illuminated regions on the OPC drum. The OPC drum now transfers the amino acid particles in a specific pattern on to the solid support which is oppositely charged.

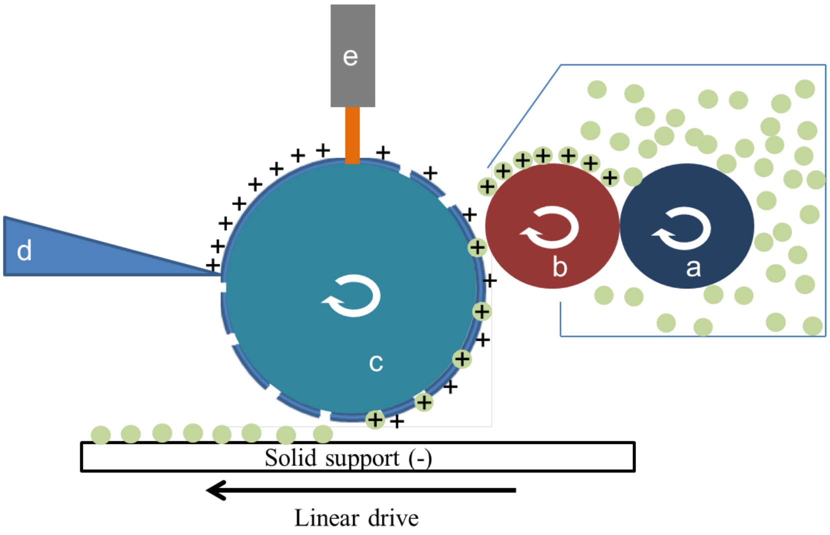

Figure I.8. Schematic representation of laser printer employed for amino acid particle deposition on a surface. a) charge drum b) transport drum c) Organic photoconductor (OPC) drum d) primary charge roller (PCR) e) Light emitting diode (LED). The PCR evenly charges an OPC drum. The LED generates a charge pattern on the OPC drum by discharging upon illumination. Particles with same charge as present on the OPC are only transferred to the discharged areas. The charge pattern is then translated into a particle pattern. The particles are printed by rolling the OPC drum over a solid support.[33, 35]

In this manner the twenty drums transfer the twenty different amino acids particles precisely onto the solid support creating the desired distribution of amino acids (Figure I.9).

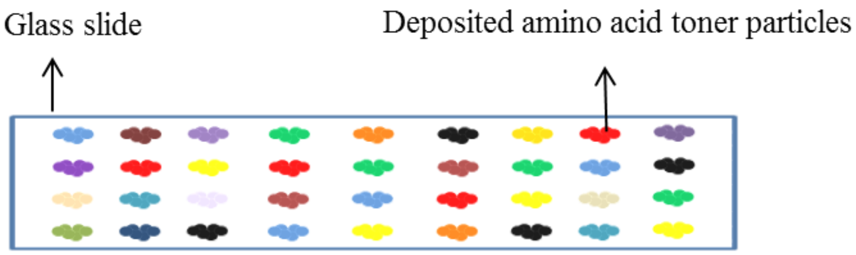

Figure I.9. Diagrammatic representation of the amino acid toner particles deposited by laser printer on a solid support. Each amino acid toner cartridge deposits the respective amino acid at the specified position on the slide.

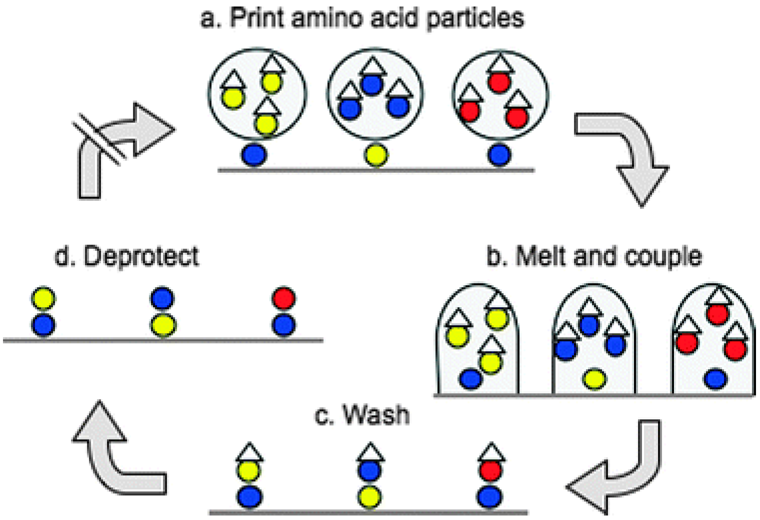

Figure I.10. Combinatorial synthesis of peptide arrays. Initially the amino acid toner particles are printed on the solid support (glass slide) by the laser printer (a). The particles are melted and the amino acids are coupled to the surface (b), then the melted matrix and the uncoupled amino acids are washed away (c), the protecting groups of the coupled amino acid particles on the surface are removed (d) so that the next amino acid can be coupled.[25]

After the deposition of the first round of amino acid particles on the functionalized substrate, the solid particles are melted to form semi-viscous spheres similar to individual reaction chambers. This step is the defining point of achieving high density of the peptide arrays. Unlike in the SPOT synthesis, where the liquid drops of amino acids disperse on the surface, in the particle based peptide synthesis, the space occupied by each amino acid is limited due to the viscosity of the matrix in which the amino acid particles are embedded. When the particles are melted, the amino acids reach the surface and couple. The melted matrix and the uncoupled amino acids are washed away in the next step (Figure I.10). Now the surface consists of precisely addressed 20 amino acids. The N-terminal Fmoc-protecting group of the coupled amino acids is removed, so that the next amino acid can be printed and coupled. The steps are repeated until the desired peptide array is completed.

I.3. Proteases

Proteins are ubiquitous in living systems and play key roles in several crucial functions. They serve as catalysts, provide immune protection, control growth and differentiation etc. However, proteins that have served their purpose must be degraded in the body so that their constituent amino acids can be recycled and used in the synthesis of new proteins. Proteins which are ingested through the diet must be broken down into fragments (small peptides and amino acids) so that they can be absorbed in the intestine. To break down the proteins, the amide bonds between the amino acids need to be hydrolyzed. However, the peptide bond is highly stable, this is due to the resonance structure which imparts partial double bond character to the peptide bond (Figure I.11). This makes the carbonyl carbon less electrophilic resulting in kinetic stability of the peptide bond.[36]

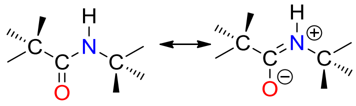

Figure I.11. Resonance structure of peptide bond. Due to the partial double bond character the hydrolysis of peptide bond is extremely slow and requires a catalyst.[36]

In the absence of a catalyst, the hydrolysis of this peptide bond has an estimated half-life of 300-600 years at neutral pH and 25^{o}C; this long time is not compatible with the bio-chemical processes where peptide bonds need to be broken down in milliseconds.[37]

Proteases are the enzymes which catalyze the cleavage of peptide bonds in proteins. They are present in all living organisms and seem to have arisen in the earliest phases of evolution.[37] They occupy a pivotal position in a variety of functions from the cellular level to the organism level, to produce cascade systems like hemostasis and inflammation.[38] They are involved in complex physiology processes and in abnormal pathophysiological conditions. Their role in some fatal diseases such as cancer and acquired immunodeficiency syndrome (AIDS) has made them potential targets for developing therapeutic agents.[39-44] In the recent trend of developing environmentally friendly technologies, proteases are being studied extensively as replacements for the chemicals which are being used (e.g. leather treatment, detergents etc.). Every year millions of tons of proteases are being produced in bulk to meet the market requirement.[45] Even though crude preparations of proteases are being used in detergent and leather industries, extensive purification is required for those proteases which are used in medicines. Proteases represent one of the three largest groups of industrial enzymes and are accounted for about 60% of the total worldwide sale of enzymes.[45-48]

Classification of proteases

Broadly proteases are divided into two groups based on their site of action.[49]

- ***Exopeptidases***: Exopeptidases cleaves peptide bond proximal to the amino or carboxy termini of the substrate. These peptidases are further classified based on their site of action
  - Aminopeptidases: Aminopeptidases acts at the free *N*-terminus of the polypeptide chain. These peptidases are in general intracellular enzymes.
  - Carboxypeptidases: Carboxypeptidases acts at the *C*-terminus of the polypeptide chain. These peptidases can be further divided into three major groups based on the nature of the amino acid residues at the active site of enzymes.
    - i) Serine carboxypeptidases
    - ii) Cysteine carboxypeptidases
    - iii) Metallocaboxypeptidaes
- ***Endopeptidases*** – Endopeptidases cleaves peptide bonds distant from the termini of the substrate.
    - a) Aspartic proteases
    - b) Metalloproteases
    - c) Cysteine proteases
    - d) Serine proteases

However, there are few proteases which do not precisely fit into the above mentioned classification (e.g. ATP-dependent proteases require ATP for activity).[50]

Mechanism of action of proteases

Proteases generate a nucleophile which is strong enough to attack the peptide carbonyl group. The nucleophile is generated with the help of the active site/catalytic site of the enzyme which include features that can help to

- Activate a water molecule or another nucleophile
- Polarize the peptide carbonyl group
- Stabilize a tetrahedral intermediate

The catalytic site of a protease is flanked on one or both sides by specific subsites. These subsites accommodate the side chains of a single amino acid residue from the substrate. The sites are numbered from the catalytic site, S_1 through S_n towards the *N* terminus and S1' through Sn' towards the *C* terminus. The amino acids of the substrate on which the proteases act are numbered P_1 through P_n and P1' through Pn', respectively.

Aspartic Proteases

As the name itself suggests these proteases depend on the aspartic acid residue for the catalytic activity (Figure I.12.c). The majority of these proteases, especially of the pepsin family, have two lobes and the active site is located between the lobes. Each lobe contributes one of the pair of aspartic acid residues that are crucial for the catalytic activity.[51-52]

Metalloproteases

These proteases depend on the availability of bound divalent cations for activity. In majority of the proteases, Zn^{+2} is the metal ion (Figure I.12.d) The cations play vital role in the mechanism of action and the proteases can be inactivated by dialysis or by the addition of chelating agents.[53]

Cysteine Proteases

In cysteine proteases, the sulphur atom of the cysteine residue in the catalytic site acts as a nucleophile (Figure I.12.b). Cysteine proteases are similar to that of serine proteases in the use of a strong nucleophile and the formation of a covalent enzyme–substrate complex.

However, the nucleophile is the sulphur atom of a cysteine residue, as opposed to the oxygen atom of a serine. These proteases catalyze the hydrolysis of the peptide bond through general acid-base formation and hydrolysis of an acyl-thiol intermediate.[54]

Serine proteases

Serine proteases consist of three amino acids (histidine, serine and aspartic acid) in the catalytic site. Each of the three amino acids fulfills a specific role in the protease mechanism. The histidine (which is stabilized by the aspartic acid) deprotonates the serine hydroxyl, enabling nucleophilic attack on the carbonyl carbon of substrate (Figure I.12a). Serine proteases follow a two-step reaction during the hydrolysis of the peptide bond, in which a covalently linked enzyme-peptide intermediate is formed. During the intermediate formation an amino acid or peptide fragment is lost. The intermediate is attacked by water which acts as a nucleophile resulting in the hydrolysis of the peptide.[55]

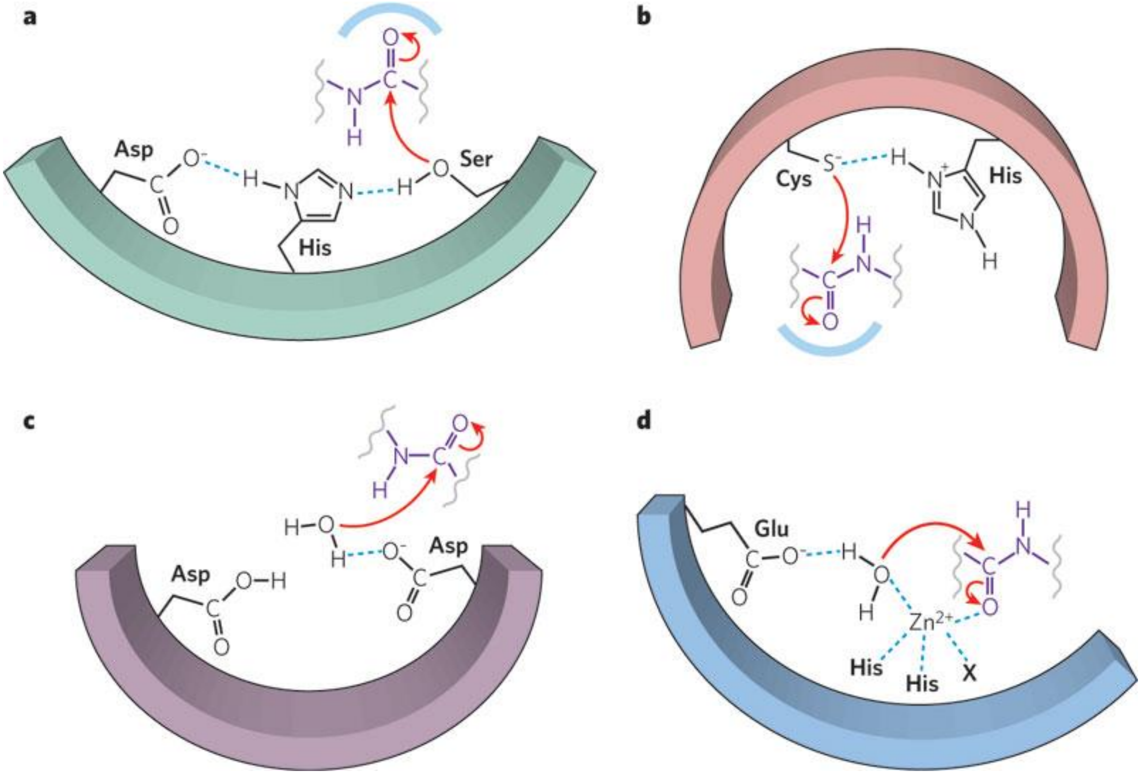

Figure I.12. Catalytic sites of various proteases. a) Serine proteases b) Cysteine proteases c) Aspartic proteases d) Metalloproteases.[56]

I.3.1. Catalytic triads

In 1967 David Blow put forward the first protease catalytic site that of α-chymotrypsin using X-ray crystallography.[57] It was shown that in total three residues are directly involved in the catalysis: Ser195, His57 and aspartate102. These three residues put together were identified as Ser-His-Asp triad, also known as catalytic triad. Each residue has a specific role in generating the nucleophilic potential at the serine side chain (-OH) which is necessary to attack the carbonyl group of the amide bond.[58]

The imidazole group of the histidine acts as a base and accepts the proton form the –OH group of the serine, generating a nucleophile which attacks the carbonyl carbon atom of the target peptide bond. The –NH group of the imidazole ring is in turn hydrogen bonded to the carboxylate group of the aspartate102. The ability of the histidine residue to accept the proton form the serine arises from the difference in the relative pKa's of the two residues. Other factors such as effects of substrate binding resulting in structural adjustments also promote the proton transfer from the serine, making it a powerful nucleophile.

Soon after the revelation of presence of catalytic triad in the chymotrypsin, an identical triad was reported in trypsin and elastase.[59-60] These two enzymes are closely related to chymotrypsin and the existence of catalytic triad was not unexpected. However, in protease subtilisin the same triad was identified.[61] What made this finding interesting was the completely different primary structure (amino acids sequence) of the subtilisin. Since then, quite a few proteases which possess a catalytic triad have been identified. Even though the residues which are present in the catalytic triad are different, the core pattern (acid-base-nucleophile) was maintained. This suggests that there was an independent convergent evolutionary path to the triad, signifying the importance of catalytic triad for the enzyme activity. Nevertheless, there are several questions to be answered regarding various events occurring during the proteolysis. The role of catalytic triad amidst the entire process takes a key position. Many enzymes, not just serine proteases are reported to have catalytic triad in their active sites (see Figure I.13).[58]

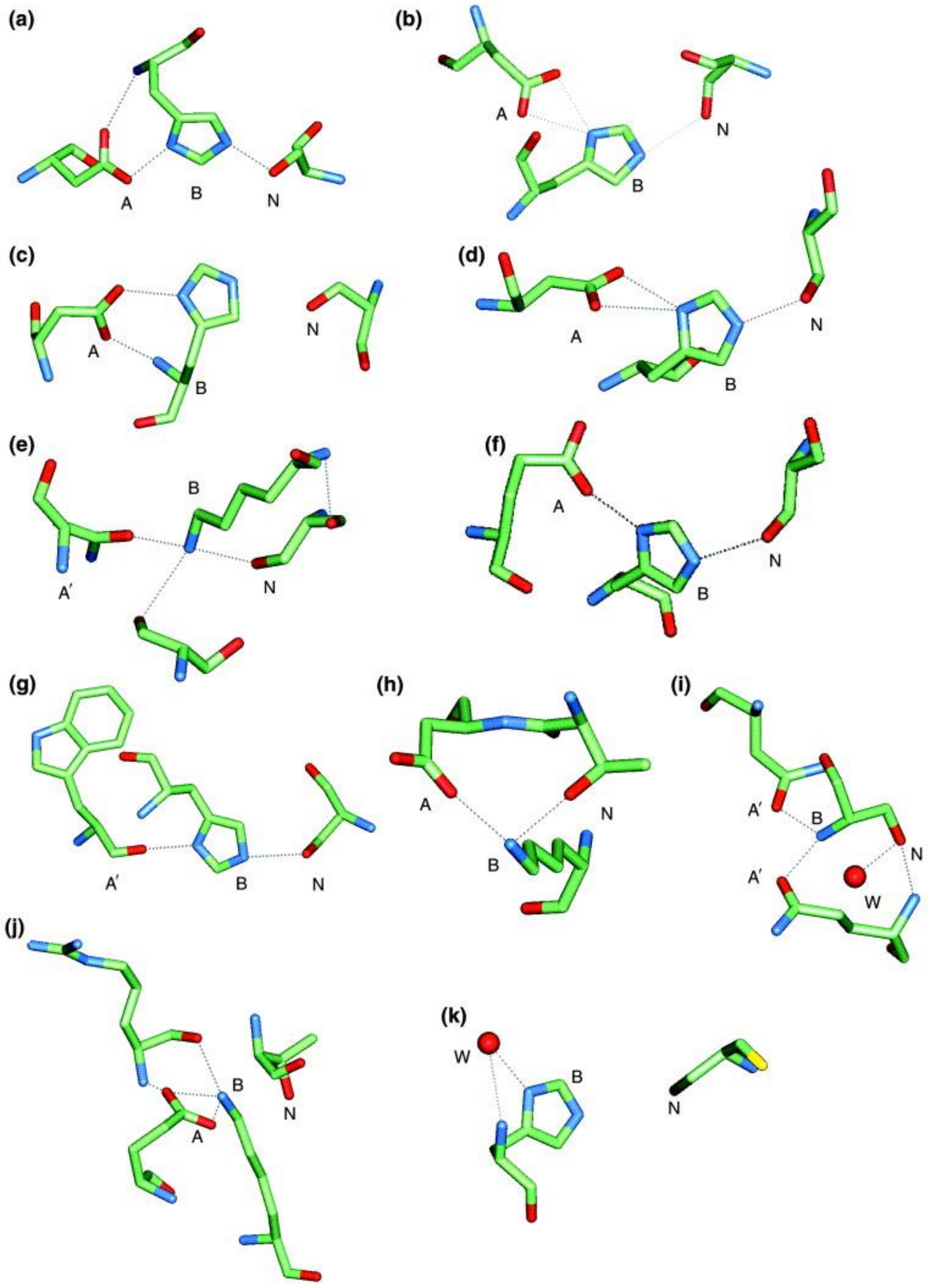

Figure I.13. The catalytic triads of enzymes. Atom (color) – nitrogen (blue); oxygen (red); sulphur (yellow). Hydrogen bonds are indicated by dotted lines. In the catalytic triads the base (B) is shown in the centre, the acid(A) and/or H-bond acceptor (A’) are shown on the left; the residue with the nucleophilic atom (N) is shown on the right. A) Trypsin b) Subtilisin c) Brain acetyl hydrolase d) Lipase e) β-Lactanase f) acetyl cholinesterase g) Streptomyces scabies esterase h) Asparaginase i) Penicillin acylase j) the prokaryotic proteasome catalytic subunit k) Trypsin like enzyme from picomavirus.[58]

I.4. Surface analytical techniques

I.4.1. UV/Vis photospectrometry

After each coupling step, the Fmoc-protecting group which is used as a temporary protecting group for the α-amino group is removed by using 20-50% piperidine in DMF. The dibenzofulvene formed during the reaction is scavenged by piperidine forming a piperidine dibenzofulvene adduct (PDFA). This adduct have an absorption maximium at 301 nm, offering a potential way to monitor the reaction completion.

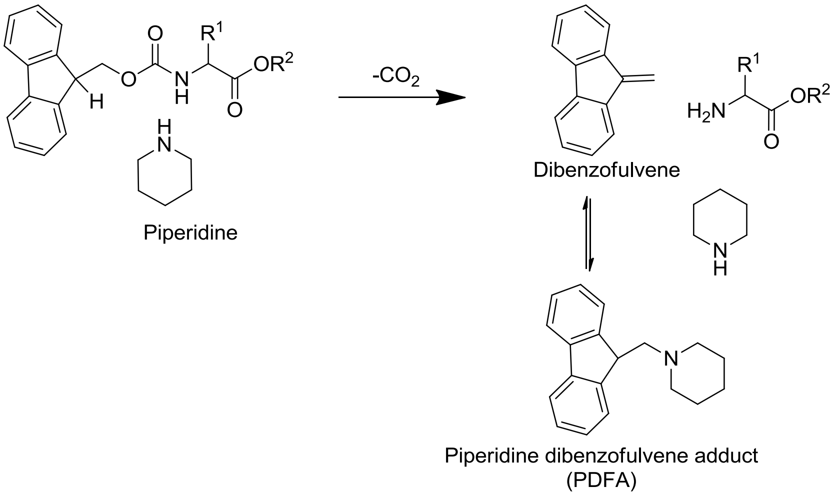

Figure I.14. Fmoc cleavage and formation of piperidine dibenzofulvene adduct. Deprotection of Fmoc-protected α-amino group with 20% piperidine in DMF results in formation of dibenzofulvene and a free amino group. Piperidine forms an adduct with dibenzofulvene which has an absorption maximma at 301 nm.

The PDFA concentration can be used to determine the number of -NH_2 groups present on the surface by comparing the absorption of PDFA obtained from the sample vs a blank solution. Derivatization grade (DG), i.e. the amino group loading on the surface in nmol/cm^2 can be obtained employing Beer-Lambert's law.[62]

$$DG = \frac{n}{A} = \frac{E.V}{\varepsilon.d.A}$$

Equation 1. Derivatization grade (DG) of surfaces calculated based on the absorption value obtained during the Fmoc release. n=amount of substance in moles, A=surface area covered with deprotection solution, E=extinction V=applied volume of 20% (v/v) piperidine in DMF, ε=extinction coffeicient, d=path length of the cuvette.

I.4.2. X-ray Photoelectron Spectroscopy

X-ray photoelectron spectroscopy (XPS) is a sensitive surface analytical technique which can give information about the elements present at the surface, the amount of each element present and the three dimensional spatial distribution of the elements. XPS is also known as electron spectroscopy for chemical analysis (ESCA). XPS can not only identify the elements present but also the chemical state of the respective elements. For example, Fe^0, Fe^{2+} and Fe^{3+} are easily distinguishable using XPS. In addition to these, XPS is also useful to find out the thickness of a polymer film and its uniformity.

When a surface is hit by a photon of sufficient energy, the atoms on the surface can be ionized resulting in ejection of electrons (Figure I.15). The Kinetic energy of the ejected electron (photoelectron) depends on the energy of the photon, given by Einstein photoelectric law.[63]

$$h\nu = E_b + KE + \Phi$$

Equation 2. Photoelectric law gives the relation between the kinetic energy of the photoelectron and the energy of the photon. E_b is the binding energy of the corresponding electron in the atom and Φ is the work function of the instrument, h is the Planck's constant, KE is the kinetic energy of the ejected electron, ν is the frequency.

In XPS, a core electron of an element is ejected from a core level by an X-ray photon of energy $h\nu$. The energy of the emitted photoelectron is then analyzed by an analyzer and the date is presented as a graph of intensity, usually expressed in counts vs electron energy.

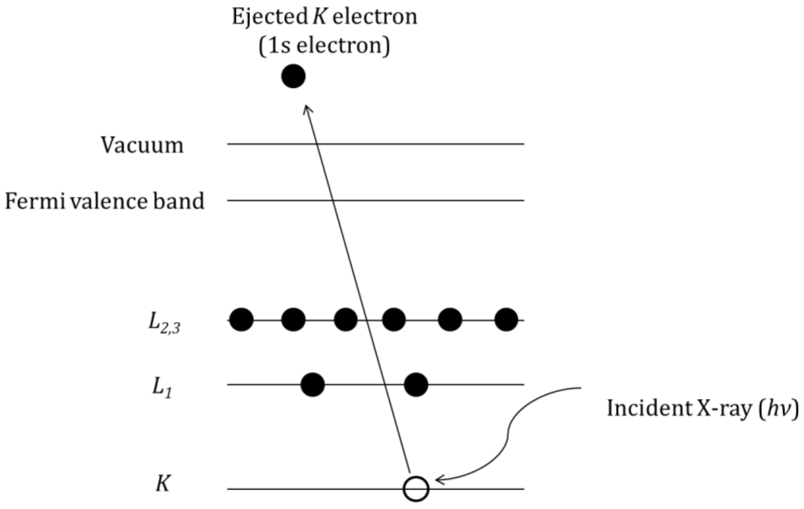

Figure I.15. Schematic representation of the XPS process showing photoionization of atom by the ejection of a 1s electron.[64]

The kinetic energy of the electron depends on the X-rays employed and therefore depends on the spectrometer. The binding energy of an electron is characteristic for both element and the atomic energy level of the electron. With most of the XPS instruments, the spatial resolution of about 10µm is possible. An advanced imaging XPS can offer spatial resolution of < 3µm.

Using XPS quantitative information of the sample composition can be obtained. Appropriate background noise subtraction (due to X-ray scattering and interaction of ejected photoelectrons in the material) from the signals followed by integration corresponding to the fraction of respective atoms in the analyzed sample improves the reliability of quantitative information. Individual calibration of the instrument and reference measurement of an internal or external standard greatly improves the accuracy of the measurement enabling quantification and valid comparisons between samples of similar type. When it comes to instrumentation, XPS consists of a primary radiation source, an electron energy analyzer and the sample under study in an ultra-high vacuum chamber. The primary radiation source produces X-rays, which are generated by bombarding an anode material with high energy electrons. The efficiency of X-ray emission from the anode is determined by the electron energy, relative to the X-ray photon energy. The X-ray source is usually an Al- or Mg- coated anode stuck by electrons from a high voltage source.

The depth analysis in XPS varies with the kinetic energy of the electrons and is determined by attenuation length (λ) of the electrons which is related to the inelastic mean free path (IMFP). The relation between the λ and the energy of the electron is proposed by Seah and Dench and is given as follows.[65]

$$\lambda = \frac{538 a_A}{E_A{}^2} + 0.41 \mathrm{a}_A (a_A E_A)^{0.5}$$

Equation 3. Equation depicting the relation between, E_A(the energy of the electron in eV), $a_A{}^3$ (the volume of the atom in nm^3) and λ (the attenuation length is in nm).

I.4.3. Time of flight secondary ion mass spectrometry

Time of flight secondary ion mass spectrometry (ToF-SIMS) is a highly sensitive surface analytical method which can be used to study the chemical composition of the top layers (~1nm) on a sample surface. The development of ToF-SIMS started with the work of Benninghoven at the University of Munster in the 1970’s.[66-68] In his work he used static ToF-SIMS to study the oxidation of metal substrates and the adsorption of organic molecules on the metal surfaces.

Generation of secondary ions

In ToF-SIMS the sample is bombarded by short pulses of primary ions. During the sputtering process, the incident ion transfers its energy to the target atoms on the sample surface thereby initiating a series of collision cascades between the atoms of the sample within about 1-2nm of the surface. As the collision cascade moves away from the bombardment site, the collisions become less energetic resulting in large molecular fragments rather than small atomic fragments (Figure I.16). The fragments produced have sufficient energy to leave the surface by overcoming the binding energy. The sputtered particles are ejected as a mixture of neutral atoms, molecules, electrons and ions.[69] Only a small fraction of the sputtered particles are charged. The polarity of the emitted fragments depends on the electronic configuration. However the actual process of sputtering is not well understood and various theories were put forward to understand the process.[70]

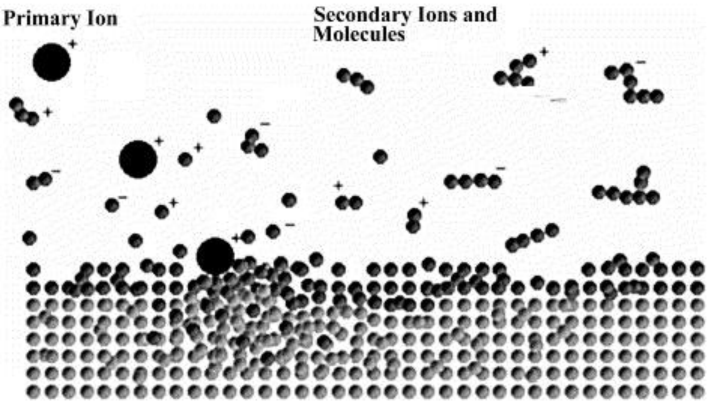

Figure I.16. Schematic representation of the secondary ion emission process initiated by the impact of primary ion. Near the site of collision extensive fragmentation occurs, producing mainly atomic particles. In the regions away from the impact point the collisions become less energetic resulting in the emission of larger molecular fragments.[69]

The secondary ion generation in ToF-SIMS can be divided into two components

- Desorption of atoms and multi-atomic clusters
- Ionization of a fraction of the sputtered particles

Primary ion sources

The primary ions can be both monoatomic (Ga, Cs, Ar, Xe, etc.) and polyatomic (Bi_n, Au_n, C_{60} and SF_5 cluster ions).[71-74] Typically the energies of the primary ions are in the range of KeV, which is higher than the binding energies of the atoms on the surface. This results in extensive fragmentation due to bond breaking near the collision site leading to the emission of particles.

The quality of the results obtained using ToF-SIMS is mainly dependent on the emission intensity of the secondary ions. The nature of primary ion source used is known to effect the secondary ion formation process. Polyatomic primary ion beams considerably increase the secondary ions yield when compared to the initially employed Ga gun. Liquid metal cluster ion guns (Au_n, Bi_n) allow high lateral resolution with high cluster current. The post ionization of sputtered particles may lead to the improvement of the sensitivity and quantification even further.

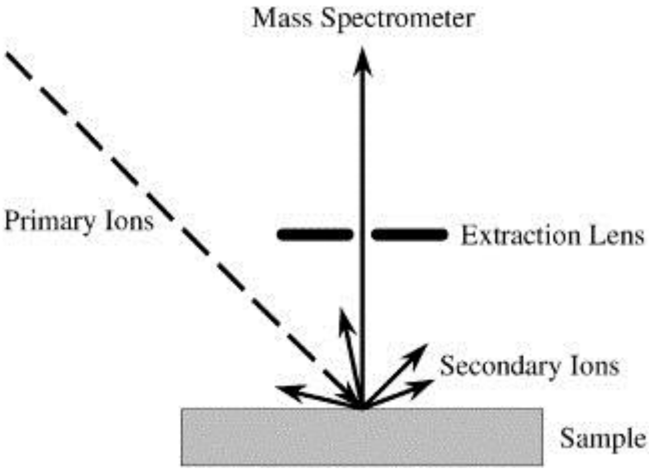

Figure I.17. The principle of secondary ion mass spectrometry. The sample surface is bombarded with energy rich primary ion beam resulting in the generation of secondary ions which are detected by the mass spectrometer.[75]

Time of flight analyzer

The secondary ion fragments generated are accelerated by an extractor with a fixed voltage to a common energy as they enter the into the TOF analyzer. The polarity of the TOF-analyzer determines whether positive or negative secondary ions are analyzed. The TOF analyzer separates the secondary ions based on the m/z (mass/charge) ratio. The mass of the ion is determined based on the time taken by the ion to travel through the field-free flight tube of length L, after the ions are accelerated to a common energy, E, in the extraction field. The relation between the time of flight and the mass of the ion can be given by the following equation

$$E = \frac{mv^2}{2} = \frac{mL^2}{2zt^2}$$

$$t = L\left(\frac{m}{2zE}\right)^{1/2}$$

Equation 4. The relation between, *E* (energy) *m* (the mass of the ion), ν (the velocity of the ion) , *L* (the length of the field-free flight tube), *z* (the charge of the ion), and *t* (the flight time).[69]

The time of flight is proportional to the square root of the mass of the secondary ion; the lighter ions travel faster and reach the detector earlier than the heavier ions.

Matrix effect

One concern regarding the quantification of ToF-SIMS spectra is the “matrix effect”, where the intensity of a given secondary ion fragments depends on its surrounding chemical environment. Therefore, the intensity of the fragment is not always directly related to its concentration on the surface. It also depends on the surrounding environment. However in most of the organic surfaces the matrix effects are minimal and by using references (along with spectral normalization) it is possible to obtain quantitative information from the sample surface.

ToF-SIMS can be used in different modes (surface spectroscopy, surface imaging, depth profiling) to obtain various kinds of information. Depending on the mode of operation, information on the chemical composition, localization and quantity of different chemical species present on the surface can be obtained.

Static SIMS and Dynamic SIMS

In static SIMS mode the sample surface is bombarded with an extremely low dose of primary ions due to which less than 1 % of the atoms present on the top surface receive an ion impact. The majority of the ions on the surface will be unaware of the sputtering event resulting in no destruction of the sample.

In dynamic SIMS the sample surface is sputtered continuously until the desired depth is reached. C_{60} cluster ions are reported to increase the yield of secondary ions during the dynamic SIMS, because they cause smaller depth of damage during the sputtering process when compared to the Ga. Due to this minimal damage C_{60} gives very good resolution during the depth profiling (Figure I.18).[76]

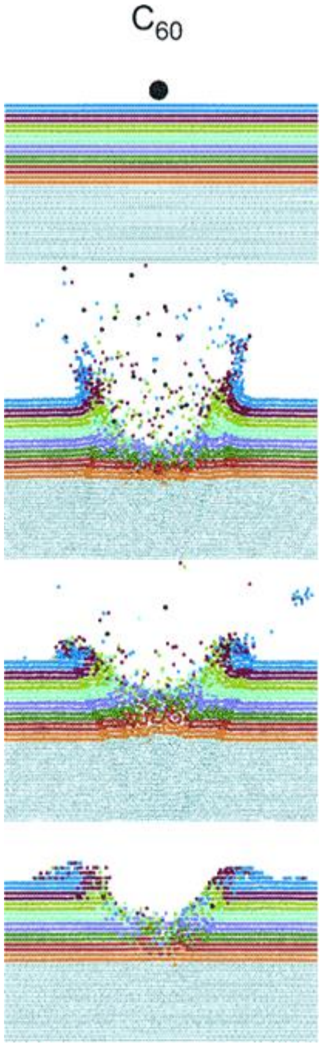

Figure I.18. Cross-sectional view of the temporal evolution of a typical collision event leading to ejection of atoms due to C60 bombardment of a gold surface at normal incidence. The atoms are colored by original layers in the substrate. The projectile atoms are black.[76]

Measurement sensitivity (detection limits in the ppb-ppm range) and depth resolutions of greater than 1 nm can be achieved during the depth profiling using ToF-SIMS.

II. Motivation and Objective of the work

Proteases play a crucial role in every living system.[38, 44] They catalyze the hydrolysis of peptide bonds via nucleophilic attack of targeted carbonyl bond. At the beginning of protein evolution, it was more likely that, proteases in primitive organisms started as destructive enzymes with simple structure for protein catabolism and generation of amino acids.[37] These primitive proteases might not have been as selective as the present proteases. However, with evolution, the proteases became more efficient both in selectivity and activity.

In a protease, which is a complex enzyme system, the catalytic ability is based on the spatial organization of the active atoms (amino acids and their side chains).[58] This work was started with a simple idea of identifying a peptide which can mimic a primitive protease (simple in structure and which can cleave a peptide bond without any selectivity, in terms of destruction). For a protease to act, it majorly requires a catalytic triad. A catalytic triad consists of an acid-base-nucleophile pattern. This pattern is conserved generally throughout the evolution in various proteases, by varying the acids and bases with different residues.[58] As J.R. Knowles put it, “Enzyme catalysis: not different, just better.”[77] With evolution, the proteases retained the catalytic triad, but got better in terms of selectivity by increasing the complexity of the protease structure. Therefore, primitive proteases can be mimicked by bringing the catalytic triad together under optimal conditions. In order to identify such a peptide with proteolytic activity, thousands of peptides must be screened to find a suitable sequence of amino acids which can mimic a spatial arrangement of a catalytic triad. The best way to do this screen is by using peptide arrays where thousands of different peptides can be screened in a single run.

The principle aim of this work was to create an assay to detect peptides with proteolytic activity in a peptide array. Peptide arrays used in this work consists of 400 different peptide spots per cm^2, therefore, the detection assay should be in such a way that, each individual peptide spot can be screened for proteolytic activity.

III. Results and discussion

III.1. First screening strategy

When developing a screen for identifying a particular moiety, the screening principle should be based on a unique property exhibited by that moiety. For example, in order to detect a particular antibody in a serum, the screening is based on the ability of antibody to bind to a particular antigen or a chemical compound. The screen for the detection of proteolytic activity was developed based on the self-digestion ability of proteases. Being proteins themselves, proteases undergo self-digestion over time.

In a peptide array, each peptide spot contains numerous peptide molecules. These peptides are closely packed in a polymer film of 10-13 nm thickness. In case of a peptide with proteolytic activity, there is a possibility of the peptide molecules present in one spot cleaving one another, resulting in a decrease of peptide molecules in the peptide spot. Tracking the loss of these peptides was utilized as the basis of the screen.

In order to study if the peptides in a spot cleave one another, the peptide array needs to be labelled with a marker which can be monitored over time under the assay conditions. In principle, a peptide array can be labelled with different kinds of markers, for example, fluorine containing molecules. The time resolved fluorine concentration is measurable by XPS or TOF-SIMS.[78] However, these surface analytical methods are time consuming, costly and slow, which makes fluorescence based assays more suitable. The loss of peptides labelled with a fluorophore in a particular peptide spot can be monitored by measuring the decrease in fluorescence intensity with a scanner in a high throughput manner.

To keep the screening conditions as simple as possible, without needing any extra equipment such as incubating system, the screen was carried out at room temperature (RT) and at neutral to slightly alkaline pH. The peptide arrays were incubated in phosphate buffered saline with surfactant Tween20 (PBS-T) at RT. Tween20 was added to ensure the optimal wetting of the surfaces.

III.1.1. Stability of the peptides under screening conditions

Once the optimal conditions of the assay were chosen, the next step was to verify the stability of the peptide arrays under the chosen assay conditions. The peptide arrays, which are to be screened for peptide candidates with proteolytic activity, should be stable in PBS-T at RT. The peptide arrays were synthesized on a copolymer film consisting of 10% (n/n) poly(ethylene glycol) methacrylate and 90% (n/n) methyl methacrylate (10:90-PEGMA-co-PMMA).[33] The stability of the polymer bound peptides in PBS-T was verified by XPS measurements. As conducting surfaces are favorable for XPS, the 10:90-PEGMA-co-PMMA polymer was synthesized on a silicon wafer, employing Surface Initiated Atom Transfer Radical Polymerization (siATRP) (see V.3.11).[79] To the available –OH groups, Fmoc-β-alanine-OH was coupled followed by the removal of Fmoc-group. To the now available free NH_2-groups, Fmoc-L-Pentafluorophenyl alanine-OH was coupled (Figure III.1).

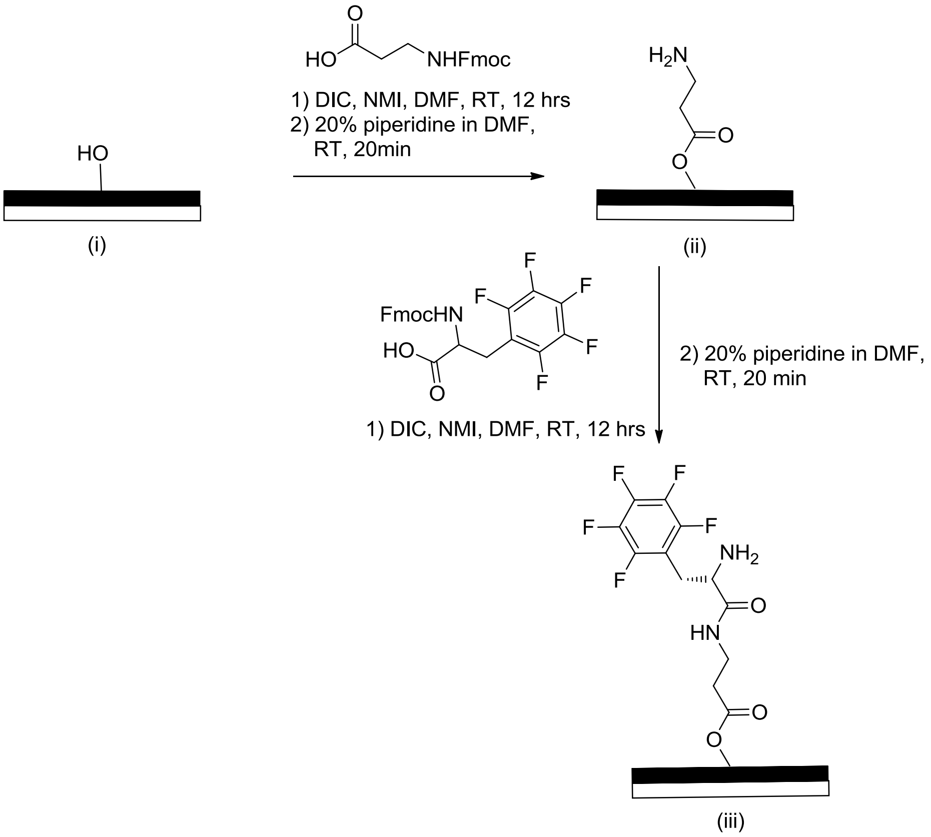
HO
NHFmoc
1) DIC, NMI, DMF, RT, 12 hrs
2) 20% piperidine in DMF, RT, 20min
HO
H2N
O
(i)
(ii)
F
FmocHN
HO
1) DIC, NMI, DMF, RT, 12 hrs
2) 20% piperidine in DMF, RT, 20 min
NH2
HN
(iii)

Figure III.1. Schematic representation of a fluorine labelled Phenylalanine coupled to the polymer surface. (i) 10:90-PEGMA-co-PMMA surface with free –OH groups (ii) surface with β-alanine, providing the NH_2-groups for the next coupling (iii) Pentafluoro-L-phenylanlanine marker coupled to the surface.

The composition of the PEGMA-co-PMMA layer obtained was verified via XPS. Table 1 shows the binding energies at which the C 1s region peaks were observed. Figure III.2 depicts the quantitative analysis of the C 1s region of the 10:90-PEGMA-co-PMMA film. The experimentally determined $C_{C=O}$:C_{C-O}:C_{C-C} peak area ratio is 1:2:3 and is in good agreement with theoretical ratio of 1:1.8:3. The pentafluorophenyl alanine bound to the polymer resulted in a distinct F 1s signal in the XPS spectrum (Figure III.3). The F 1s signal is used as a marker to test the time resolved stability of the peptides on the 10:90-PEGMA-co-PMMA surface, when incubated in PBS-T.

Table 1. The C 1s region of 10:90-PEGMA-co-PMMA film on silicon wafer

C1s region	Binding energy [eV]
$C_{C-C;}$ C_{C-H}	285.0
$C_{C-O;}$ C_{C-N}	286.5
$C_{O=C-O}$; $C_{O=C-N}$	288.8

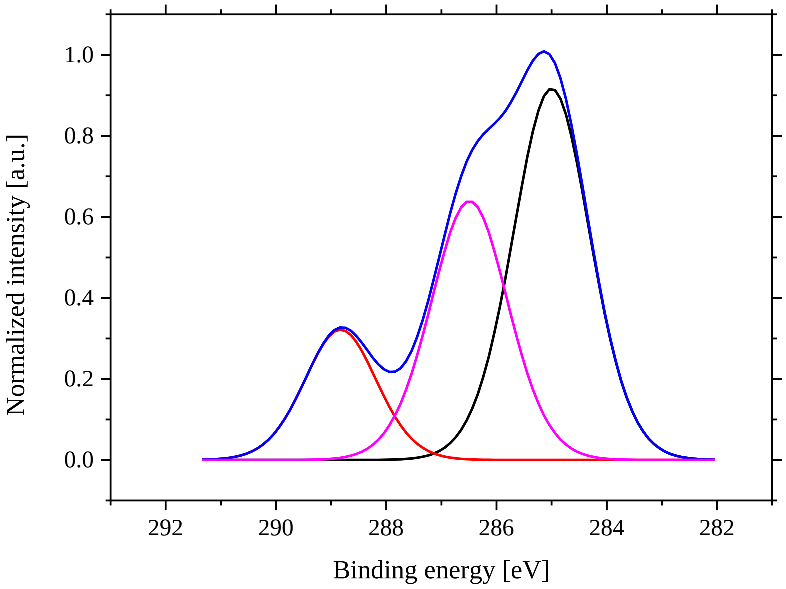

Figure III.2. C 1s region in the XPS spectrum of the 10:90-PEGMA-co-PMMA polymer film on a silicon wafer. The polymer should result in a $C_{C=O}$:C_{C-O}:C_{C-C} peak ratio of 1:1.8:3. The experimental ratio of 1:2:3 is in good agreement. The small variations in the composition can be caused by variations in the PEGMA side-chain length which contains 3-5 ethylene glycol units basing on the number average of the molecular weight.

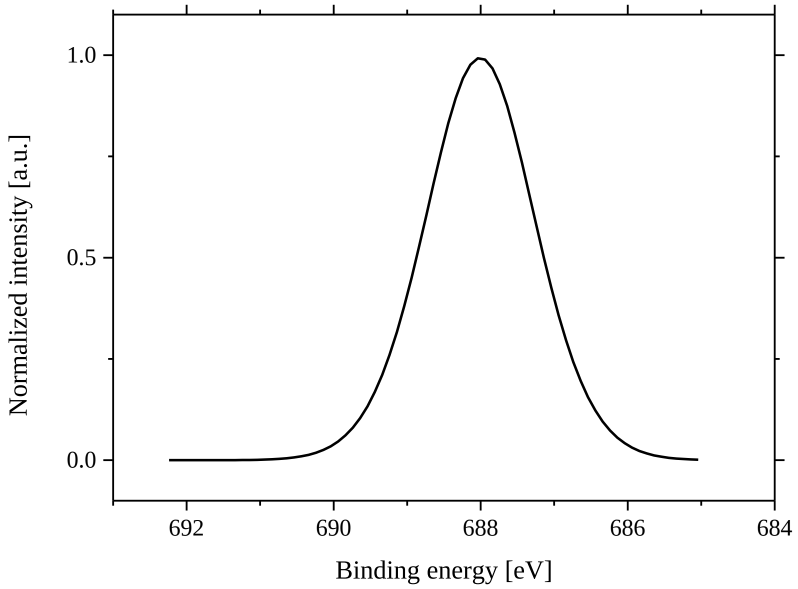

Figure III.3. F 1s region in the XPS spectrum of the 10:90-PEGMA-co-PMMA polymer film on a silicon wafer.

To determine the stability of the peptide bound to the polymer, the F 1s signal was quantitatively analyzed after exposing the wafer to PBS-T. The silicon wafer was cut into five small pieces and the pieces were incubated in PBS-T for 0,1,2,3 and 4 days respectively. After the specified time, the pieces were taken out of the PBS-T solution, washed with milli-Q water to remove the buffer salts and possible cleavage products and were dried under a stream of argon. A XPS measurement was done for each of the samples, to measure the amount of fluorine on the sample. Each sample was measured at three different locations and the final reading is an average of the three readings. All the readings were normalized so that the data from the five samples can be compared.

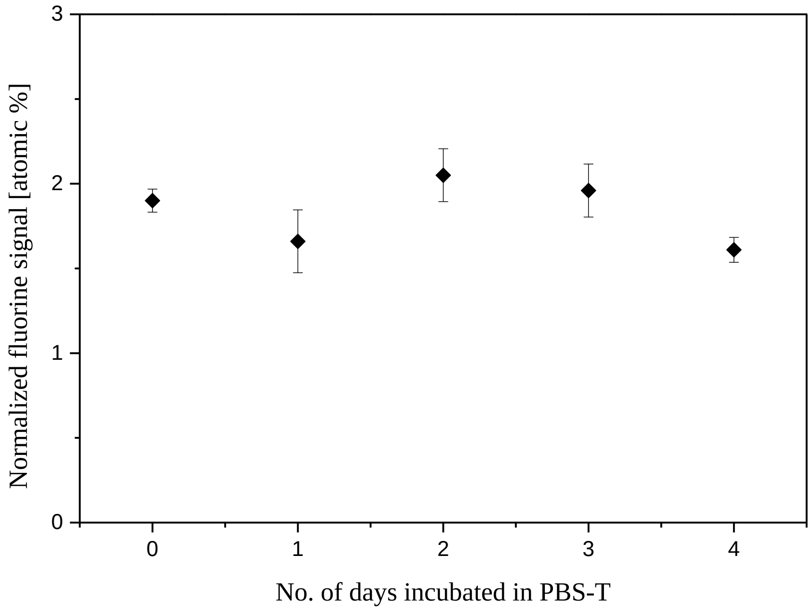

Figure III.4. Trend of the normalized fluorine concentration on the silicon wafer over time on incubation in PBS-T. Each measurement is an average of three measurements and all the measurements were normalized for comparison.

From the Figure III.4 it can be noted that the concentration of fluorine on the surface remains relatively constant within the error range of 10 % of the instrument. No significant decrease in the fluorine signal due to the incubation of samples in PBS-T was observed. This measurement indicates that the arrays can withstand the PBS-T conditions (at least for 4 days) without any inherent damage.

III.1.2. Labelling of peptide arrays

The next step in the screening was to identify a suitable fluorophore which can be used to label the peptide arrays. Two scanners (*Genepix 4000B microarray scanner* and *Odyssey LICOR Infrared imaging system*) were available during the course of this work (see Table 2), which made a compatible label mandatory.

Table 2. Possibilities of scanners, their corresponding wavelengths and highest resolutions.

Scanner	Excitation wavelengths (nm)	Resolution possible
Genepix 4000B	532 635	21µm
Odyssey infrared imaging system	700 800	5µm

It is necessary to label the peptide array before deprotecting the side chains, otherwise the side chains of the amino acids in the peptide sequence will be labelled along with the *N*-terminal end of the peptide. Therefore, the dyes need to be resistant to the TFA, which is used for side chain deprotection. Based on these criteria, three different dyes were chosen which are compatible with the scanners and resistant to the TFA (see Table 3).

Table 3. Dyes and the corresponding compatible scanners

Dye	Scanner	Excitation wavelength (nm)
5(6)-carboxytetramethylrhodamine (TAMRA)	Genepix 4000B	532
DyLight 680	Odyssey	700
DyLight 800	Odyssey	800

Three similar peptide arrays with side chains protected were labelled at the *N*-terminal amino group with *N*-Hydroxysuccinimide (NHS) ester derivatives of the above dyes (see section V.3.1). After labelling, the side chains were deprotected using TFA (see section V.3.3). The labelled arrays were scanned before and after deprotection to verify the stability of the dyes under TFA conditions (see Figure III.5, Figure III.6 and Figure III.7).

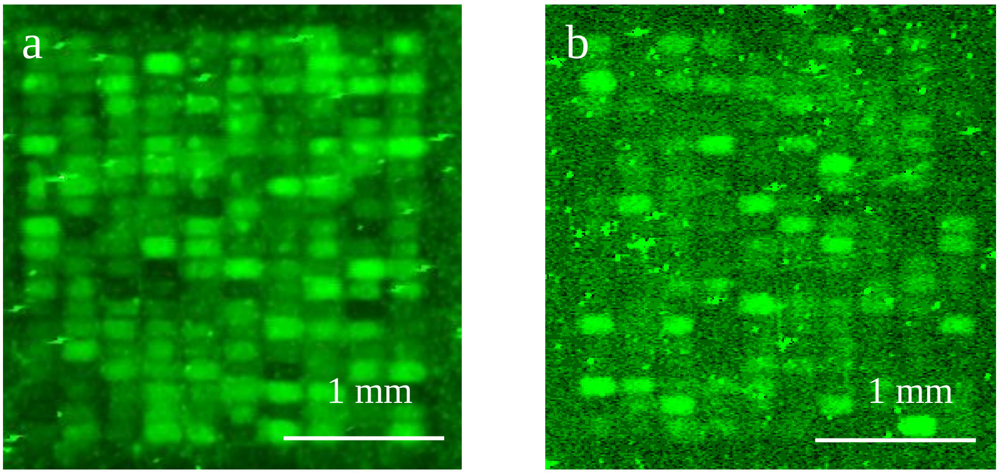

Figure III.5. Peptide array labelled with DyLight 800 NHS ester a) before TFA treatment b) after TFA treatment. Images acquired using Odyssey Infrared Imager at 800 nm excitation wavelength.

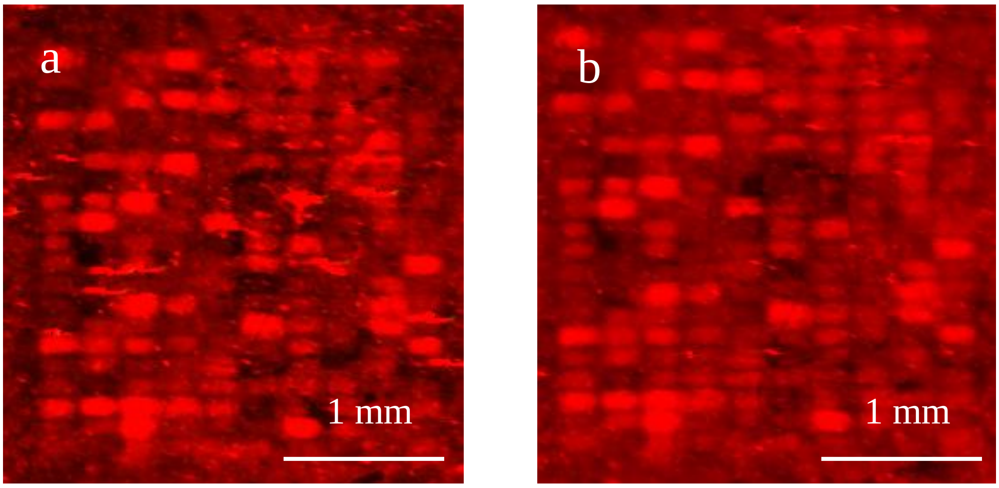

Figure III.6. Peptide array labelled with DyLight 680 NHS ester a) before TFA treatment b) after TFA treatment. Images acquired using Odyssey Infrared Imager at 700 nm excitation wavelength.

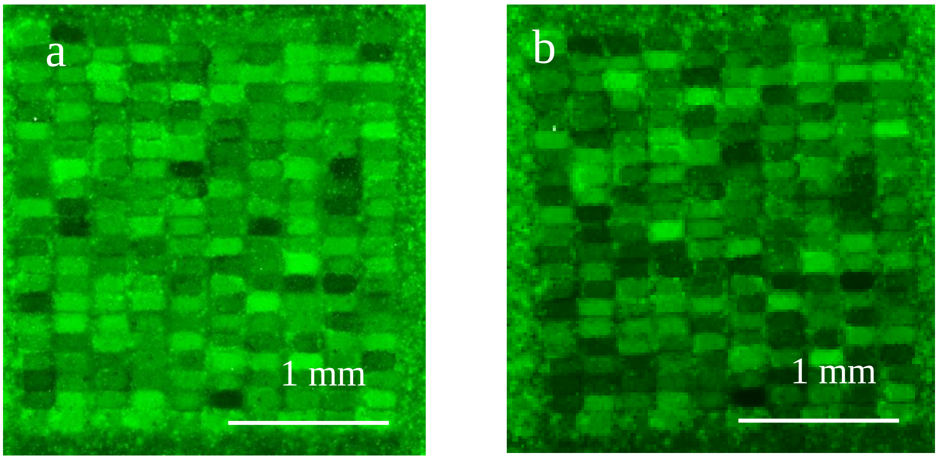

Figure III.7. Peptide array labelled with TAMRA-NHS ester a) before TFA treatment b) after TFA treatment**.** Images acquired using Genepix 4000B scanner at 532 nm excitation wavelength.

The difference in the pattern of fluorescence of the spots before and after TFA treatment is due to different amount of peptides per spot. In peptide synthesis, yield of a peptide depends on the peptide sequence, therefore, all the peptide spots in an array vary in the amount of peptides. The relative intensity of the spots also changed after the side chain deprotection because the dye was quenched by the protecting groups of the different amino acids. Once the protecting groups were removed the quenching effect was eliminated, resulting in change in pattern of fluorescence.

From the fluorescence images (Figure III.5, Figure III.6, Figure III.7), it can be noted that all the three dyes are resistant to the TFA which was used for deprotecting the side chains. However, the quality of the images acquired with the Genepix 4000B scanner was much better than the Odyssey scanner. The Genepix 4000B scanner also exhibited a good signal to noise ratio. Therefore, TAMRA was selected for labelling the peptide arrays.

III.1.2.1. Labelling with Fmoc-Lysine(5/6)-TAMRA)-OH

As mentioned in the previous section, labelling with TAMRA was optimal for this work. In principal, there were two ways to introduce the dye. One approach was to use the TAMRA-NHS ester which can react with the free amino group at the *N*-terminus of the peptide. The other approach was to couple a fluorescently labeled amino acid to the peptide. Fmoc-Lys(5/6-TAMRA)-OH was commercially available and can be coupled to the peptide array using DIC/NMI chemistry. Fmoc-Lys (5/6-TAMRA)-OH was chosen considering that the amino acid can be converted into an OPfp ester, embedded into the toner particles and can be used directly during production of peptide arrays using laser printer. This enables the introduction of the fluorescently labelled amino acid at different positions within the peptides. Therefore, coupling of the fluorescently labelled lysine was preferred over TAMRA-NHS ester labelling.

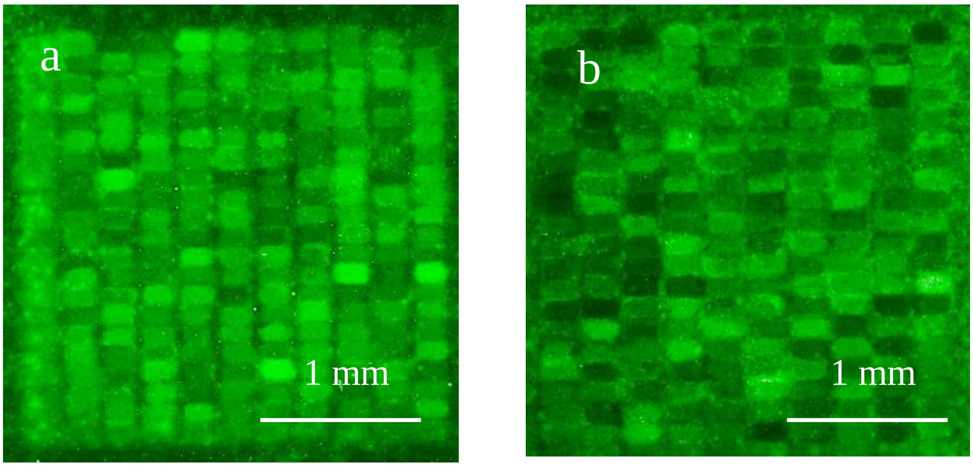

Figure III.8. Peptide array labelled with Fmoc-Lys (5/6-TAMRA)-OH; a) before TFA b) after TFA**.** Images acquired using Genepix 4000B scanner at 532 nm excitation wavelength.

From the Figure III.8 it can be noted that the labelling of the peptide array with Fmoc-Lys (5/6-TAMRA)-OH was successful (see section V.3.2). The fluorescent label remained fluorescent after TFA treatment.

III.1.3. First screen

The principle of the first screen is based on the self-digestion character of the peptidases. Peptides having “proteolytic” properties should cleave each other, resulting in the loss of peptides, which can be monitored by the decrease of fluorescence intensity within labelled peptide spots.

A peptide array with random peptides (containing mostly the amino acids from the catalytic triad-serine, histidine, aspartate, cysteine, glutamate and lysine) was chosen for the primary screen. Each peptide sequence was in double spots to ensure that the data was not affected by artefacts.

Every peptide sequence consists of two glycines (‘GG’) in the middle of the sequence. The goal of the introduction of this ‘GG’ linker is to provide flexibility for the peptides so that they have chance to bend and form secondary structures if possible. The three dimensional structure of an enzyme is determined in part by the flexibility of the protein which in turn is based on the amino acids. Of the 20 natural amino acids, glycine, which is found in most of the beta hair pin loops, plays an extraordinary role in making the local peptide structure flexible by providing high flexibility.

The array was labelled with the fluorescent amino acid, Fmoc-Lys (5/6-TAMRA)-OH, by coupling it to the N-terminal end of the peptide sequence using DIC/NMI (see section V.3.2). After the removal of Fmoc-group (see section V.3.13), the side chains were deprotected using TFA (see section V.3.3). The array was incubated in PBS-T for 12 hours followed by washing of the array thoroughly with milli-Q water to remove buffer salts and possible cleavage products. After every step, the array was scanned using a Genepix 4000B scanner. The parameters of all the scans were kept constant so that the scans could be compared to the track of the changes in the fluorescent intensity of the spots. The fluorescent images obtained before and after the PBS-T incubation were analyzed using the PepAnalyzer software.

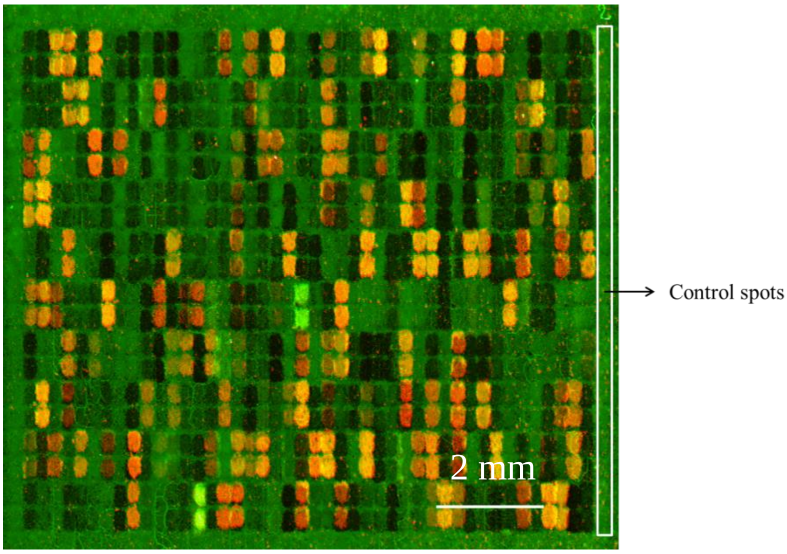

Figure III.9. One part of the array used in the first screen. Each peptide spot was given a color code based on the amount of fluorescence lost. The dark red spots indicate that the loss of fluorescence is higher when compared to the bright yellow spots. A frame of HA and FLAG epitopes was taken as control.

In the first screen 2,000 peptides were analyzed, 3.35% of the peptides lost >95% of the fluorescence. From the Table 4, it can be noted more than half of the peptides lost >50% of initial fluorescence.

Table 4. Summary of the fluorescence lost by the labelled peptides after incubation in PBS-T buffer. In total 2,000 peptides were screened in an array format.

Loss of fluorescence (%)	Peptides which lost fluorescence (%)
>95%	3.35%
>90%	15.65%
>80%	36.35%
>70%	49.85%
>60%	58.95%
>50%	65.50%

Summary

In the first screen significant number of peptides (65.50%) lost more than half of the initial fluorescence. This loss of fluorescence suggests the possibility of proteolytic activity in the peptide arrays. However, the loss of fluorescence might also be due to some unknown artefacts. To find out the actual reason for the loss of fluorescence further experiments were conducted. The peptide sequences which lost > 90% of fluorescence were taken and further screenings were done. The details of the screenings conducted are given in Figure III.10.

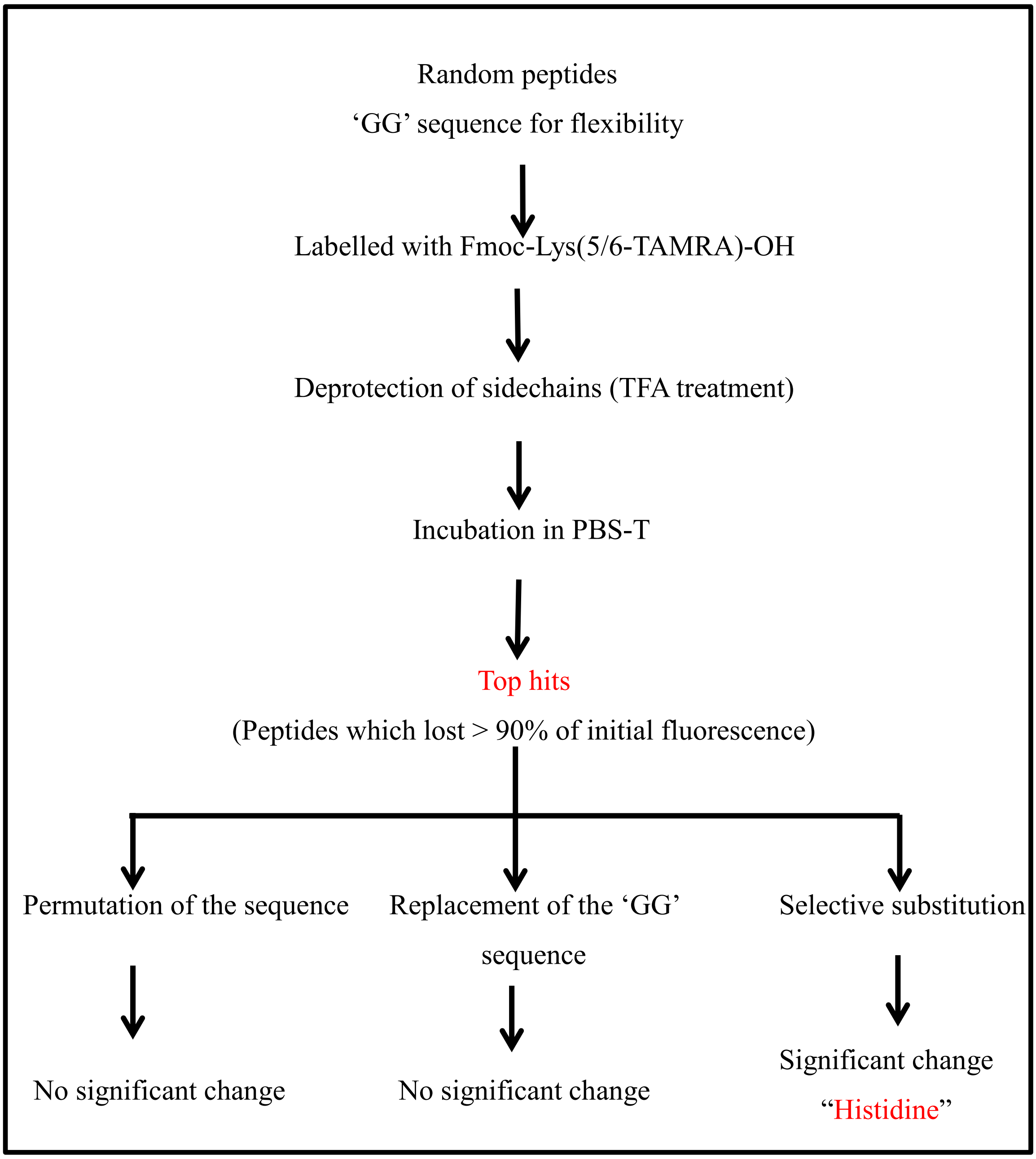
Random peptides
'GG' sequence for flexibility
Labelled with Fmoc-Lys(5/6-TAMRA)-OH
Deprotection of sidechains (TFA treatment)
Incubation in PBS-T
Top hits
(Peptides which lost > 90% of initial fluorescence)
Permutation of the sequence
Replacement of the 'GG' sequence
Selective substitution
No significant change
No significant change
Significant change
"Histidine"

Figure III.10. Flow chart indicating the further experiments carried out after the first screen. All the screens were carried out under similar conditions and the data of each screen was analyzed using the PepAnalyzer software.

III.1.3.1. Permutation of the sequences of top peptide hits

In proteases, few amino acids which are part of the catalytic site play crucial role in the proteolytic activity.[58, 80] Replacing a particular amino acid involved in the catalytic activity result in the decrease or loss of the protease activity.[81] In order to distinguish artifacts from real proteolytic activity, the peptides which lost > 90% of fluorescence from the previous digestion assay were permutated at each position by exchanging every amino acid in the sequence with the 19 other amino acids. The array was labelled and incubated in PBS-T similar to the previous assay. All the peptide spots lost fluorescence irrespective of the amino acid replaced. After the data analysis, it was evident that none of the amino acid was solely responsible for the observed loss of fluorescence and no specific proteolytic motif could be identified.

III.1.3.2. Replacement of the ‘GG’ sequence

All the peptides in the first screen had a glycine-glycine (GG) sequence in the middle to impart flexibility to the peptides. In order to study if the ‘GG’ sequence had any role in the loss of fluorescence, a new array was designed with the peptides which lost > 90% fluorescence in the first screen. In the peptide sequences of this array the two glycines were replaced with a combination of different amino acids and the screen was repeated. All the peptides lost fluorescence indicating that ‘GG’ sequence did not play any role in the loss of fluorescence in the first screen.

III.1.3.3. Selective substitution

The assay conducted with arrays of permutated peptides (III.1.3.1) suggested that the activity showed by the peptides is not due to a single amino acid. However every peptide in the array contained more than one amino acid related to the catalytic triad. For example, a peptide sequence, DWDSSGGCWHHVSCS, which showed 99% decrease in fluorescence intensity, contains 4 serine, two histidine and 2 aspartic acids. During the permutations of the peptides if only one of the histidines is replaced, the un-replaced histidine might still be able to participate in the proteolytic activity. In order to verify if the total removal of the catalytic triad amino acids would cause any effect, another array was designed. This array consisted of peptide sequences which lost > 90% fluorescence during the first assay. However, instead of permutating the sequences as was done in section III.1.3.1, in this array all the copies of a particular amino acid in a peptide sequence were replaced with neutral and similarly charged amino acid (Table 5).

Table 5. Amino acids which were selectively substituted. A, G - neutral amino acids; R,K,E,C,T,Y – amino acids with similar charge as the replaced parent amino acid.

Parent amino acid	Replaced with
H	A,R,K,
D	G,E,K
S	A,C,T,Y

Table 6. Selective substitutions. In this example all the histidines in the sequence are replaced with neutral (A) and similarly charged (R,K) amino acids.

Parent sequence	DWDSSGGCWHHVSCS
‘H’ replaced with ‘A’	DWDSSGGCWAAVSCS
‘H’ replaced with ‘R’	DWDSSGGCWRRVSCS
‘H’ replaced with ‘K’	DWDSSGGCWKKVSCS

Table 6 depicts the example of the selective substitution done at Histidine positions in a peptide sequence. The array with the selected substitutions was labelled followed by incubation in PBS-T.

After the analysis of the results it was noted that none of the substitutions had significant effect on the decrease of fluorescence signal expect for Histidine. All the peptides in which histidines were replaced with other amino acids (A/R/K/W), showed no significant decrease in the fluorescence intensity (Figure III.11). This might be an indication for the importance of histidine in the mechanism of decrease of fluorescence.

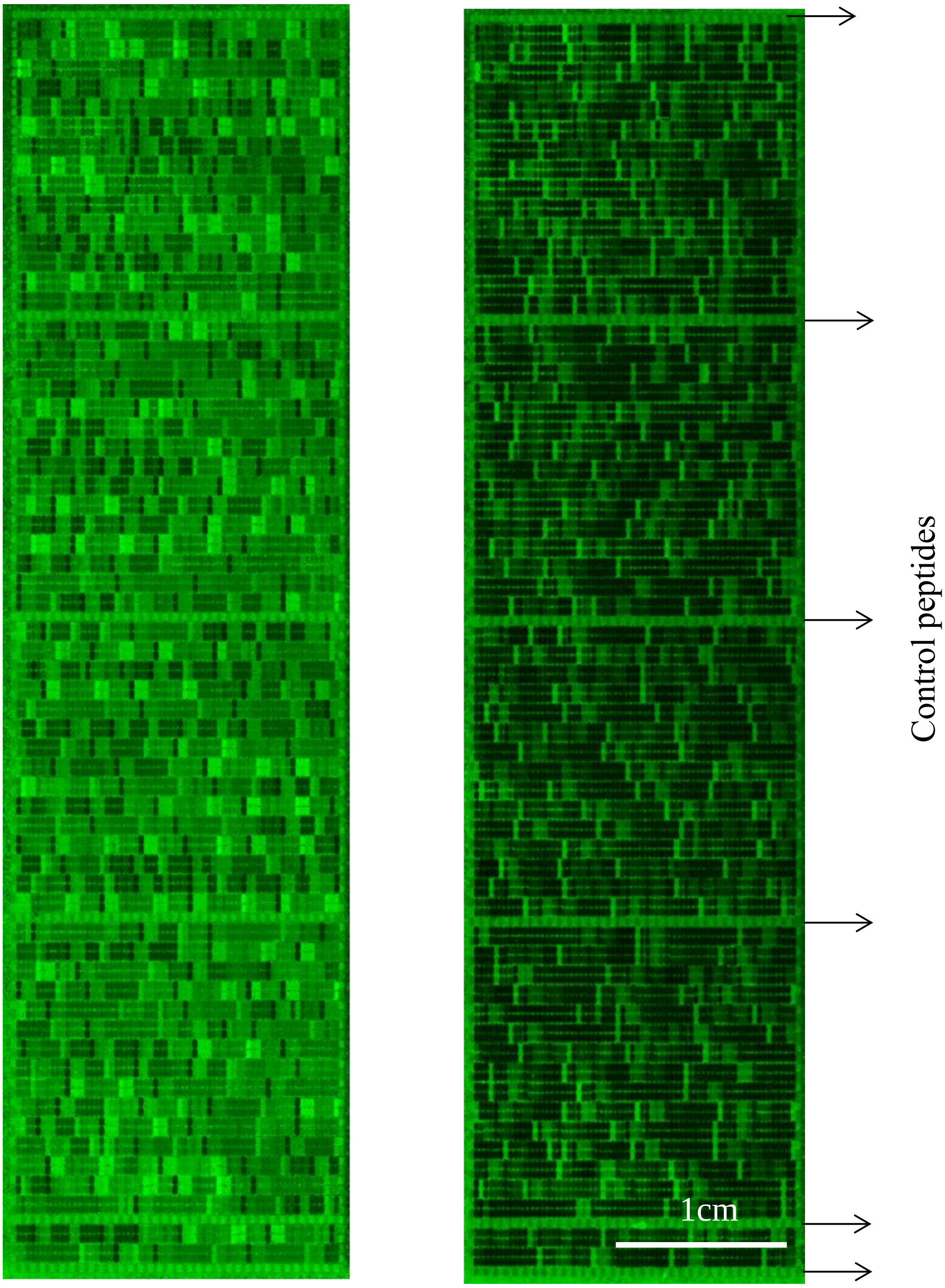

Figure III.11. Peptide array labelled with Fmoc-Lys (5/6-TAMRA)-OH a) before PBS-T incubation b) after PBS-T incubation. The spots which retained fluorescence after incubation in PBS-T (all the green spots except the control spots in the right picture) are the peptide spots in which all the histidines in the sequence are replaced with other amino acids.

III.1.3.4. Quenching by tryptophan

During the labelling of the peptide arrays it was noticed that some peptide spots are darker when compared to other peptide spots. Initially this low fluorescence was attributed to the low peptide concentration in the spot due to different yields during the synthesis. However, upon closer investigation, it was noticed that this low fluorescence follows a trend related to the tryptophan position in the respective peptide. If a tryptophan was present at the *C*-terminal end of the sequence, the quenching was more pronounced and as the tryptophan position moved towards the *N*-terminal end, the quenching decreased (see Figure III.12).

Table 7. The trend of fluorescence quenching based on position of tryptophan in the peptide sequence. Dark fields equal low fluorescence. The quenching due to tryptophan increased from top-left to the bottom-right. The peptide sequence shown in the table is one of the sequences from Figure III.12**.** A1-*C*-terminus of the peptide, A15-*N*-terminus of the peptide.

N-terminus												C-terminus		
A15	A14	A13	A12	A11	A10	A9	A8	A7	A6	A5	A4	A3	A2	A1
W	H	K	L	V	F	F	A	E	D	V	G	S	N	K
H	W	K	L	V	F	F	A	E	D	V	G	S	N	K
H	K	W	L	V	F	F	A	E	D	V	G	S	N	K
H	K	L	W	V	F	F	A	E	D	V	G	S	N	K
H	K	L	V	W	F	F	A	E	D	V	G	S	N	K
H	K	L	V	F	W	F	A	E	D	V	G	S	N	K
H	K	L	V	F	F	W	A	E	D	V	G	S	N	K
H	K	L	V	F	F	A	W	E	D	V	G	S	N	K
H	K	L	V	F	F	A	E	W	D	V	G	S	N	K
H	K	L	V	F	F	A	E	D	W	V	G	S	N	K
H	K	L	V	F	F	A	E	D	V	W	G	S	N	K
H	K	L	V	F	F	A	E	D	V	G	W	S	N	K
H	K	L	V	F	F	A	E	D	V	G	S	W	N	K
H	K	L	V	F	F	A	E	D	V	G	S	N	W	K
H	K	L	V	F	F	A	E	D	V	G	S	N	K	W

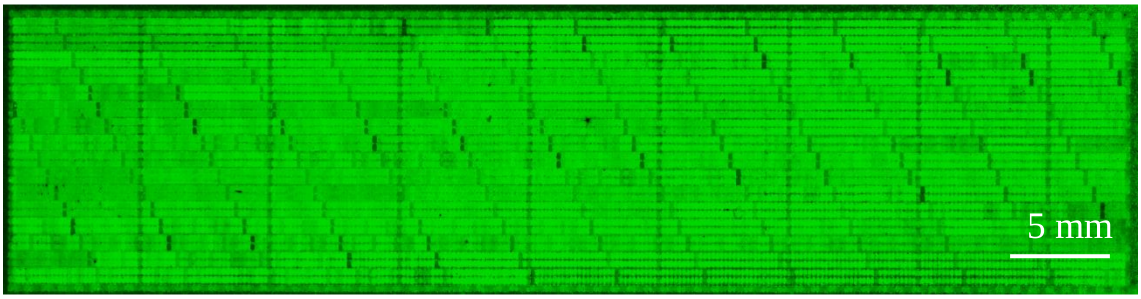

Figure III.12. Quenching effect due to tryptophan. The array was labelled with Lysine-TAMRA, followed by side chain deprotection. The image was acquired with Genepix 4000 B scanner at an excitation wavelength 532 nm. The ladder-like structures are formed due to the quenching effect caused by tryptophan at various positions in the sequence.

As the tryptophan position moved from the *N*-terminal to the *C*-terminal end of the peptide, the fluorescently labelled peptide spots got darker suggesting that the quenching phenomenon observed was linked to the distance between tryptophan and the fluorophore (Table 7).

Fluorescence quenching, that is the non-radiative relaxation of an electronically excited state, can be caused by a variety of processes including internal conversion, intersystem crossing, molecular collision, energy transfer, and electron transfer. Förster resonance energy transfer (FRET) and photoinduced electron transfer (PET) are two mechanisms that lead to variation of fluorescence emission by distance-dependent fluorescence quenching between a fluorophore and a quenching moiety.[82-83]

FRET is a long range fluorescence quenching mechanism where the donor and acceptor can effectively quench each other at Forster distance which is typically in the ranges of 2-8 nm.[84-85]

$$E = \frac{R_0^{\;6}}{R_0^{\;6} + r_0^{\;6}}$$

Equation 5. Forster equation to calculate the quenching efficiency of the fluorophore. *E* is the transfer effieiciency, R_0 is Förster distance, r_0 is distance between the fluorophore and the quencher.

The transfer efficiency (*E*) should decrease as the distance between the fluorophore and the quencher decreases(r). As the transfer efficiency (*E*) decreases the quenching decreases.

However, from the Figure III.12, it is evident that this is not the case. On the contrary, the quenching increases as the distance between tryptophan and the TAMRA increases. Moreover, for FRET to take place, the absorption spectrum of the acceptor (tryptophan) should overlap with the emission spectrum of the donor (TAMRA). Tryptophan has an absorption maximum at around 280 nm, whereas TAMRA has an emission maximum at around 575 nm, this rules out the possibility of quenching of TAMRA by tryptophan due to FRET.

Another possibility of the quenching is by photoinduced electron transfer, which requires contact formation (van der Waals contact) between the fluorophore and the quencher.[82] However, the fluorophore and the quencher were further away when the quenching was observed.

It is essential to study and understand various factors which can affect fluorescent signals as the same fluorescent signal loss was used as the basis for this assay. Therefore, in order to investigate the effect caused by tryptophan on the fluorescence further experiments were conducted.

Quenching due to tryptophan

Tyrptophan has been used to measure fluorescence fluctuations in peptides at a single-molecule level. The fluorescence of the excited fluorophore (e.g. an oxazine derivative dye (MR121)), was efficiently quenched by tryptophan upon contact formation.[86] This method has been used to determine the conformational changes in a peptide or a protein molecule by labelling a peptide with a fluorophore at one terminus and a tryptophan at the other terminus, when the peptide changes conformation and folds bringing the tryptophan and the fluorophore together, it results in quenching due to the photoinduced electron transfer (PET). The same phenomenon of fluorophore quenching by tryptophan was employed in developing a sensitive protease assay.[87] In this assay a fluorophore was coupled to one end of a peptide and tryptophan to the other end of the peptide. In solution, the flexibility of the peptide back bone leads to conformations in which the fluorophore and the tryptophan residue come into contact. This contact enables photoinduced electron transfer resulting in quenching. In the presence of a protease, the peptide is cleaved in the middle preventing contact formation due to conformations. Thus, the fluorescence intensity of the fluorophore increases signifying the presence of protease in solution (Figure III.13).

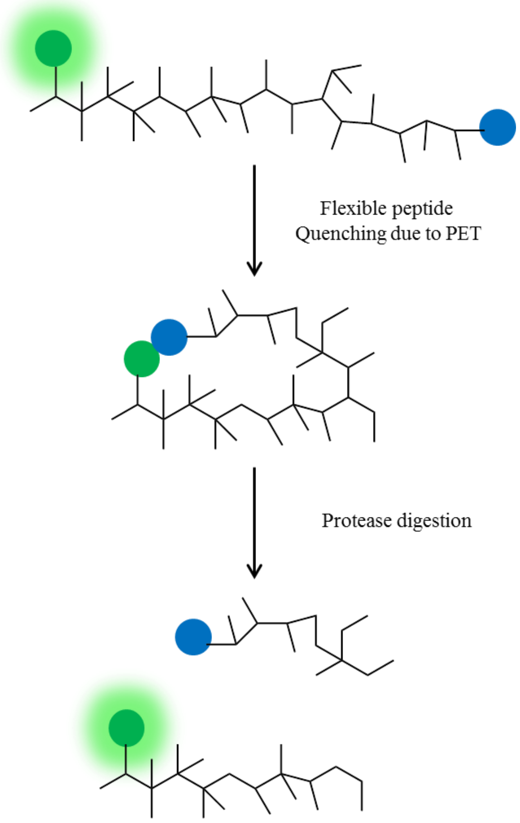

Figure III.13. Quenching of a peptide with fluorophore and tryptophan. Green moiety – fluorophore; blue moiety – tryptophan.

Many reports and findings were put forward regarding quenching due to PET in solution. However, the effect of dye quenching in peptide arrays which is a totally different system compared to quenching in solution is not studied thoroughly. In order to verify if the same photoinduced electron transfer is the reason for the quenching observed in the peptide arrays due to tryptophan, an experiment was conducted. As the quenching observed in the peptide arrays appeared to be related to the distance between the fluorophore and the tryptophan, three peptides having similar sequences but with varied distances between the fluorophore and tryptophan were used in the experiments.

Each 16meric peptide consisted of

- A fluorphore near *C*-terminus

- A tryptophan near *N*-terminus
- An arginine in the middle as cleavage site for trypsin
- A cysteine at the *N*-terminus

Cysteine was introduced at the *N*-terminal end of the peptide so that the peptide can be bound to a maleimide functionalized solid support via the thiol group of cysteine.

Table 8. Peptides used in the digestion experiments. Z = Lys(5/6-TAMRA)-fluorophore, the three peptides have varied distance between fluorophore and tryptophan**.**

	Peptide sequence	Distance between fluorophore and tryptophan (W)
PW-1	CGSAZSNRVEAGIILW	10 amino acids
PW-2	CGSAZSNRVEAGIWIL	8 amino acids
PW-3	CGSAZSNRVEAWGIIL	6 amino acids

From here on these three peptides will be mentioned as ‘PW-peptides’.

Two experiments were performed to identify the cause of the quenching due to tryptophan

1) Digestion of PW-peptides in solution.
2) Digestion of PW-peptides bound to a surface.

Digestion of PW-peptides in solution

Peptides were digested using trypsin in a black-96 well plate. Each well was filled with the appropriate peptide solutions and trypsin in PBS-T was added to the respective wells. As a control, to equal number of wells containing peptides, PBS-T was added without trypsin. As soon as the addition was complete, the fluorescence measurement was started. The measurement was performed using a microplate reader, TECAN infinite 200. The gain of fluorescence was monitored overnight by measuring fluorescence in 10 min intervals (see section V.3.4).

All the peptides had high initial fluorescence intensity suggesting that quenching was unlikely. It can be noted that none of the three peptides showed any gain of fluorescence on trypsin digestion irrespective of the distance between the fluorophore and the quencher (see Figure III.14). This suggests that the quenching observed in the array was not distance related.

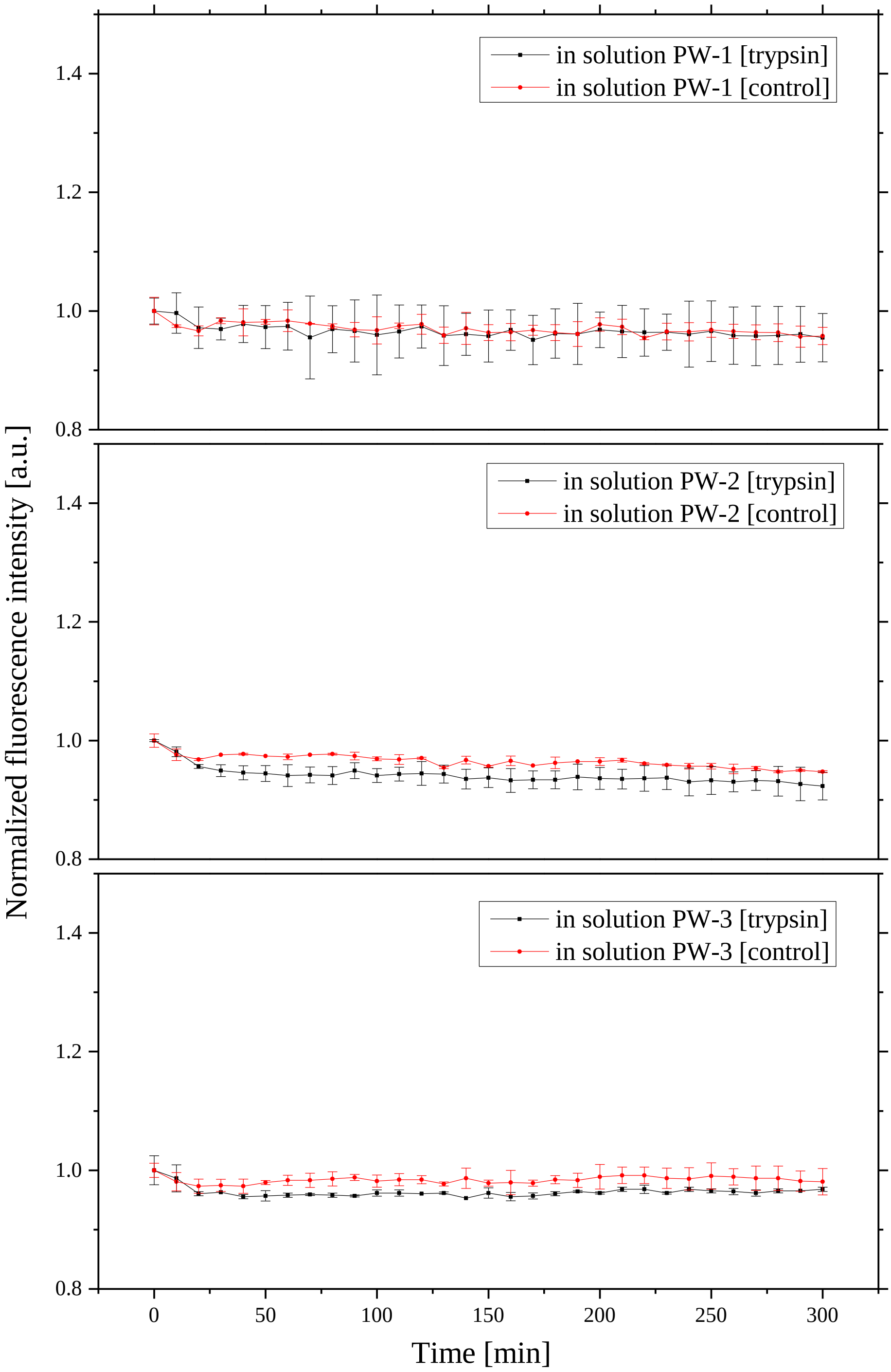

Figure III.14. Digestion of PW-peptides in solution with trypsin. The distance between the fluorophore and tryptophan is 10 amino acids in PW-1, 8 amino acids in PW-2 and 6 amino acids in PW-3. None of the three PW-peptides gained fluorescence on trypsin digestion, suggesting that there was no quenching due to tryptophan.

Digestion of PW-peptides bound to a surface

In order to study if immobilization of peptides has any effect on the quenching of the fluorophore by the tryptophan, the digestion experiment was repeated after binding the peptides to a maleimide coated black 96-well plate. The peptides were bound to the well plate via the *N*-terminus cysteine (-SH side chain). Maleimides react with free sulfhydryl group(s) forming stable thioether linkages (see Figure III.15).

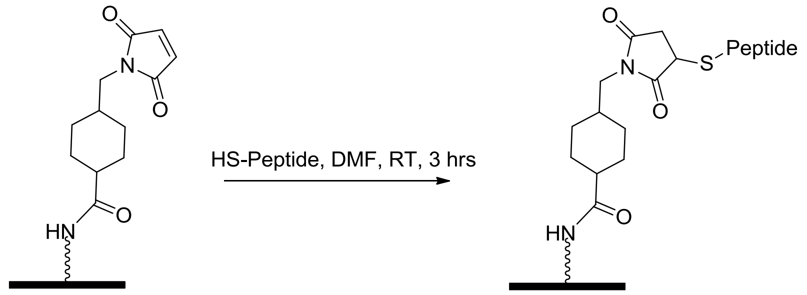

Figure III.15. Binding of a peptide with cysteine (thiol side chain) to a maleimide coated surface.

The peptides were bound to the maleimide well plate over night at 4 ^{o}C. The free maleimide groups to which the peptides did not bind were blocked using cysteine. HCl. After the blocking, trypsin digestion was carried out by adding trypsin to the respective wells. PBS-T was added to an equal number of wells as control. As soon as the addition was done the fluorescent measurements were performed using a microplate well reader, TECAN infinite 200 (see section V.3.5).

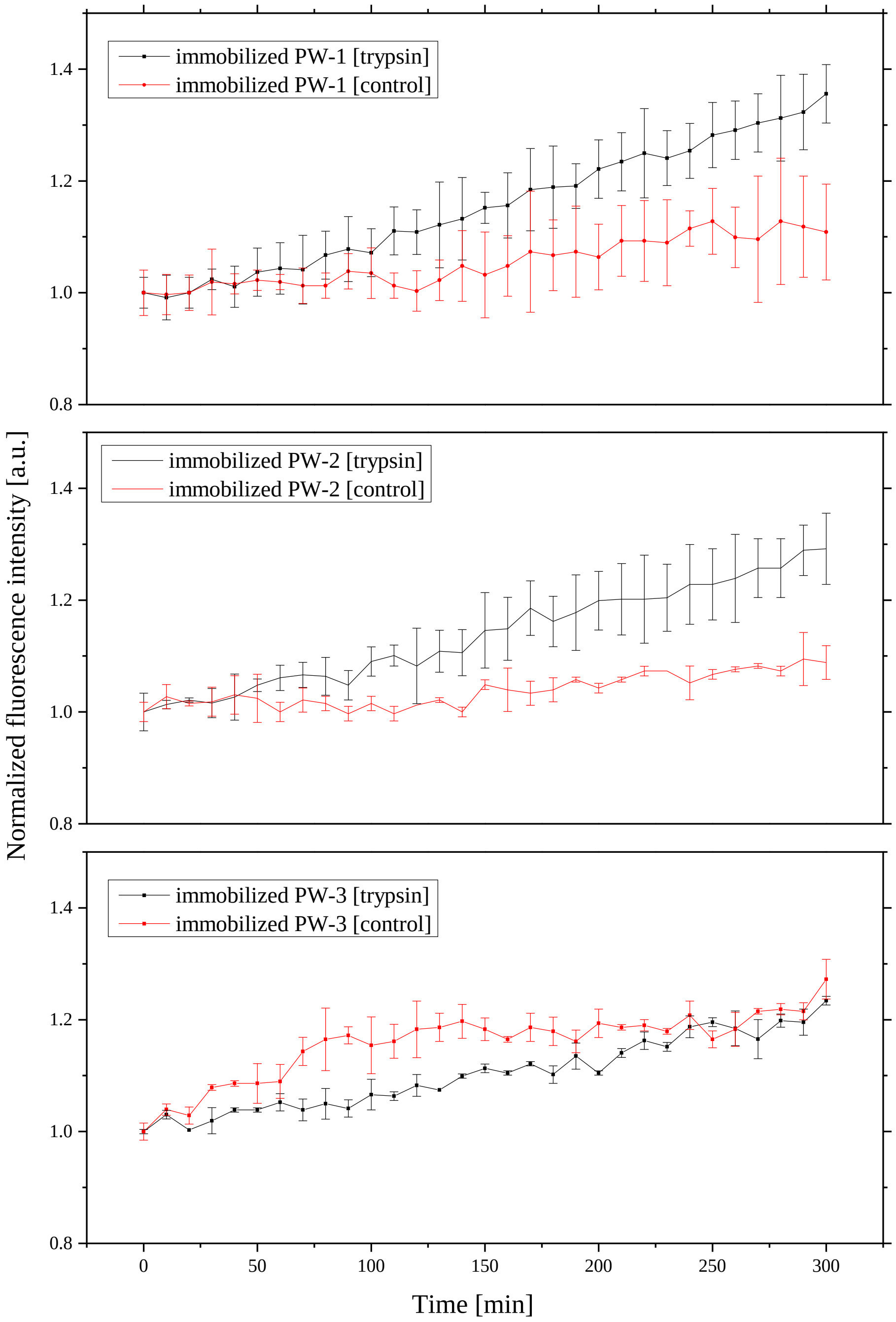

Figure III.16. Digestion of PW-peptides bound on a surface with trypsin. The distance between the fluorophore and tryptophan is 10 amino acids in PW-1, 8 amino acids in PW-2 and 6 amino acids in PW-3. In peptides PW-1 and PW-2 trypsin digestion resulted in an increase of fluorescence intensity.

From Figure III.16, it can be noted that the peptides PW-1 and PW-2 gained fluorescence on digestion with trypsin. No gain of fluorescence was noticed in the case of PW-3 peptide. One reason for this might be that the trypsin was not able to reach the cleavage site due to steric hindrance caused by the short distance between the fluorophore and the tryptophan. Nevertheless, the gain in fluorescence in the PW-1 and PW-2 peptides suggests that there might be quenching of the fluorophore by the tryptophan before the digestion of the peptides.

III.1.3.5. Conclusion of the quenching effect due to tryptophan

In order to understand the quenching effect of tryptophan (located near the *C*-terminus of a peptide) on the fluorophore (located near the *N*-terminus of a peptide) two different digestion experiments were conducted. Three peptides with varied distance between the tryptophan and the fluorophore were digested using trypsin. One set of digestion was done in solution where the peptides can have free movement in solution. The other set of digestion was done after binding the peptides to a surface, thereby restricting the movement of the peptides.

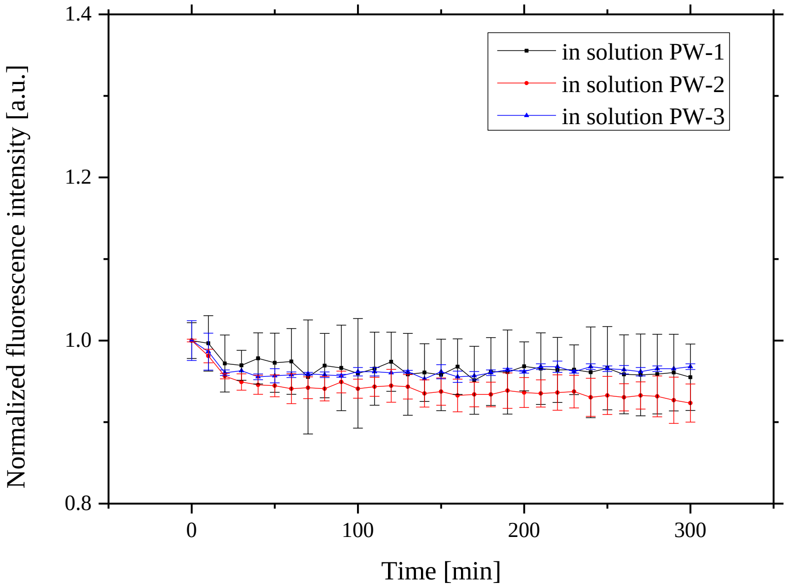

Figure III.17. Comparison of net gain of fluorescence intensity by PW-peptides in solution when digested with trypsin. None of the three peptides showed an increase in fluorescence indicating the absence of quenching of fluorophore by the tryptophan.

From Figure III.17 it can be noted that none of the peptides (PW-1, PW-2 andPW-3) gained fluorescence during digestion with trypsin in solution. This suggests that the fluorophore is not quenched by the tryptophan before digestion, therefore, after digestion there is no sign of increase in fluorescence.

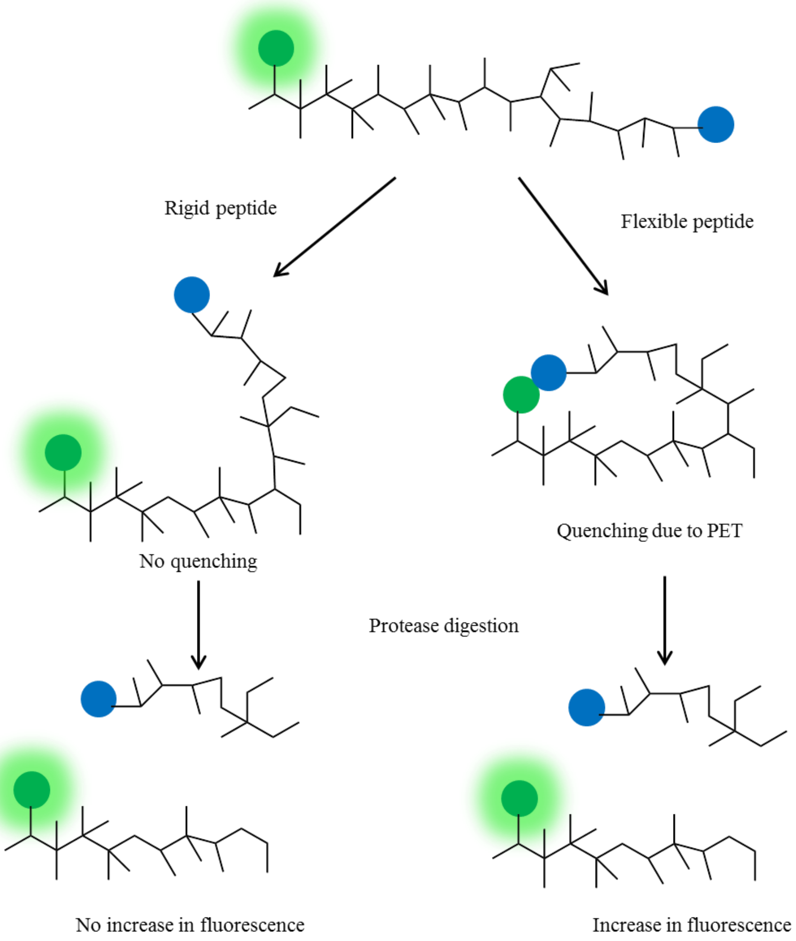
Rigid peptide
Flexible peptide
No quenching
Quenching due to PET
Protease digestion
No increase in fluorescence
Increase in fluorescence

Figure III.18. Diagrammatic representation of a peptide with fluorophore (green) near one end and tryptophan (brown) near the other end. In the right side scheme, the fluorophore on the peptide is quenched by the tryptophan due to PET, this occurred due to the contact between the fluorophore and the tryptophan due to the flexibility of the peptide. On the left side of the scheme, on the occasion of the rigid peptide the fluorophore and the tryptophan cannot come in to contact, therefore no quenching is observed.

When in solution the peptide is in equilibrium with its possible conformations that can lead to two possibilities (Figure III.18).

1) The peptide is flexible enough to bring the fluorophore and quencher into contact resulting in quenching of the fluorophore by tryptophan due to PET.

2) The peptide is rigid and cannot bring the flurophore and the tryptophan together, therefore no quenching of the fluorophore takes place.

In the first scenario, when the peptides are digested with a protease, the fluorophore and the quencher get separated and the tryptophan can no longer quench the fluorophore, resulting in an increase of fluorescence.[87] In the second scenario, the protease digestion results in the separation of fluorophore and quencher similar to the first scenario. However, even before the digestion, the fluorophore is not quenched by the tryptophan therefore the digestion and separation of the fluorophore and the tryptophan does not result in increase of fluorescence. From Figure III.17 it can be noted that there was no quenching before digestion, suggesting that the peptides might not have been flexible enough for the tryptophan and the fluorophore to get into contact resulting in quenching due to PET.

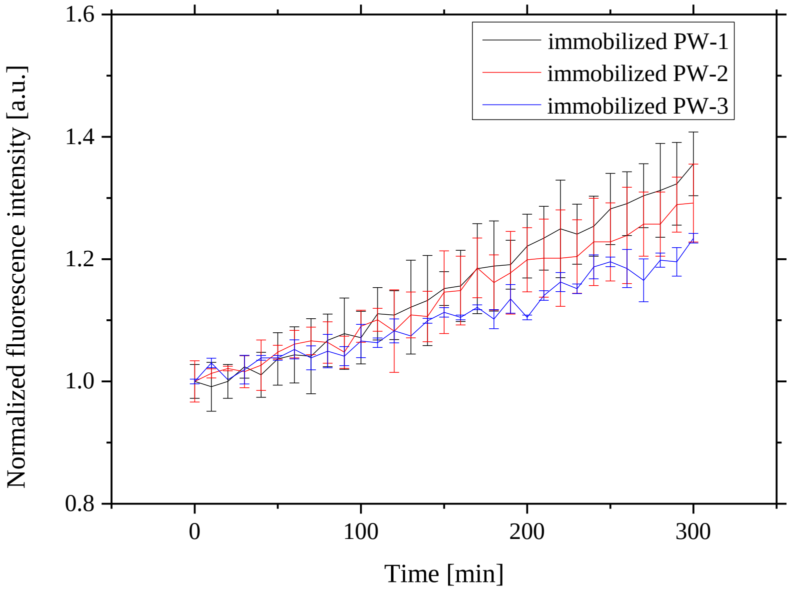

Figure III.19. Comparison of net gain in fluorescence intensity by peptides PW-1, PW-2, PW-3 bound to a surface on digestion with trypsin.

From the Figure III.19 it can be noted that peptides PW peptides when bound to a surface gained fluorescence after trypsin treatment. On the other hand, the same peptides did not gain fluorescence when digested in solution. This suggests that when peptides were bound to a surface the tryptophan quenched the fluorophore to some extent. One possible reason for this could be intermolecular quenching. When in solution the peptides have a high degree of freedom and the molecules are in equilibrium. However, when the peptides are bound to a three dimensional polymer network, the movement is restricted, thereby increasing the chances of intermolecular quenching (Figure III.20)

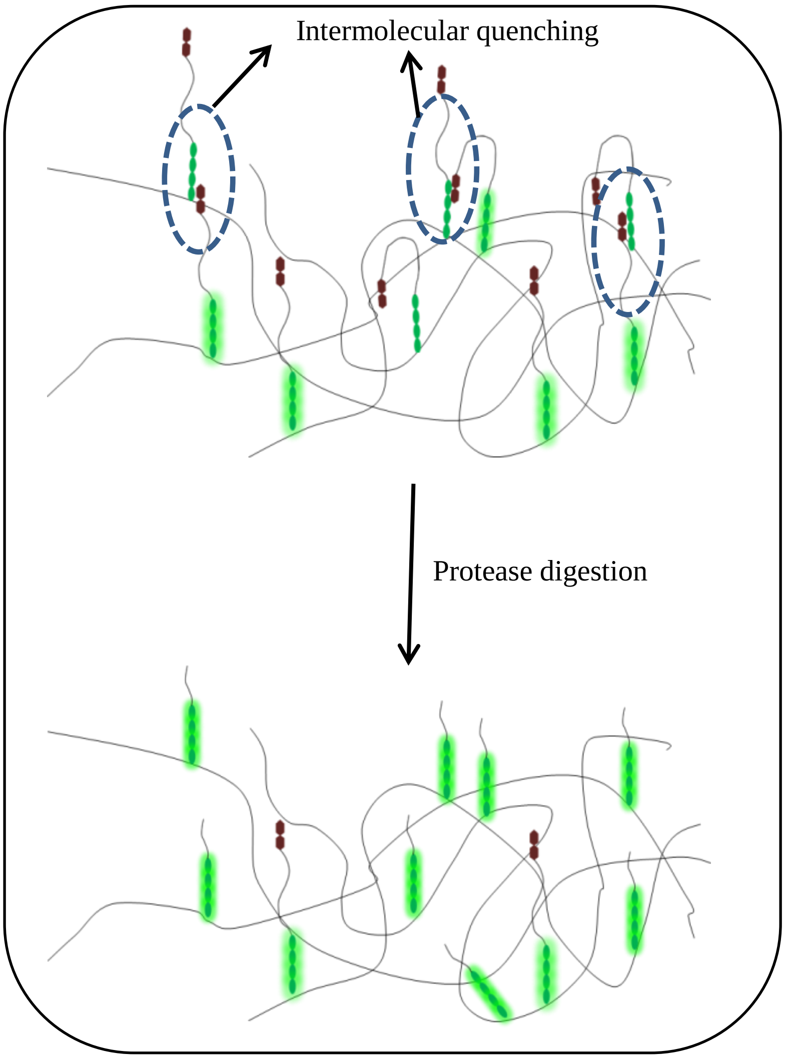

Figure III.20. Phenomenon of intermolecular quenching of fluorophore (green) by tryptophan (brown) when peptides are bound to a polymer network on surface. The fluorophore on a peptide is quenched by a tryptophan from an adjacent peptide resulting in intermolecular quenching. On trypsin digestion the tryptophan leaves the polymer leaving behind the fluorophore resulting in an increase of fluorescence.

When the peptides are bound to a surface, the movement of the peptides is restricted (opposed to the free movement when peptides are in solution). The possibility of intermolecular quenching is high as the peptides are immobilized. On digestion with trypsin, the tryptophan leaves the polymer resulting in gain of fluorescence by the fluorophore.

The quenching of fluorophore by 'W' observed in bound (PW) peptides gives an insight into the quenching phenomenon observed in the peptide arrays. During the synthesis of the peptide arrays (from the *C*-terminal to the *N*-terminal) the amount of coupled amino acid decreases. For example, in a peptide sequence 'NH_2-HKLVFFAEDVGSNKW-COOH' the amount of tryptophan coupled at the *C*-terminal end of the peptide is more when compared to the amount of histidine coupled at the *N*-terminal. When the peptide array is labelled at the *N*-terminal, the amount of fluorophore is relatively in low amounts when compared to the tryptophan. Therefore, in the 3D polymer network, the fluorophore which is positioned at the *N*-terminal is surrounded by excessive amount of tryptophan from the adjacent peptides resulting in intermolecular quenching by photoinduced electron transfer (Figure III.21).

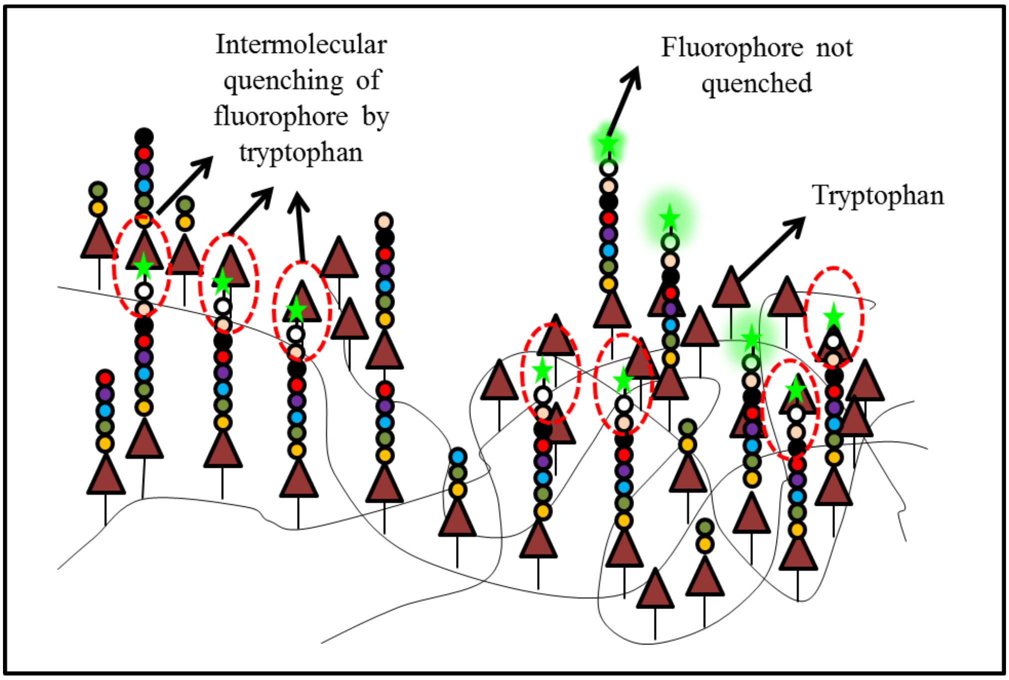

Figure III.21. Intermolecular quenching of the fluorophore by the tryptophan – observed in peptide arrays. In a 3D polymer network the fluorphore on the N-terminus of a peptide is quenched by tryptophan on an adjacent peptide resulting in intermolecular quenching.

Therefore, the quenching of fluorophore by tryptophan noticed during the labelling of peptide arrays is possibly related to the amount of tryptophan in the array rather than the distance between the fluorophore and the tryptophan.

III.1.4. Drawbacks of the first screening process

The first screen developed to identify peptides with proteolytic characters in a peptide array was based on the measuring the decrease in fluorescence intensity of the individual peptide spots after incubating the peptide array in PBS-T buffer. However, the loss of fluorescence intensity was caused by many other factors (e.g. quenching) not just proteolytic activity. Intermolecular quenching of the fluorophore by tryptophan due to PET is another drawback of the screening. All the peptide sequences exhibited quenching to some extent depending on the position of the tryptophan. Excluding the tryptophan totally from the entire peptide array sequences is not ideal when screening random peptide arrays. In this screen the peptide arrays were labelled by coupling a fluorophore to the NH_2 group at the *N*-terminal end of the peptide sequence. This results in modifying the properties of the peptide. Minimum chemical modification of the peptides is favorable so as not to change the properties.[87] Peptides are embedded in a 3D polymer network, where a cloud of functional groups is created due to the side chains of the various amino acids from the adjacent peptides. Therefore, the properties exhibited in the peptide arrays during the screens might not have been due to individual peptides but were rather due to this cloud environment (cloud effect), which was rich of all the catalytic triad amino acids. Due to all these drawbacks, the first screening method was discarded and a new screening method was developed.

III.2. Second screening strategy

Considering all the shortcomings noticed in the first screen, the second screen was developed taking into account the following points:

1) The screen should be done by employing peptide arrays without modifying the properties of peptides – no coupling of fluorophore to the peptide array.
2) Peptides in the array should be cleaved so that they can move freely in solution during the assay – this minimizes the cloud effect (see section 0).
3) If a peptide possesses proteolytic activity, the screening signal should be gain of fluorescence intensity – during the first screening strategy loss of fluorescence resulted in false positive signals due to quenching, a gain in fluorescence is a much more reliable way to identify a real proteolytic activity.
4) An independent reporter surface that facilitates a gain in fluorescence intensity on detection of proteolytic activity would be ideal.

Cleaving of the peptide array from the synthesis slide

Instead of conducting the screening while the peptides in the array are bound to the surface (creating a cloud environment with closely packed amino acid side chains from neighboring peptides), it is preferable to carry out the screen with peptides which are cleaved from the array and have the freedom to move in solution. The screening was designed in a way that each peptide spot represents a small reaction unit which allows peptides to be in solution. The peptide array can be cleaved from the synthesis surface by incubating the slide under dry ammonia vapor. In the presence of ammonia the ester bond which is the link between the peptides and the polymer support will be cleaved thus releasing the peptides.

A schematic representation of the whole screen for proteolytic activity detection applying these mandatory prerequisites is shown in Figure III.22.

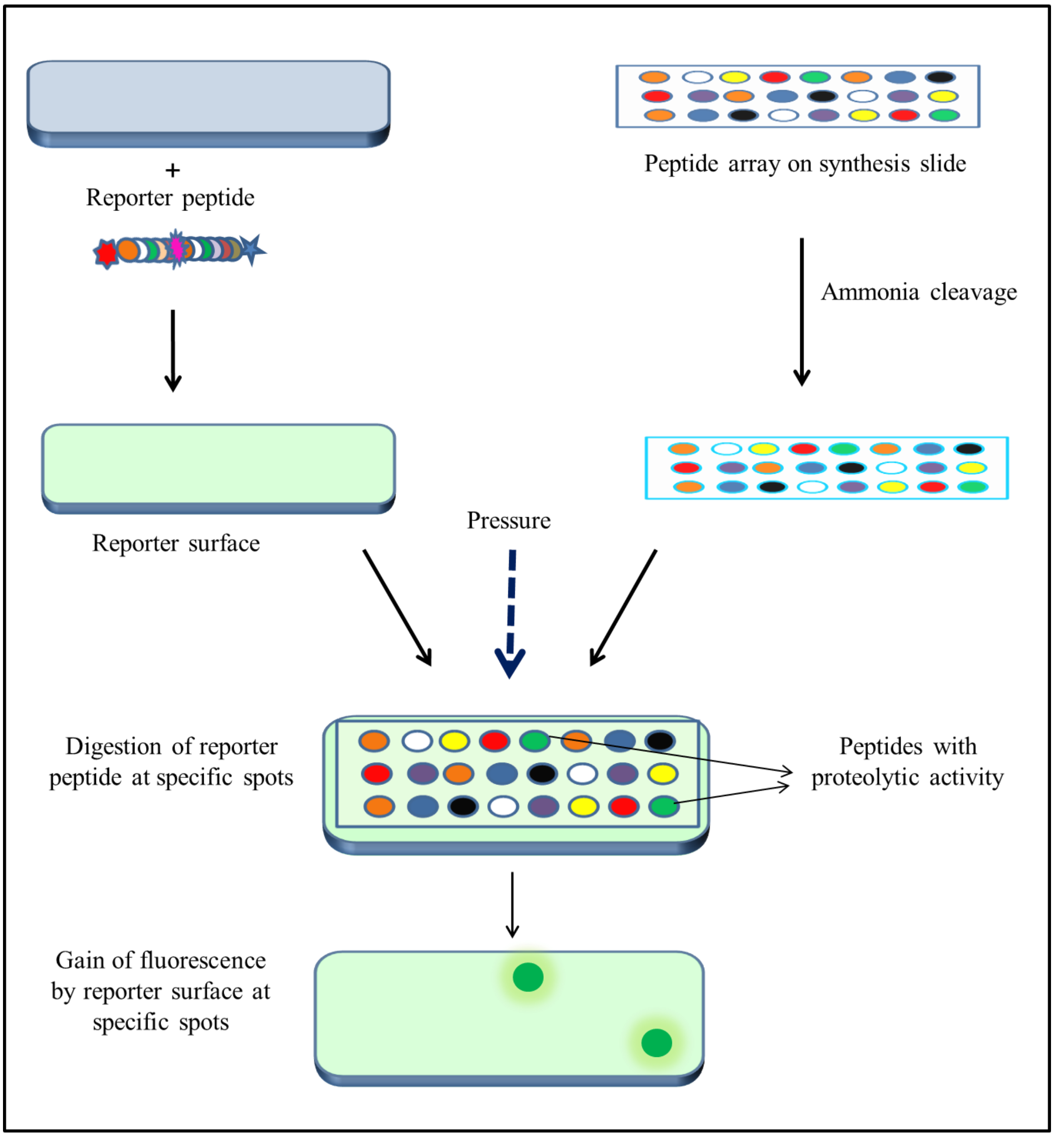
+
Reporter peptide
Peptide array on synthesis slide
Ammonia cleavage
Reporter surface
Pressure
Digestion of reporter peptide at specific spots
Peptides with proteolytic activity
Gain of fluorescence by reporter surface at specific spots

Figure III.22. Schematic representation of the second screening for detection of a peptide with proteolytic activity in a peptide array format.

The central idea in the second screening assay was to develop an independent reporter surface which can interact with a proteolytic peptide in a peptide array and can gain fluorescence on detection of proteolytic activity. In order to achieve the aim, the following were needed.

a) Design of a suitable reporter peptide
b) Design of a suitable surface to bind the reporter peptide. The surface should be compatible with the proteolysis, in order not to repel the potential proteolytic candidates from the surface.

III.2.1. Design of a reporter peptide

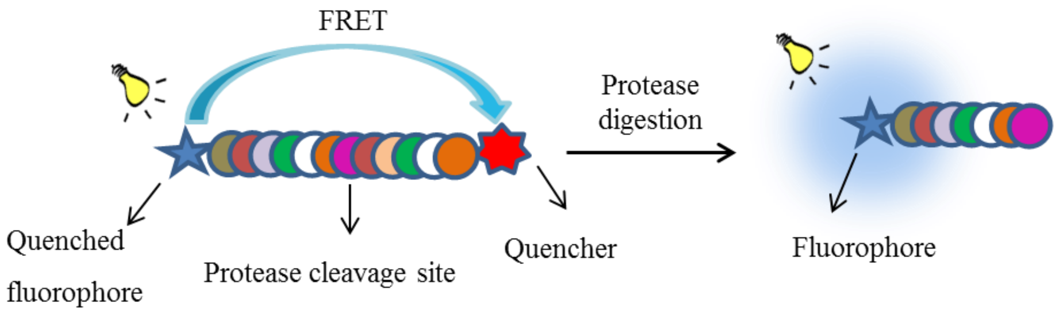

Figure III.23. Diagrammatic representation of a Reporter Peptide. A reporter peptide contains a fluorophore and a quencher placed at an optimal distance for the Förster resonance energy transfer (FRET). Due to FRET the fluorophore is quenched by the quencher. When a protease cleaves the peptide, separating the quencher from the fluorophore, the fluorescence of the fluorophore is restored.

A reporter peptide, which can gain fluorescence upon detection of proteolytic activity, was designed, thus eliminating the problems related to quenching during the screening process. The reporter peptide was designed based on a phenomenon named 'Förster resonance energy transfer (FRET)'.

The theory of FRET was developed by Förster in the late 1940's and have been used in various fields of biology such as in protein research, real time monitoring of bio-chemical reaction in in-vivo studies.[82-85, 87-92] FRET is a non-radiative transfer of excitation energy between a donor molecule and an acceptor molecule, and it can occur if the emission spectrum of the donor overlaps with the absorption spectrum of the acceptor molecule (Figure III.24). When the vibronic transitions of the donor have the same energy as the corresponding transitions in the acceptor molecule, the transitions are in resonance and thus the name 'Resonance Energy Transfer'.

The efficiency of quenching due to the resonance energy transfer depends on the distance between the fluorophore and the quencher. Förster calculated the efficiency of the resonance energy transfer based on Equation 6.

$$E = \frac{R_0^{\,6}}{R_0^{\,6} + r_0^{\,6}}$$

Equation 6. Forster equation. *E* is the efficiency of the resonance energy transfer, R_0 is Förster distance, r_0 is the distance between the fluorophore and the quencher. R_0 is the distance at which the energy transfer efficiency is 50%.

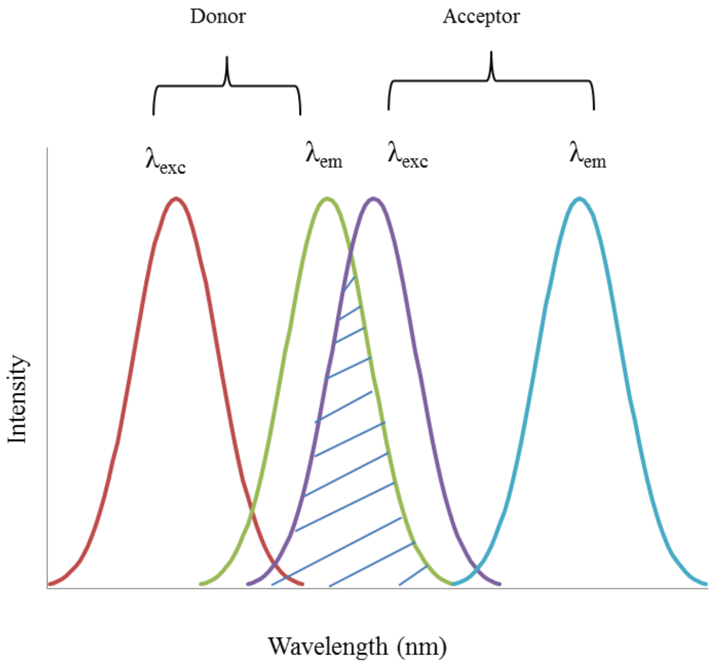

Figure III.24. The absorption and emission spectra of donor and acceptor. The emission spectrum of the donor should overlap with the absorption spectrum of the acceptor for an efficient Resonance energy transfer (FRET).

Different combinations of fluorophore and quencher were considered and finally TAMRA was selected as a fluorophore (donor with inherent fluorescence) and TQ3 as a quencher (acceptor). The absorption spectrum of the TQ3 quencher overlaps with the emission spectrum of the fluorophore (TAMRA) making the pair suitable for FRET experiments (Table 9). TQ3 is a dark quencher which absorbs the energy from the excited fluorophore (donor) and emits the energy as heat instead of as fluorescence (which is typical for fluorescent quencher).

Table 9. Excitation and emission wavelengths of the fluorophore (TAMRA) and quencher (TQ3).

	Excitation (nm)	Emission (nm)
TAMRA	~549	~577
TQ3	~570	-

According to Equation 6, as the distance between the fluorophore (TAMRA) and the quencher (TQ3) increases, the quenching efficiency decreases. The distance between the quencher and fluorophore, should not be too small (as this might affect the accessibility of the cleavage site by the protease due to steric hindrance) or too large (as this might lead to incomplete quenching of the fluorophore by quencher). Therefore, the distance between the fluorophore and quencher should be optimized as such that both the quenching efficiency and the rate of cleavage by the protease are optimal.

In order to find the optimal distance between the fluorophore and the quencher, four 15mer peptides with a fluorophore and a quencher placed at varied distances were tested (see Table 10). The sequence of the peptide was selected at random with enough polar amino acids, in order not to make the peptide too hydrophobic. The peptide sequence was designed so that it has the following characters

1) A cysteine at the N-terminus – for binding the peptide to a surface via a linker.
2) A glycine spacer after cysteine.
3) An arginine in the middle of the sequence as cleavage site for trypsin

Table 10. List of reporter peptides and the corresponding distance between the fluorophore and the quencher.

Reporter peptide code	Sequence	Distance between 'Z' and 'X'
RP-1	CGZSALEVRALYAXAG	10
RP-2	CGSAZLEVRALYAXAG	8
RP-3	CGSAZLEVRALXYAAG	6
RP-4	CGSAZLEVRXALYAAG	4

Z = Fmoc-Lys(5/6-TAMRA)-OH -------- Fluorophore

X = Fmoc-Lys(TQ3)-OH) -------- Quencher

From here on, these four peptides will be referred to as reporter peptides (RP).

III.2.1.1. Digestion of reporter peptide candidates in solution

In order to verify the cleavage of the reporter peptides by trypsin, the digestion was tested in solution. The peptides were digested in a black 96-well plate. Each peptide was received as HPLC-purified product. The well plate was filled with appropriate reporter peptide solutions and trypsin in PBS-T was added to the respective wells. To equal number of wells pure PBS-T was added as control experiment (see section V.3.4).

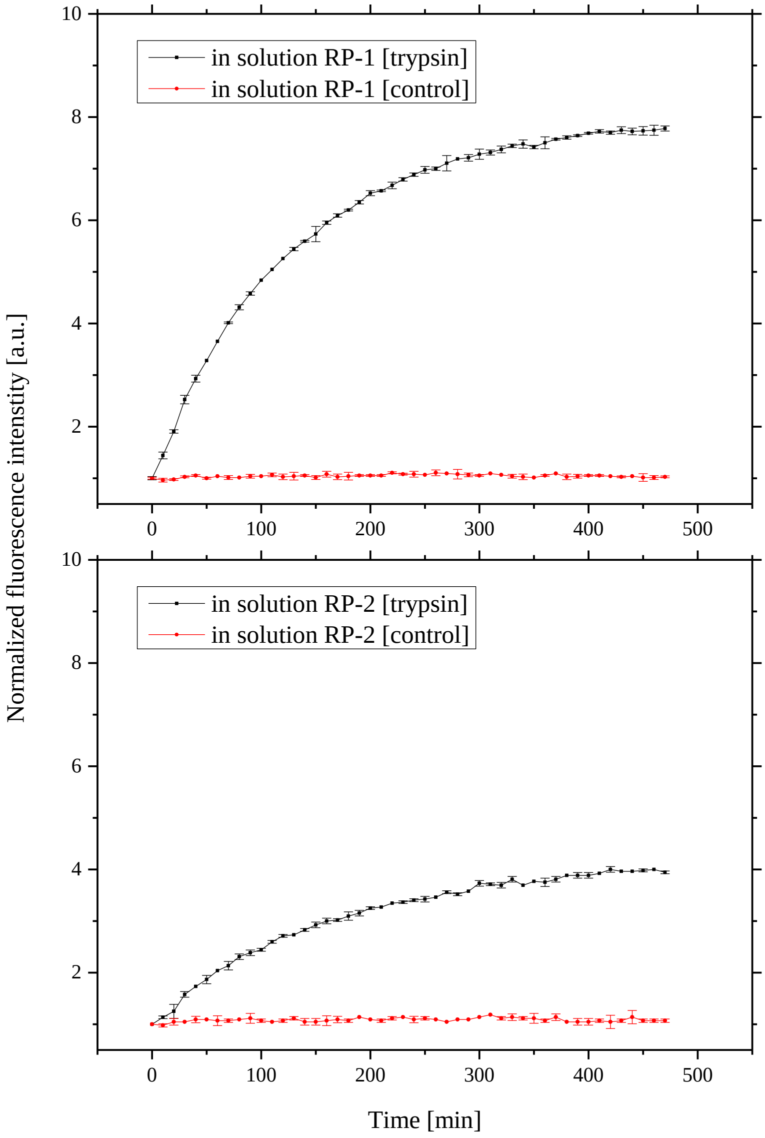

Figure III.25. Gain of fluorescence by RP-1 and RP-2 over time on digestion with trypsin. RP-1 has 10 amino acids between the fluorophore and the quencher whereas RP-2 has 8 amino acids.

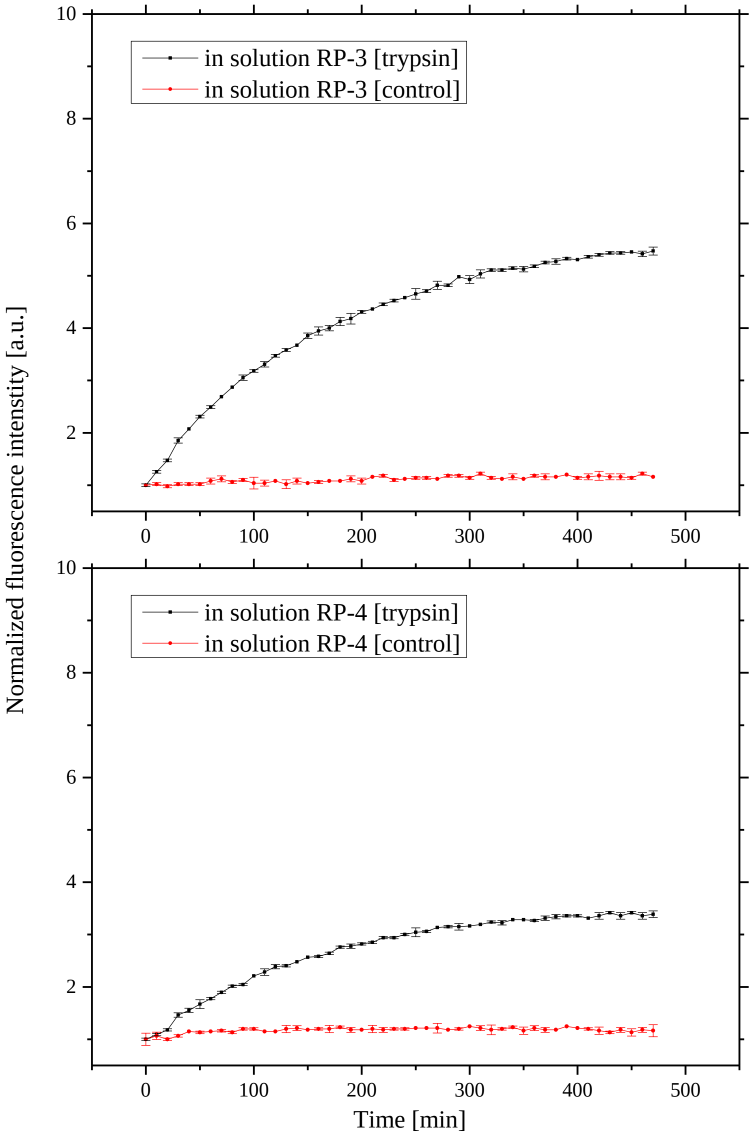

Figure III.26. Gain of fluorescence by RP-3 and RP-4 in solution over time on digestion with trypsin . RP-3 has 6 amino acids between the fluorophore and the quencher whereas RP-4 has 4 amino acids.

From Figure III.25 and Figure III.26, it can be noted that all four reporter peptides gained fluorescence over time upon digestion with trypsin. This indicates that both cleavage and separation of the quencher from the peptides were successful.

Table 11. Average initial fluorescence of reporter peptides.

Reporter peptide	Distance between fluorophore and quencher	Average initial fluorescence (a.u.)
RP-1	10 amino acids	43
RP-2	8 amino acids	26
RP-3	6 amino acids	27.5
RP-4	4 amino acids	33.5

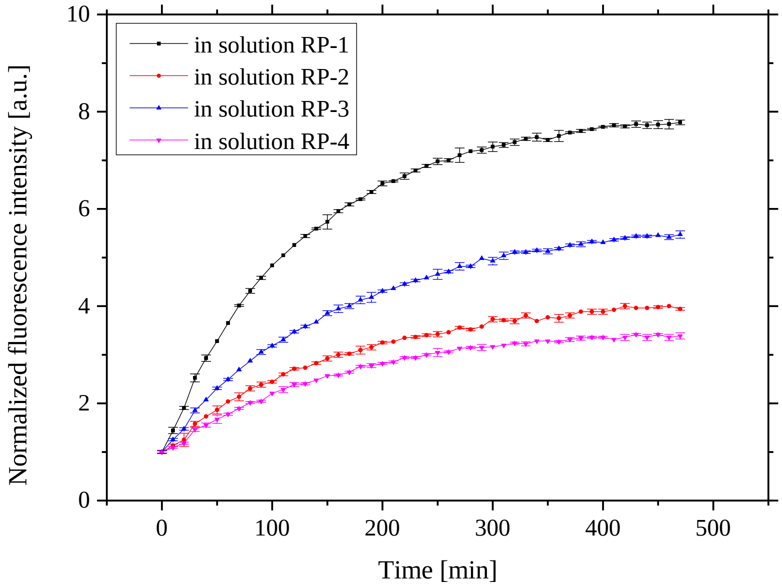

Figure III.27. Comparison of net gain of fluorescence intensity by peptides RP-1, RP-2, RP-3 and RP-4 in solution on digestion with trypsin.

When the initial fluorescence of the peptides was compared (see Table 11), it was noted that, RP-2, which has a distance of 8 amino acids between fluorophore and quencher showed the best quenching efficiency when compared to the other peptides. However, when the relative net gain of fluorescence of the four peptides was spotted in a graph (see Figure III.27), it was noticed that RP-1 gained fluorescence rapidly over-time when compared to the other reporter peptides. This suggests that RP-1, where there is a distance of 10 amino acids between the fluorophore and quencher, has better cleavage efficiency over time, even though the initial quenching is not as high as in RP-2. This indicates that a distance of 10 amino acids is optimal for trypsin to reach the cleavage site and digest the peptide at an optimal level. Due to the bulky nature of the fluorophore and quencher, as the distance between the two decreases, the steric hindrance increases resulting in slower cleavage kinetics. There is a possibility that if the distance between the fluorophore and the quencher is increased further, the cleavage might be faster. However, the quenching efficiency of the quencher drops further, as the quenching efficiency is inversely proportional to the distance between the quencher and the fluorophore. Based on these observations, RP-1 with a distance of 10 amino acids between fluorophore and quencher appeared to be a better candidate.

III.2.1.2. Digestion of reporter peptide candidates immobilized on a surface

In order to investigate if the cleavage kinetic is affected by immobilizing the peptides onto a surface, restricting the accessibility of the cleavage site to the protease, the digestion experiment was repeated with peptides bound to maleimide coated black well plate. The peptides were coupled to the maleimide surface via the *N*-terminal cysteine-SH group. Maleimides react with free sulfhydryl group(s) at pH of 6.5-7.5, forming stable thioether linkages (Figure III.15). The peptides were bound to the maleimide groups on the well plate followed by blocking of the left over maleimide groups with cysteine.HCl solution (see section V.3.5). After the blocking step, enzyme digestion was carried out by adding trypsin to the respective wells. To equal number of wells pure PBS-T without trypsin was added as control.

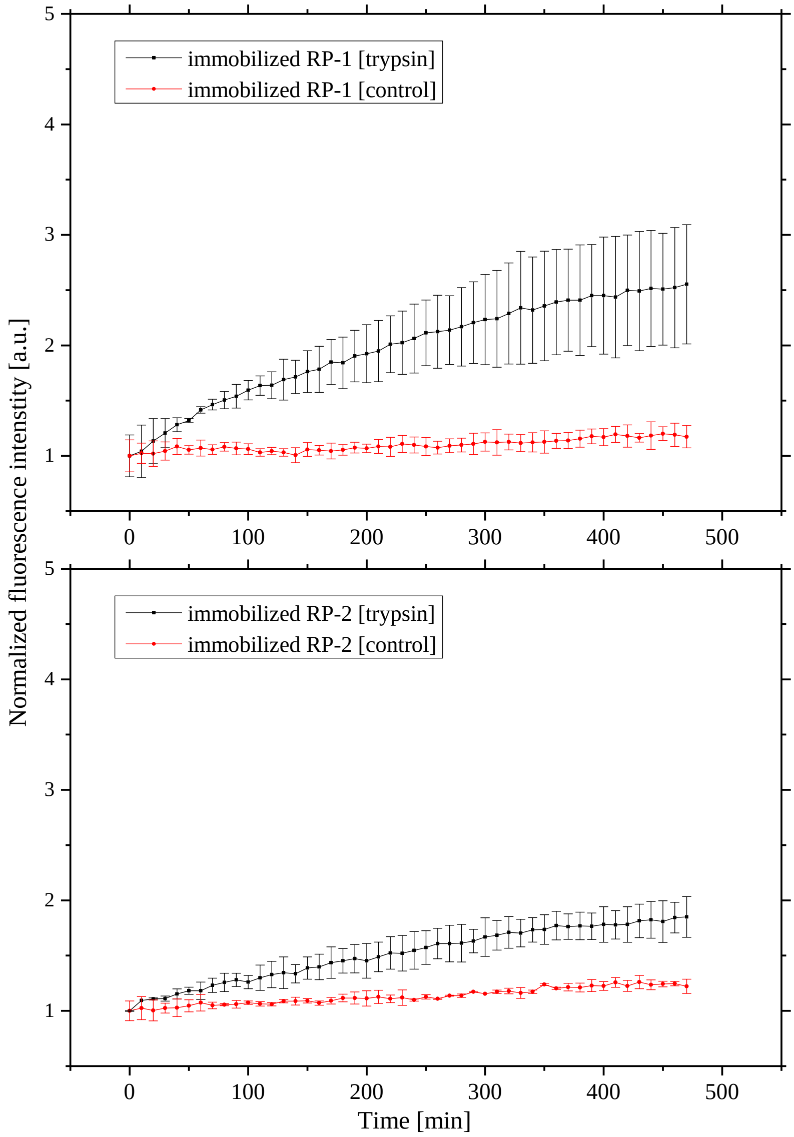

Figure III.28. Gain of fluorescence by RP-1 and RP-2 immobilized on a surface over time on digestion with trypsin. RP-1 has 10 amino acids between the fluorophore and the quencher whereas RP-2 has 8 amino acids.

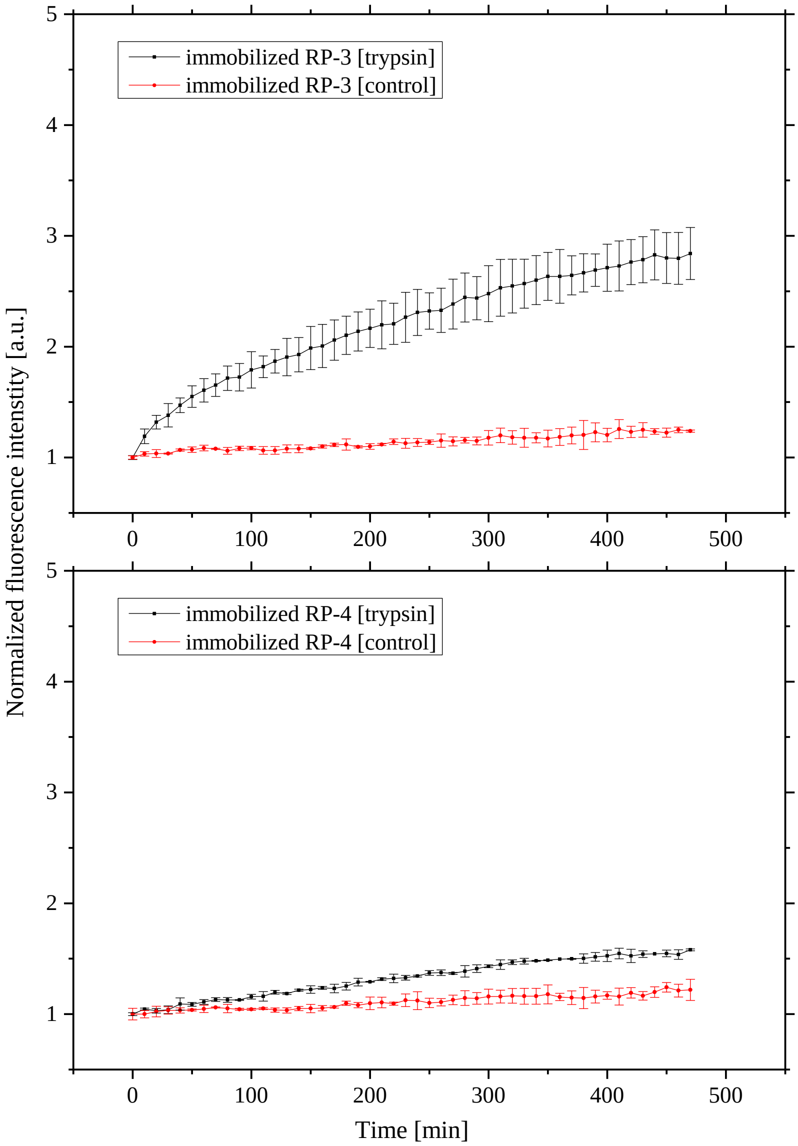

Figure III.29. Gain of fluorescence by RP-3 and RP-4 immobilized on a surface over time on digestion with trypsin. RP-3 has 6 amino acids between the fluorophore and the quencher whereas RP-4 has 4 amino acids.

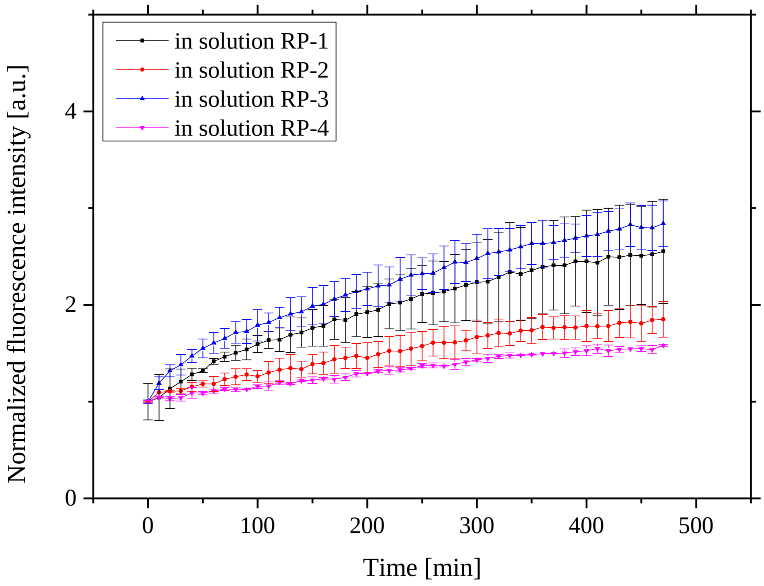

Figure III.30. Comparison of relative net gain of fluorescence by the bound reporter peptides RP-1, RP-2, RP-3 and RP-4 on trypsin digestion.

From Figure III.28, Figure III.29 and Figure III.30, it can be noted that all four immobilized reporter peptides gained fluorescence over time upon digestion with trypsin, similar to the digestion in solution. This suggests that binding of the reporter peptides on surface does not prevent the digestion of peptides.

Summary

Four peptides with a varied distance between the fluorophore and the quencher were designed. Using trypsin, these peptides were digested in solution and when immobilized on a surface. All the four peptides gained fluorescence on digestion with trypsin both in solution and when immobilized on the surface, indicating that the fluorophore and the quencher are successful in creating a FRET pair. When in solution, RP-1 gained relatively more fluorescence over time upon digestion with trypsin, whereas, when immobilized on a surface, RP-3 appeared to have gained more fluorescence. However, the nature of the surface to which the peptides were bound is not known. The supplier of the maleimide coated well plates did not offer the chemical composition of the surface. Therefore, in order to find out which reporter peptide is the better candidate, all the four peptides were spotted on three different surfaces of known chemical composition.

III.2.2. Design of a suitable surface for protease activity detection

The interaction of molecules (proteases) with a surface is influenced by the chemistry of the surface. Therefore, it was important to find a suitable surface for the immobilization of the reporter peptide. The reporter surface should not be too hydrophilic since such surfaces are known to repel the proteins.[93-94] This is not an ideal as the protease should be able to interact with the reporter peptide on the surface. On the other hand, the reporter surface should also not be too hydrophobic, as they are known to adsorb proteins.[95] Therefore, three different surfaces were compared in order to find the most suited surface for the digestion of the reporter peptide with a protease.

- Three-dimensional polymer networks
  a) 100% PEGMA surfaces
  b) 10:90-PEGMA-co-PMMA surfaces
- Two-dimensional self-assembled monolayers
  a) AEG_3 surfaces

III.2.2.1. Three dimensional (3D) polymer network surfaces

These surfaces in general have a high density of functional groups when compared to the 2D surfaces,. Two kinds of 3D polymer surfaces that differ in both polymer thickness and hydrophobicity were used for further experiments.

- ***100% PEGMA surface***

These 3D polymer surfaces have a high functional group density of up to 40 nmol/cm^2.[93] The polymer surface constitutes of 100% polyethylene glycol methacrylate (PEGMA) units. Due to the high hydrophilicity of the surface, the surfaces are expected to prevent adsorption of proteins.[94] These surfaces were chosen to study if the high loading capacity of the surface improves the sensitivity of the surface to detect protease activity.

- **10:90 PEGMA-co-PMMA surface**

These surfaces are composed of 10 % (n/n) PEGMA and 90 % (n/n) methylmethacrylate (MMA). Beyer *et al.* reported that this 3D polymer exhibited low unspecific adsorption of proteins (BSA, fibrinogen, diluted human serum etc.).[93] The surface was chosen in order to test if the low unspecific adsorption improves the proteolytic activity of proteases on the surface.

Preparation and characterization of 3D polymer surfaces

These surfaces were created using the surface-initiated atom transfer radical polymerization (siATRP).[35, 79, 96-99] The ATRP technique results in fast rates of polymerization with narrow molecular weight distributions and precise control of polymer compositions. [100] The monomers are statistically inserted into the growing polymer chain in the case of 10:90-PEGMA-co-PMMA. Prior to the functionalization, the surfaces were cleaned and activated to make them reactive. To the now activated surface, containing –OH groups, a silane was coupled followed by an initiator molecule. The initiator molecule contains a –Br which acts as the starting point for the atom transfer radical polymerization (ATRP), also known as living polymerization (Figure III.31).

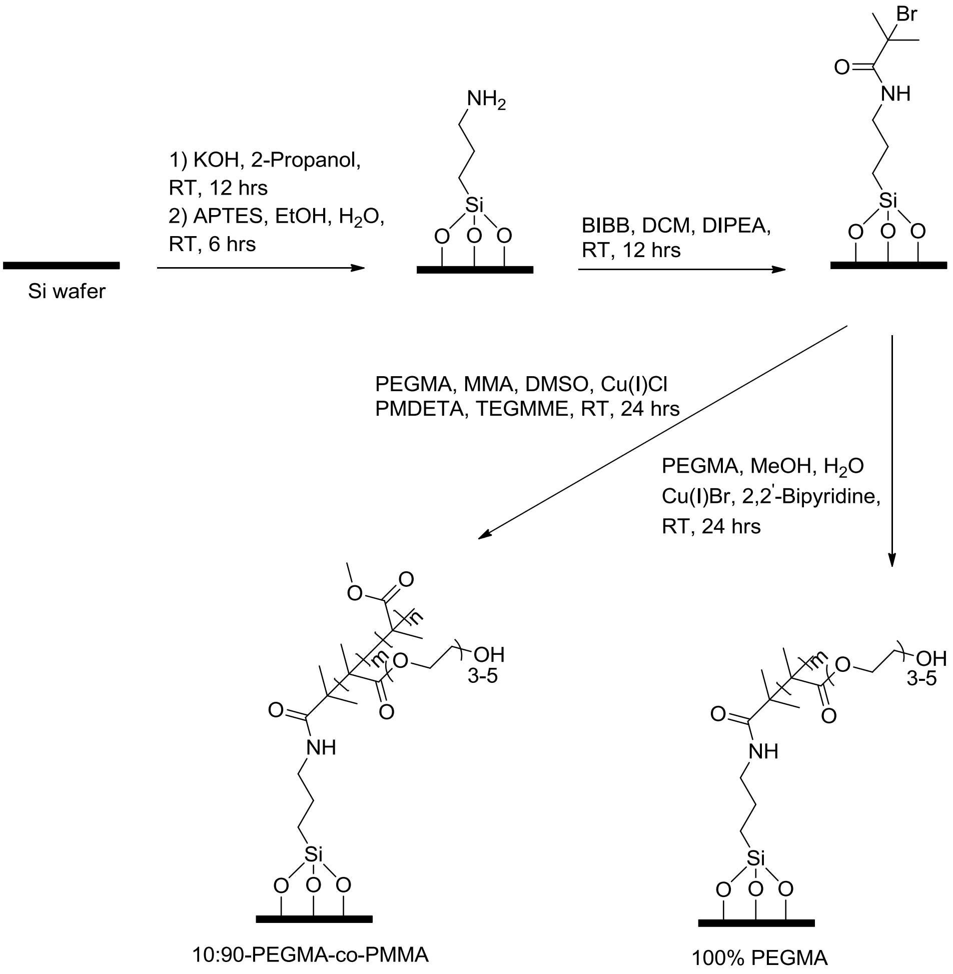
Si wafer
1) KOH, 2-Propanol, RT, 12 hrs
2) APTES, EtOH, H_2O, RT, 6 hrs
NH_2
Si
O O O
BIBB, DCM, DIPEA, RT, 12 hrs
Br
O
NH
PEGMA, MMA, DMSO, Cu(I)Cl PMDETA, TEGMME, RT, 24 hrs
PEGMA, MeOH, H_2O Cu(I)Br, 2,2'-Bipyridine, RT, 24 hrs
OH
3-5
10:90-PEGMA-co-PMMA
100% PEGMA

Figure III.31. Schematic representation of preparation of three dimensional polymer network surfaces.

While preparing the surfaces, a small silicon wafer was added at every step of the process so that the surfaces can be characterized by XPS. (3-Aminopropyl)triethoxysilane (APTES) was added to the activated surfaces to provide functional groups for further chemistry. From the Figure III.32(i) it can be noted that N 1s peak at 401 eV was observed on the surface after silanization confirming the success of the reaction.

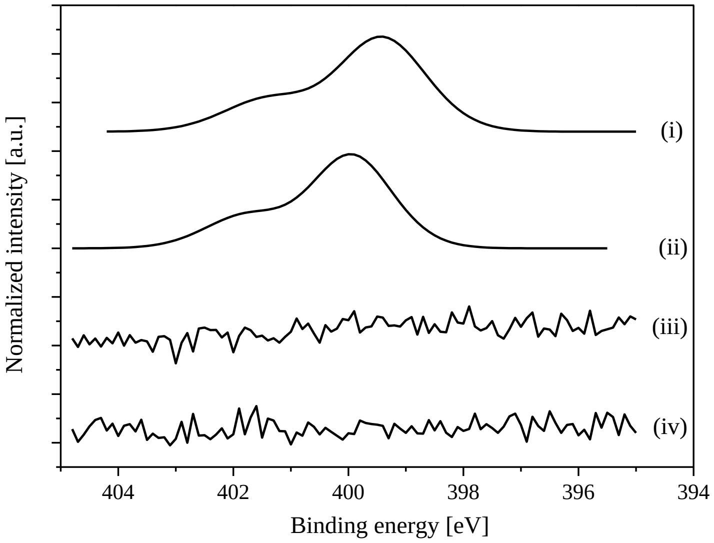

Figure III.32. XPS spectra of the N 1s region of the surface after each step of polymer film preparation. (i) after silanization with APTES (ii) after coupling the –Br initiator (iii) 10:90 PEGMA-co-PMMA polymer film (iv) 100% PEGMA polymer film.

Following silanization, an initiator, α-Bromoisobutyryl bromide (BIBB), was coupled. From the Figure III.33 (ii), it can be noted that a Br 3d peak is present at 68.1 eV confirming the successful addition of the initiator for siATRP. The surfaces with polymer film did not exhibit any N 1s peak. In the polymer, the NH bond is deep within the polymer film so it cannot be detected anymore by the XPS.

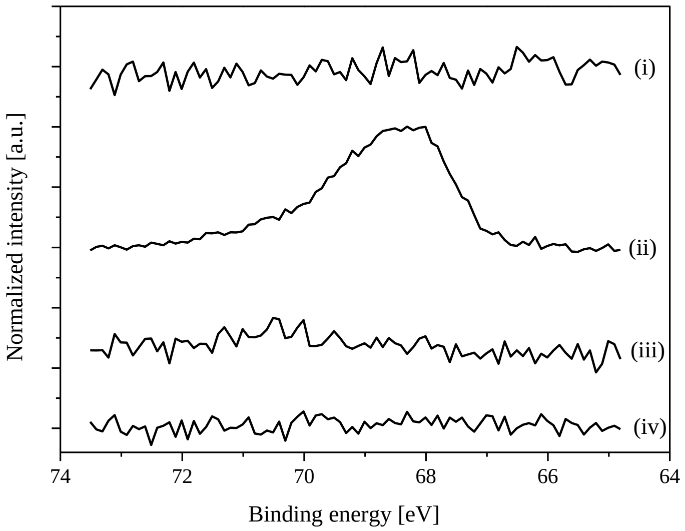

Figure III.33. XPS spectra of Br 3d region of the surface after each step of polymer film preparation. . (i) after silanization with APTES (ii) after coupling the –Br initiator (iii) 10/90 PEGMA-co-PMMA polymer film (iv) 100% PEGMA polymer film. Bromine is only present when the initiator is added on the surface before siATRP polymerization (ii)

In the C 1s region spectra of the polymer surfaces, peaks were noticed at 285.0 eV, 286.5 eV and 288.9 eV due to the C=O, C-O, C-C bonds. The composition of the polymer films obtained by the siATRP was verified. In theory, the peak areas $C_{C=O}$: C_{C-O} : C_{C-C} should constitute a ratio of 1 : 1.70 : 3 in 10:90-PEGMA-co-PMMA film and 1 : 8 : 3 in 100% PEGMA film. The observed ratios 1 : 1.87 : 2.40 and 1 : 7.70 : 2.45 were in good agreement with the expected values (Table 12). The small deviations in the ratios are attributed to the variations in the PEGMA side-chain lengths which contain 3-5 ethylene glycol units.

Table 12. Quantitative analysis of the C 1s area of 10:90-PEGMA-co-PMMA and 100% PEGMA polymer film. The expected ratios of peak areas, $C_{C=O}$: C_{C-O} : $C_{C-C,}$ are in good agreement with the observed ratios in both the polymer surfaces.

	Expected	Observed
10:90-PEGMA-co-PMMA	1 : 1.70 : 3	1 : 1.87 : 2.40
100% PEGMA	1 : 8 : 3	1 : 7.70 : 2.45

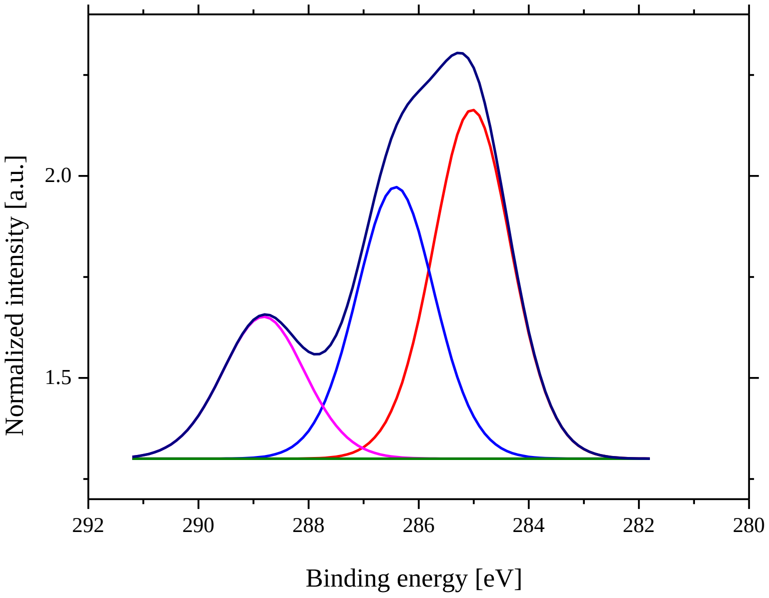

Figure III.34. C 1s region in the XPS spectrum of the 10:90-PEGMA-co-PMMA polymer film.

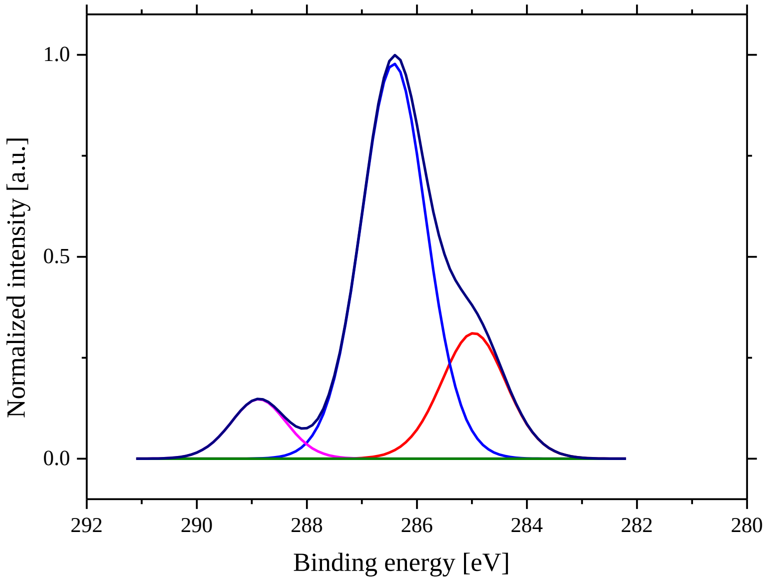

Figure III.35. C 1s region in the XPS spectrum of the 100% PEGMA polymer film.

The PEG-OH side chains on both the polymer surfaces were further modified with Fmoc-β-alanine-OH to yield amine groups required for the further reactions (see Figure III.36).

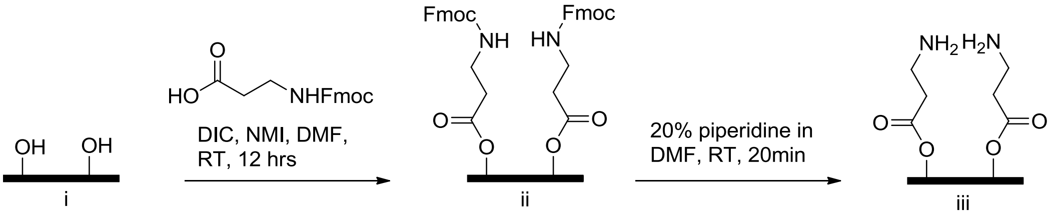

Figure III.36. Introduction of amine (-NH2) groups onto a 3D polymer surface. The PEG-OH side chains are further modified by coupling Fmoc-β-alanine-OH to yield amino groups i) PEG-OH groups on 10:90-PEGMA-co-PMMA and 100% PEGMA iii) surfaces with free amine groups.

III.2.2.2. Two-dimensional self-assembled monolayers

Self-assembled monolayer (SAM) surfaces are versatile two dimensional (2D) surfaces.[101] The properties of these surfaces can be changed with minimum effort.[102-103] 2D SAM surfaces have a lower density of functional groups when compared to 3D polymer surfaces (both 10:90 PEGMA-co-PMMA and 100% PEGMA). However, a reporter peptide attached to a 2D surface should be easily accessible for a potential protease than a reporter peptide embedded in a 3D polymer network. It was noted by Prime K.L. *et al.* that SAMs with several ethylene glycol units suppress non-specific adsorption.[104] The number of ethylene glycol (EG) units must be optimal. Very high density of EG units might result in completely repelling the protease from the surface before the activity, and a very low density results in unspecific adsorption of proteins resulting in denaturation. This system was intensively studied by Dr. Schirwitz in his dissertation[35], therefore the monolayers were synthesized according to the protocols optimized in his work for further reporter peptide digestion studies.

The 2D surfaces were prepared by depositing a monolayer of 3-(glycidyl)oxypropyl trimethoxysilane (3-GPS) followed by the epoxide ring opening using 4,7,10-Trioxa-1,13-tridecanediamine (DATT).[105]

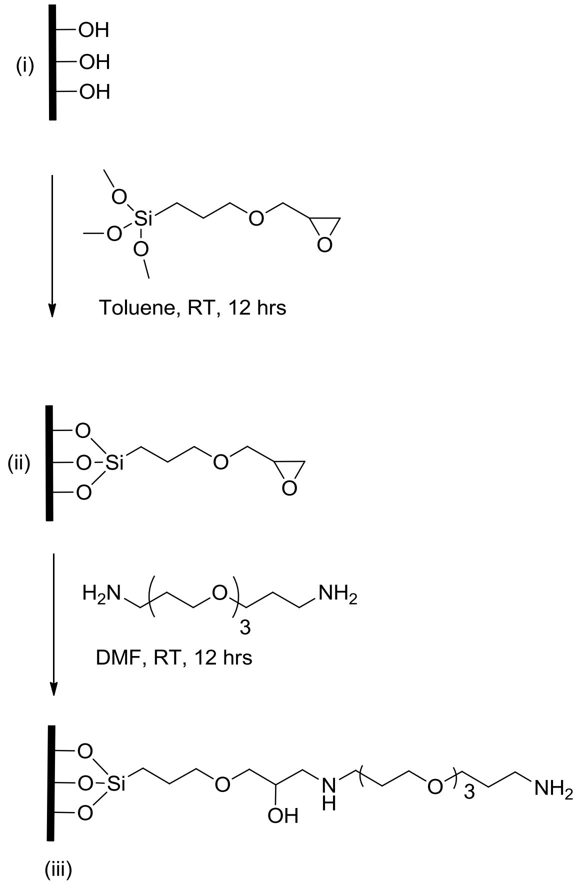

Figure III.37. Schematic representation of preparation of AEG_3- self assembled monolayers. i) activated surface, ii) epoxide surface iii) AEG_3 surface

The prepared AEG_3 surfaces were characterized by XPS. The ratio of C-O/C-N bonds to C-C bonds is higher on the AEG_3 surface when compared to the epoxide surface (Figure III.37). From the C 1s spectra region of the surfaces (Figure III.39 and Figure III.39) it can be noted that the XPS spectra reflects this. The peak area $C_{C\text{-}O}$+$C_{C\text{-}N}$:$C_{C\text{-}C}$ ratio was higher on AEG_3 surface (1.52:1) when compared to the ratio obtained from the epoxide surface (1.28:1).

A theoretical $C_{C\text{-}O}$: $C_{C\text{-}C}$ ratio of 2:1 would be expected for the epoxide surfaces. For the AEG_3 surfaces the same ratio should be 3 : 1. However, the experimental $C_{C\text{-}O}$+$C_{C\text{-}N}$: $C_{C\text{-}C}$ ratios were lower on AEG_3 surface indicating that probably the ring opening reaction with the DATT was incomplete. DATT consists of two amine groups and there is possibility that both amine groups react with two epoxides on the surface resulting in ring formation. From the Figure III.40 it can be noted that two peaks were present in the N 1s spectral region of the AEG_3 surface. The peak at 399.3 eV was due to –NH bond corresponding to C-NH- C moiety formed by the reaction of DATT amines with the epoxide rings. The peak noticed at 401.5 eV signifies the presence of protonated –NH_2 suggesting the presence of free NH_2 groups on the AEG_3 surface.

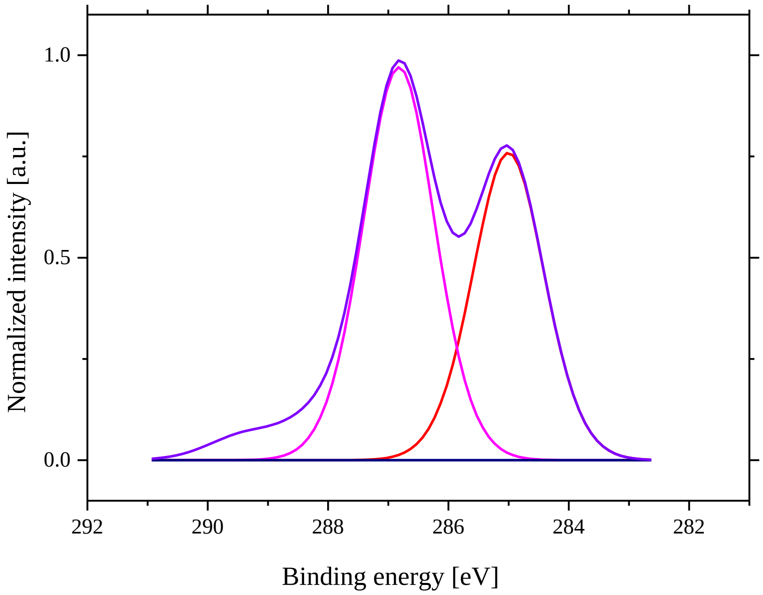

Figure III.38. C 1s region in the XPS spectrum of the epoxide surface.

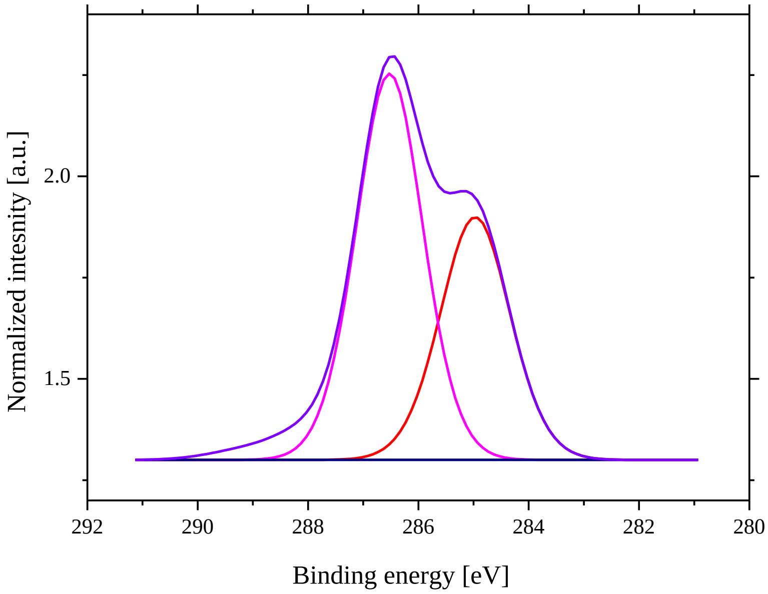

Figure III.39. C 1s region in the XPS spectrum of the AEG_3surface.

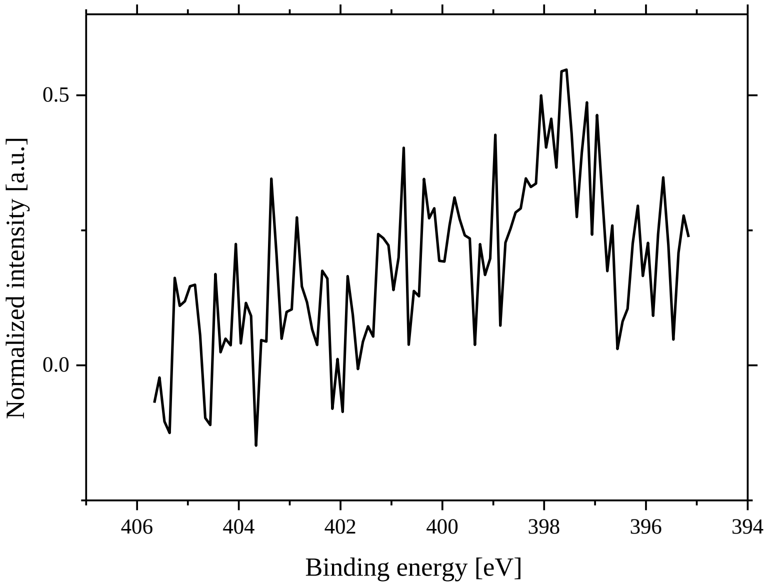

Figure III.40. N 1s region in the XPS spectrum of the epoxide surface.

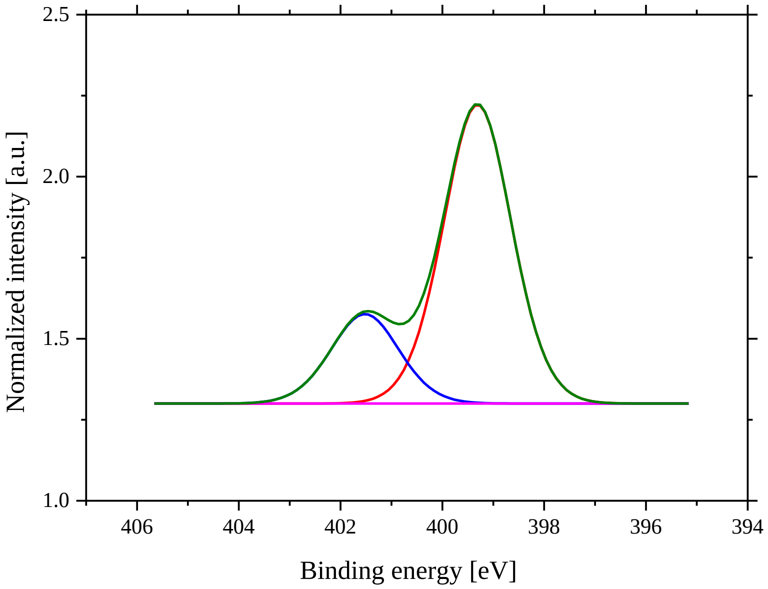

Figure III.41. N 1s region in the XPS spectrum of the AEG$_3$ surface.

III.2.2.3. Fluorescence measurements

In order to bind the reporter peptides covalently to the surfaces by spotting technique, linker 4-(N-maleimidomethyl)cyclohexanecarboxylic acid N-hydroxysuccinimide ester (SMCC) was coupled to the free -NH_2 groups on the three surfaces (AEG_3-SAM; 10:90-PEGMA-co-PMMA and 100% PEGMA). The addition of the linker provides maleimide groups via which the peptides can bind to the surface (see Figure III.42).

Using a spotting robot (NanoPlotter NP2.1, GeSiM GmbH, Germany) the reporter peptides (RP-1, RP-2, RP-3 and RP-4) were spotted onto the three surfaces (see section V.3.16). After drying, each spot is approximately 300 µm in diameter. For the spotting, HPLC purified peptides were used. The spotter used 2 nL of solution in each spot. Therefore, all the spots on a surface should contain equal concentration of peptides bound to the maleimide groups.

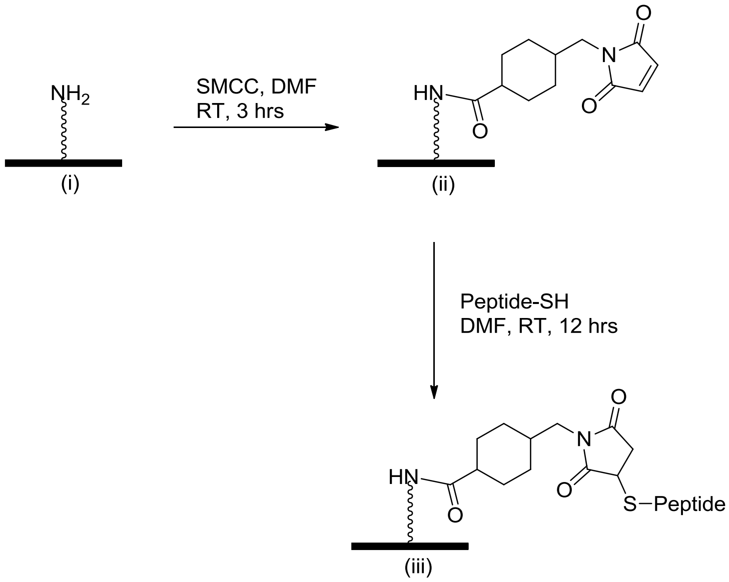

Figure III.42. Schematic representation of addition of maleimide linker to the surfaces. (i) NH_2 groups on the AEG_3-SAM, 10:90-PEGMA-co-PMMA and 100% PEGMA surfaces (ii) surfaces functionalized with SMCC linker (iii) Reporter peptide coupled to the maleimide group via the-SH group of the cysteine, which is at the N-terminus of the peptide.

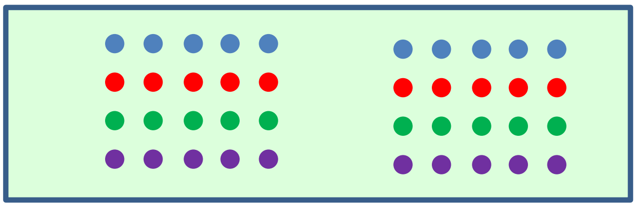

Figure III.43. Schematic representation of layout of the peptide spots spotted in an array format on the surfaces. Each slide consists of two similar sub-arrays of reporter peptides. Each color spot represents a reporter peptide. Blue: RP-1, Red: RP-2, Green: RP-3, violet: RP-4. Five copies are made for each peptide spot.

The spotting was done in such a way that each glass slide had 2 sub arrays (Figure III.43). Each sub array contained 4 different peptide spots in a column, each row contained multiple spots of the same peptide. The average fluorescence intensity of five spots of each peptide was used for the calculations.

After spotting the peptides on the surfaces, the free maleimide groups were blocked (see section V.3.17). After blocking, each glass slide was scanned using Genepix 4000B scanner. The slides were then placed in a special staining/incubation chamber containing a silicone seal to separate the two sub-arrays for the digestion experiments. Due to this silicone ring, the liquid which was added in the specific chambers stayed in the respective chambers without leaking into the other chamber. To one sub-array chamber PBS-T (control) was added, to the other sub-array chamber PBS-T and trypsin was added. The entire set up was covered using an aluminum foil to prevent any bleaching of the fluorophore and the setup was left overnight. The slides were scanned again using the same parameters that were used after the blocking step so that the comparison of the fluorescence intensity can be made before and after digestion experiments. Using Genepix analysis software the fluorescence intensity of each spot was calculated before and after trypsin digestion.

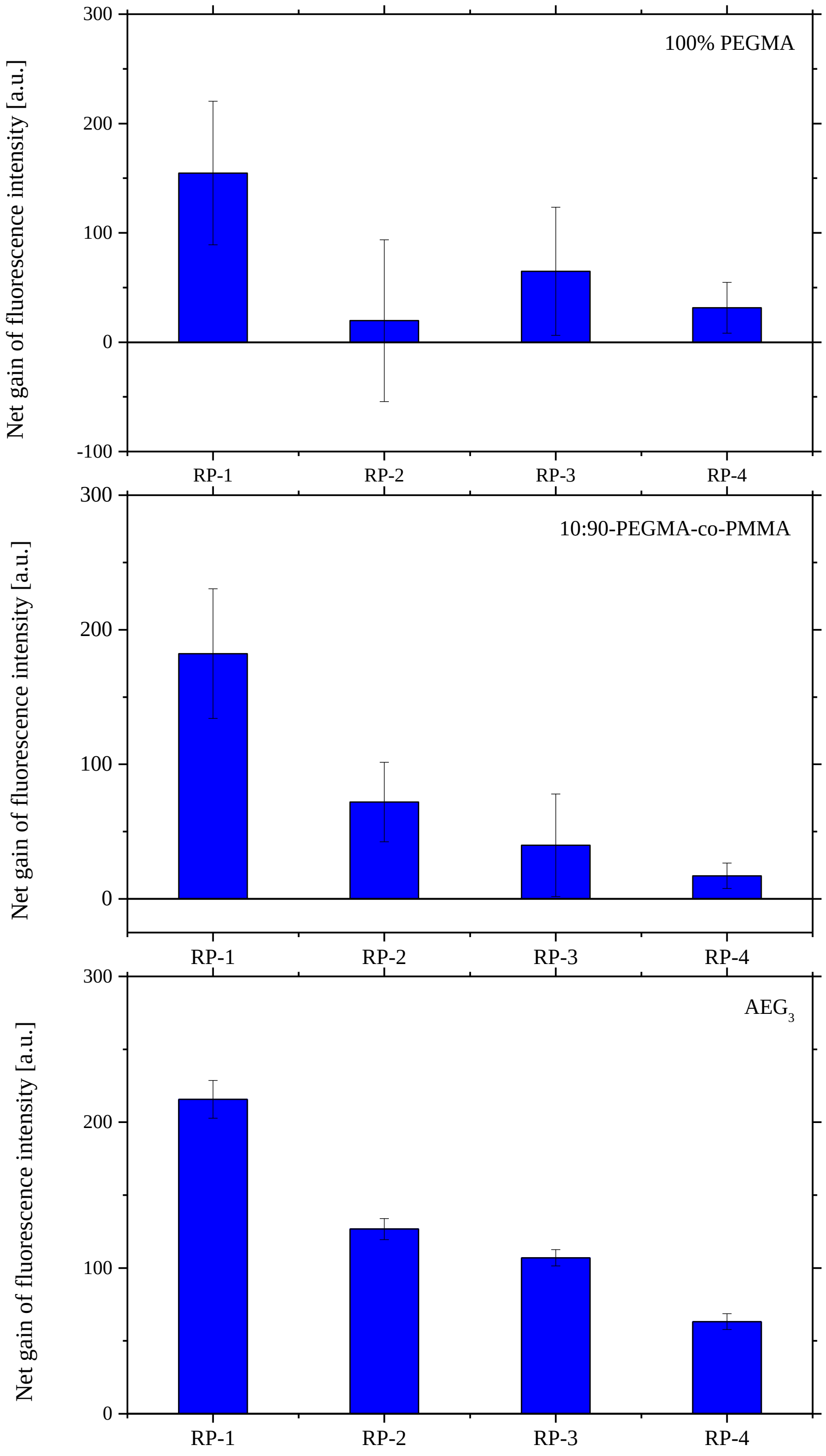

Figure III.44. Net gain of fluorescence intensity by the reporter peptides, RP-1, RP-2, RP-3 and RP-4 immobilized on three different surfaces on digestion with trypsin.

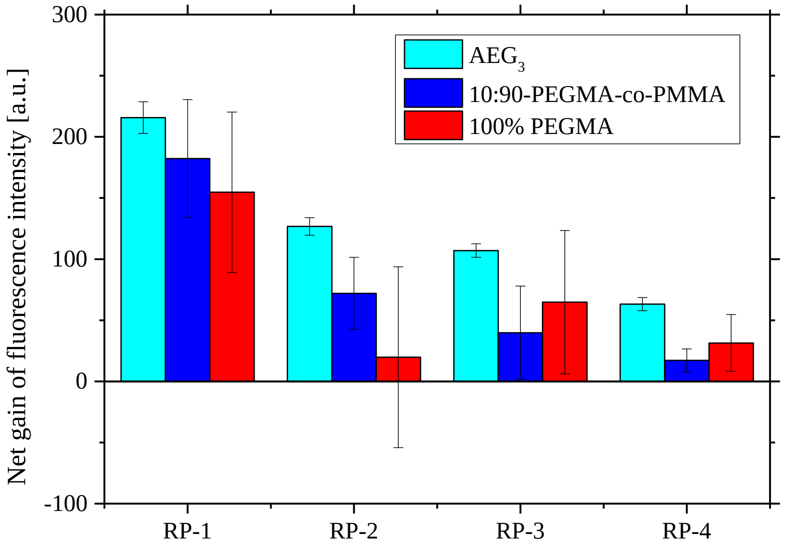

Figure III.45. Comparison of net gain of fluorescence intensity by reporter peptides on different surfaces.

Net gain of fluorescence by each spot was calculated by subtracting the initial fluorescence intensity from the final fluorescence intensity followed by calculating the percentage gain of fluorescence. From Figure III.44 and Figure III.45 it can be noted that all the reporter peptides gained fluorescence on digestion with trypsin. On all three surfaces, RP-1 showed the highest relative increase in fluorescence intensity. When different surfaces were compared, AEG$_3$-SAM, showed promising increase in fluorescence intensity. AEG$_3$-SAM surfaces also showed less standard deviation values compared to the other two surfaces suggesting the uniformity of the surface and peptide binding. From the above result it can be interpreted that for the preparation of reporter surface, RP-1 is the preferred reporter peptide and AEG$_3$-SAM is the preferred surface.

III.2.2.4. ToF-SIMS measurements.

From the fluorescence measurements it was evident that AEG$_3$-SAM surfaces were the most promising for the protease activity detection. However, in order to verify the results, Static Time-of-Flight Secondary Ion Mass Spectrometry (ToF-SIMS) measurements were carried out.

For the protease digestion experiment, a labelled peptide was bound to the surfaces and the peptides were digested using protease-trypsin so that the label is removed from the surface after the digestion. The label was followed using the ToF-SIMS to depict the rate of protease digestion. A peptide with a *C*-terminal Pentafluoro-L-phenylalanine was bound to the surface. The peptide was digested using trypsin and the ‘F^-’ and ‘$C_6F_5^-$’ anion signals of the Pentafluorophenyl ring were monitored after specific time intervals of digestion.

Table 13. Labelled peptide used in the ToF-SIMS experiment.

Peptide	Component	purpose
CGSGRGEX	X	Label – Pentafluoro-L-phenylalanine
	R	Arginine – trypsin cleavage site
	C	Cysteine – for peptide coupling via maleimide linker
	GSG	Spacer between the surface and trypsin cleavage site

For the measurements the three surfaces (10:90-PEGMA-co-PMMA; 100% PEGMA and AEG$_3$-SAM) were synthesized on a silicon wafer. A β-alanine was coupled to the 10:90-PEGMA-co-PMMA and 100% PEGMA surfaces so that there were free NH_2 groups for the coupling of SMCC linker.

After coupling of the SMCC linker, the three wafers were cut into small pieces. One wafer piece of each surface was put aside as a control for a ToF-SIMS measurement. To the other wafer pieces the fluorine labelled peptide (1mg/ml) was covalently bound via the *N*-terminal cysteine.

The silicon wafers of the three surfaces with and without the labelled peptide were used to check for background signals at the m/z values 19 and 167 related to 'F^-' and '$C_6F_5^-$' anions. From the Figure III.46, it can be noted that the reference measurements showed no significant background at m/z ranges of 'F^-' and '$C_6F_5^-$' (19 and 167 respectively). In the '$C_6F_5^-$' region of the 10:90-PEGMA-co-PMMA and 100% PEGMA polymer surfaces, a signal was present very close to the m/z value 167. However, there is no overlap between this peak and the $C_6F_5^-$ peak. This peak is found only in the polymer surfaces and is absent in the AEG_3-SAM surfaces suggesting that the peak might be due to the fragment from the polymer.

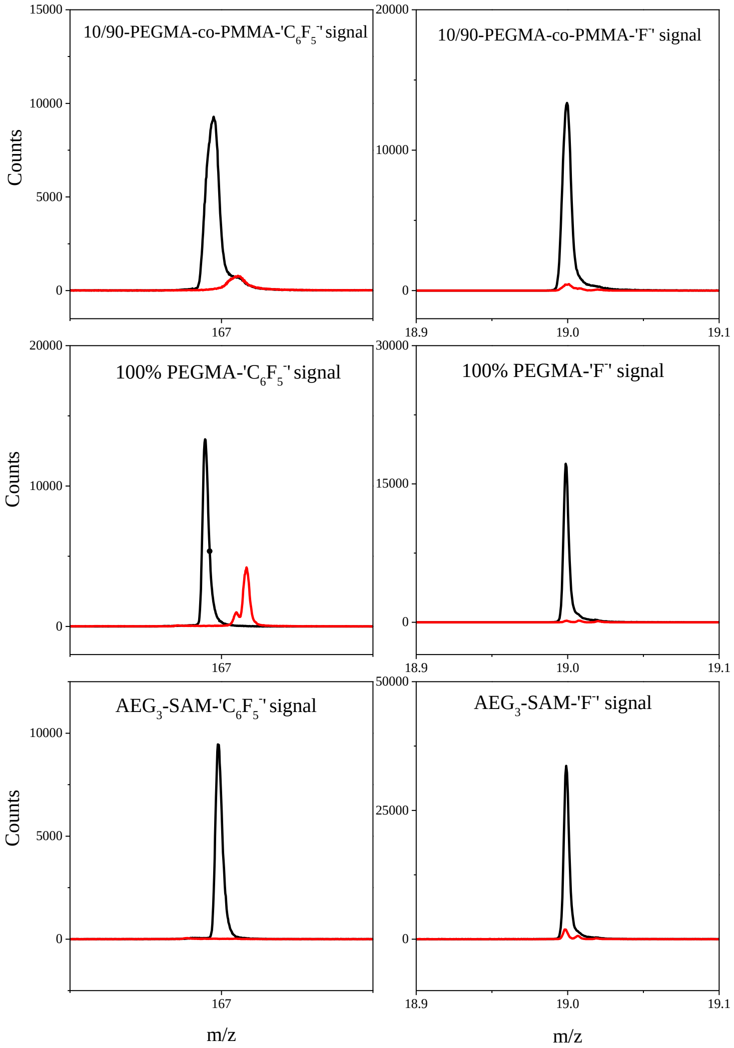

Figure III.46. Comparison of m/z signals of $C_6F_5^-$ and F^- anions on silicon wafers with fluorine labelled peptide (black) and without fluorine labelled peptide (red).

Pieces of each surface sample were incubated in trypsin solution (2.00 µmol) for the respective times followed by washing and drying of the surfaces thoroughly before ToF-SIMS measurement. The digestions were conducted for 0 min, 5 min, 10 min, 15 min, 30 min and 60 min on each surface (see Table 14). Each sample was measured at three different locations on the surface and the average of the three is taken as the final reading. The measurements showed that the total ion count varied from measurement to measurement. Therefore, instead of using the raw data, the data was normalized by dividing the fragments (F^- and $C_6F_5^-$) count by the total ion count. The standard deviation is less than 2% in majority of the measurements.

Table 14. Different surfaces incubated in trypsin. A small piece of each sample surface was incubated in trypsin solution for the respective time period followed by washing and ToF-SIMS measurement.

Surface	Time of incubation in trypsin [min]
AEG_3-SAM	0, 5,10,15,30,60
100% PEGMA	
10:90-PEGMA-co-PMMA	

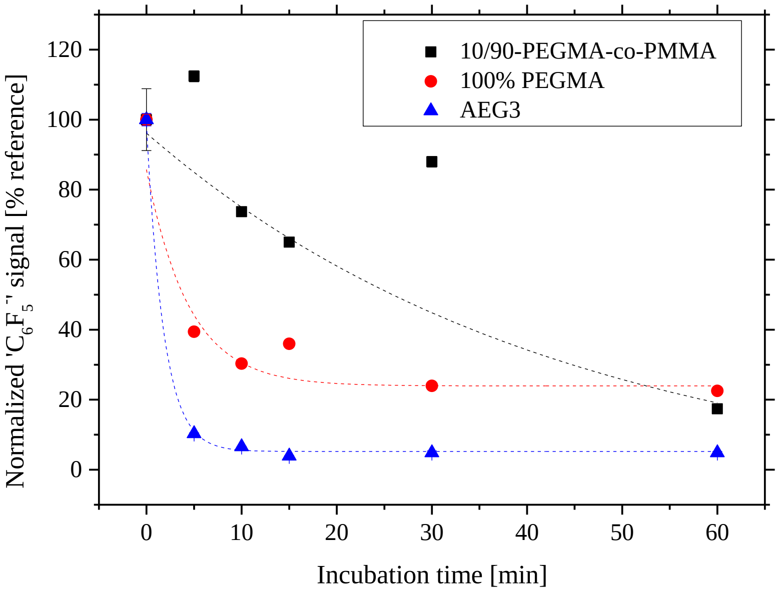

Figure III.47. Time resolved signal of $C_6F_5^-$ ion on different surfaces which were incubated in trypsin.

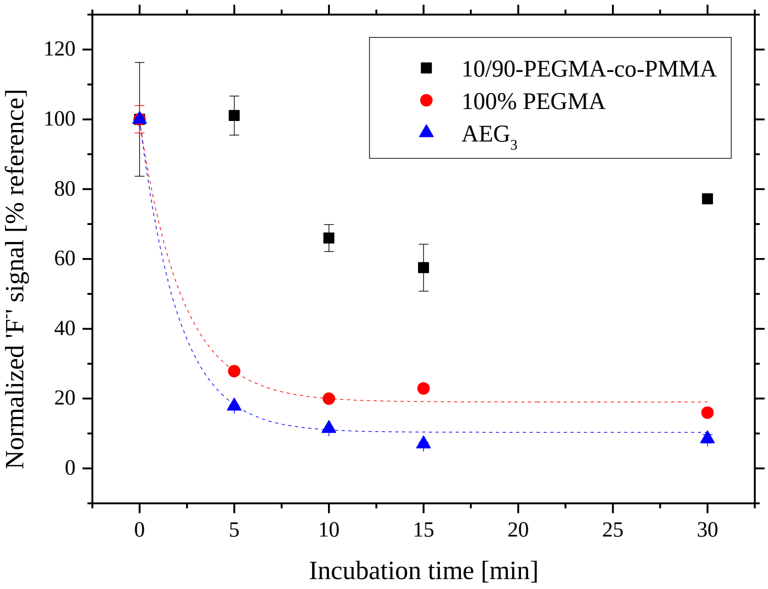

Figure III.48. Time resolved signal of F^- ion on different surfaces which were incubated in trypsin.

From the Figure III.47 and Figure III.48 it can be noted that during the first five minutes the digestion of the labelled peptide by trypsin is very rapid. The digestion is complete at around 15 min. The measurements of the 100% PEGMA and AEG$_3$-SAM surfaces follow a clean trend with less than 2% SD. However, the 10:90-PEGMA-co-PMMA surface showed the signals scattered with greater than 10% error most of the times. Therefore these measurements were not included in the evaluation. Nevertheless, it is evident that on AEG$_3$-SAM surface the proteolytic activity is better when compared to the 3D polymer surface. This observation is in agreement with the result obtained from the fluorescence measurements. Therefore, 2D AEG$_3$-SAM surfaces were considered the best choice to detect proteolytic activity.

Depth profiling

To determine if trypsin is able to enter the polymer and cleave peptides embedded inside the polymer network, a depth profile scan was done on 100% PEGMA polymer surface using ToF-SIMS. 10:90-PEGMA-co-PMMA polymer layers and AEG$_3$ monolayers were too thin (< 20nm) to do a depth profile scan. The 100% PEGMA polymer film had a thickness of 200 nm and was suitable for depth profile scans.

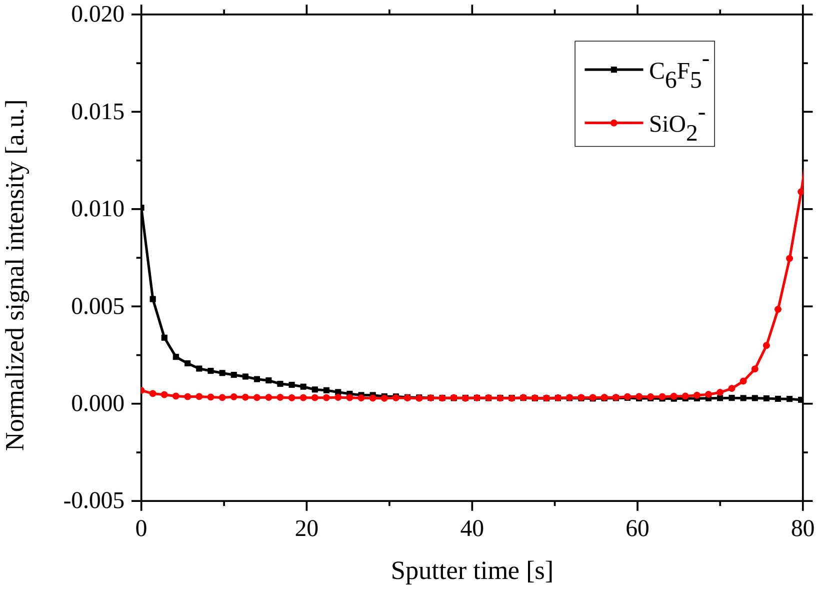

Figure III.49. ToF-SIMS depth profile scan of 100% PEGMA film loaded with fluorine labelled peptide before digestion with trypsin.

The depth profiling was done on the same wafer pieces (0 min, 5 min) which were used in the previous section for the digestion experiments. The wafer piece at time scale 0 min was not exposed to trypsin; therefore, the fluorine label should be intact in the polymer. From the Figure III.49, it can be noted that as the sputtering time progresses, the amount of fluorine ($C_6F_5^-$) decreased until it was completely absent around 35 s sputter time. This suggests that the peptide was only coupled in the top layer of the polymer. After 70 s into sputtering, SiO_2^- signal appears, which suggests that the entire polymer film was sputtered away, leading to characteristic silicon-related signals from the wafer.

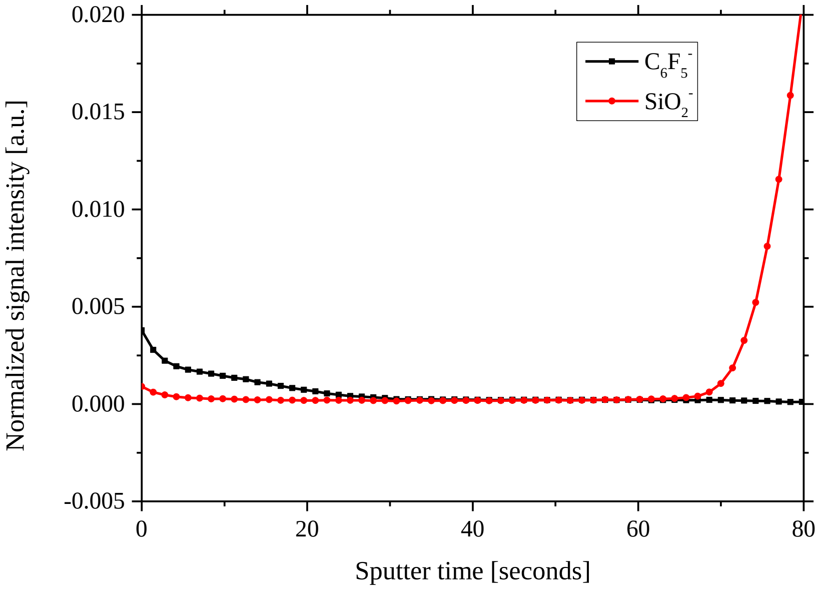

Figure III.50. ToF-SIMS depth profile scan of 100% PEGMA film loaded with fluorine labelled peptide after digestion with trypsin.

Another depth profiling was done with the wafer which was incubated in trypsin for 5 min (the same wafer which was measured during the static measurement). From the Figure III.47 and Figure III.48 obtained from static ToF-SIMS measurements, it can be noted that the fluorine intensity dropped exponentially on this sample when compared to the sample at 0 min (no trypsin digestion). However, static SIMS only measures the top layers (1-3 nm) of the surface. Therefore, the drop in the fluorine intensity is confined to the top layers. From the depth scan of the sample, Figure III.50, the composition of layers present deep in the surface were obtained. From the scan it is evident that although fluorine intensity dropped significantly in the top layers of the polymer, the fluorine in the deep polymer layers was still intact. This suggests that the trypsin, due to its bulkiness, might not have been able to reach the deeper layers of the polymer.

Summary

A labelled peptide was coupled to a 2D monolayer and a 3D polymer network. This peptide was digested using a protease, trypsin, and the label was monitored using fluorescence and ToF-SIMS measurements. The goal of this digestion experiments was to find whether 2D or 3D surfaces are optimal for the detection of proteolytic activity.

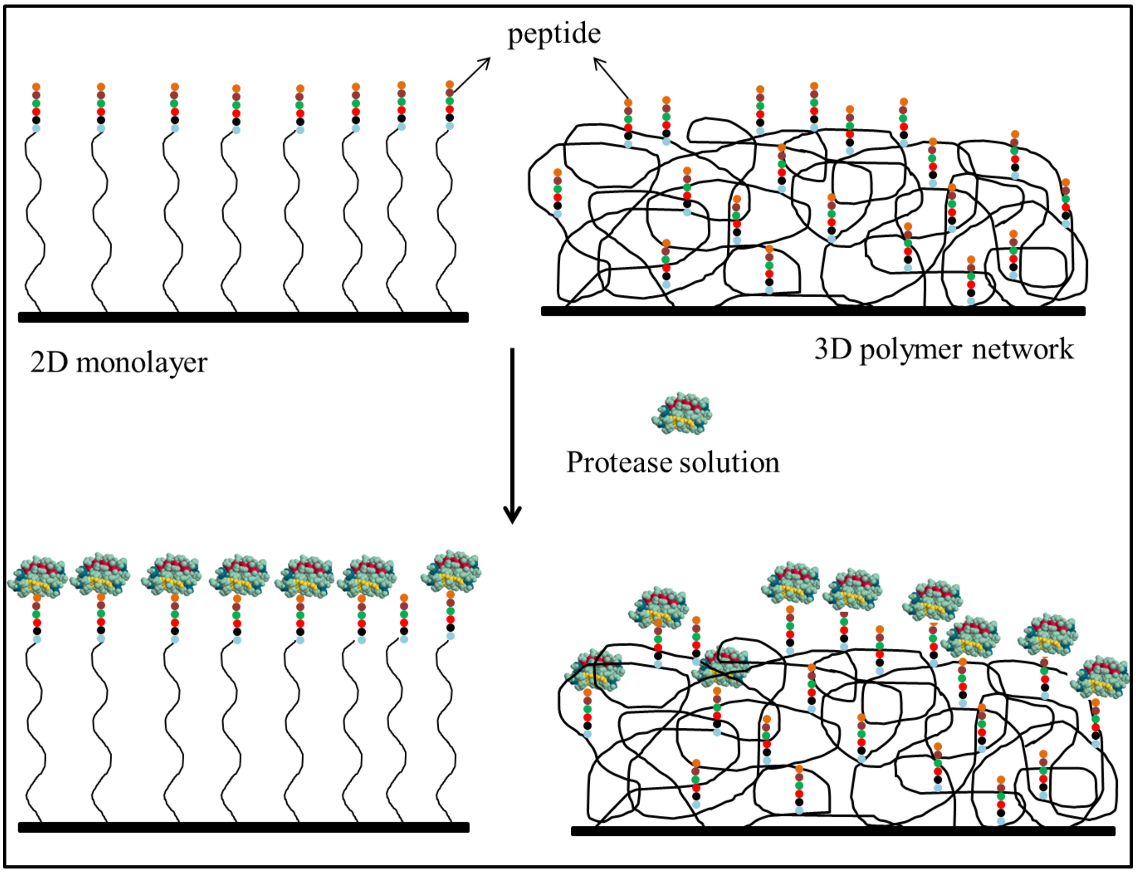

Figure III.51. Schematic representation of accessibility of peptides which are present on a 2D and 3D surfaces to a protease for proteolytic activity. Peptides present on a 2D surface are easily accessible to a protease, when compared to peptides embedded in a 3D polymer network.

Both the results obtained from fluorescence and ToF-SIMS measurements indicate that 2D surfaces are better for proteolytic activity. 2D surfaces provide better accessibility to the protease for the digestion of molecules present on the surface. Even though 3D surfaces can be loaded with large amount of substrate (for proteolytic activity), only the molecules present in the top layers of the 3D polymer network are accessible for proteolytic activity. Therefore, 2D AEG_3-SAM surfaces were used for creating a reporter surface which can detect proteolytic activity.

Reporter surface

The reporter surface is created based on the results obtained from section III.2.1 and section III.2.2. Reporter peptide-1 (RP-1) turned out to be an optimal FRET peptide that can be coupled to a 2D AEG_3-SAM surface to create a reporter surface favorable for proteolytic activity detection.

III.2.3. Sensitivity of the reporter surface

It is essential to determine the detection sensitivity of the reporter surface. A peptide array which is synthesized on a 100% PEGMA surface has peptide density of 1-5 nmol per cm^2. In order to use the reporter slide to screen for proteolytic peptide candidates, the reporter surface should be able to gain fluorescence on detection of a protease of concentration 1 nmol or less.

A series of digestion experiments were conducted with different concentrations of trypsin to determine the sensitivity of the reporter surface. A single reporter surface was separated into 16 small chambers (using incubation chamber with silicon seal) and trypsin solution of different concentrations was added to the respective chambers. As a control, to two of the chambers PBS-T with protease activity inhibitor was added. The slide was incubated overnight and the fluorescence image was obtained using Genepix 4000B scanner. The image was analyzed using the Genepix analysis software to quantify the gain of fluorescence.

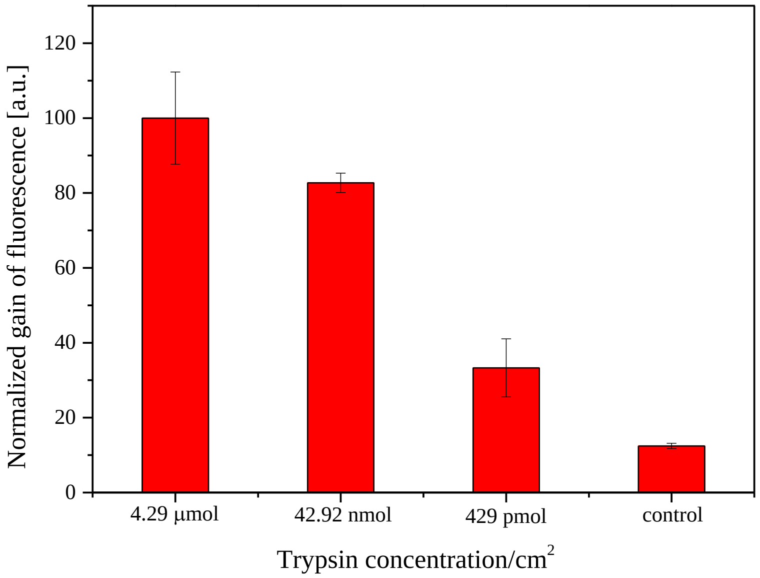

Figure III.52. Gain of fluorescence by the reporter surface on incubation with trypsin solution of different concentrations**.**

The fluorescence gain achieved by high concentration of trypsin is given the value of 100 and the gain of fluorescence by the other concentrations is normalized to this value for reference. Each chamber to which the trypsin solutions were added was of 1 cm^2 area. This means in the chamber with 429 pmol trypsin, the reporter surface was exposed to protease of concentration ≤ 429 pmol/cm^2. From the Figure III.52 it can be noted that the reporter surface gained around 30% of fluorescence on digestion with 429 pmol of trypsin per cm^2. However, when the slide was incubated in PBS-T with a protease inhibitor (control), there was a 10% gain of fluorescence. Therefore, the net fluorescence gain due to 429 pmol of trypsin was 20%. The surface did not show significant fluorescence gain for protease concentrations less than 429 pmol/cm^2. This indicates that the reporter surface can be used to detect proteolytic activity in solution when the protease concentration is 429 pmol/cm^2 or more.

Screening of a peptide array with reporter surface

A peptide array was created with the peptides which lost > 95% fluorescence during the first screening process (see section III.1.3). In total the array consisted of 700 peptides. The array was placed in a desiccator with dry ammonia vapor and was left for 48 hours to cleave the peptides from the surface. Cleaving the peptides off the surface allows them to move, thus avoiding the cloud environment (crowding of functional groups from adjacent peptides when peptides are immobilized). Following ammonia incubation, the array was taken out and vacuum was applied to remove any ammonia trapped inside the polymer network.

A reporter slide was covered with PBS-T and using a stamping machine, the array slide was stamped on the reporter slide and a pressure of 2 bar was applied. Applying pressure during the transfer using a stamping machine is crucial because the peptides in the array are free (due to ammonia cleavage) and can diffuse in all directions mixing up the peptide spots. The stamping machine also helps in bringing the two surfaces together and separating them after the assay without any sliding.

The arrays were kept pressed to each other for 24 hours, following which the slides were separated and the reporter slide was washed with milli-Q water to remove buffer salts, dried and scanned. No gain of fluorescence was observed on the reporter surface, suggesting that the 700 peptides in the array do not possess the desired proteolytic activity. This result suggests that the significant (> 95%) loss of fluorescence noticed during the first assay might not be due to proteolytic activity of the individual peptides. However, 700 peptides is a very small number of peptides compared to the possible combinations of amino acids for 15 meric peptides. Further screenings with multiple peptide arrays need to be done to find a peptide with robust proteolytic activity.

It is to be noted that a single peptide of short length (15mer) might not be enough to create the 3D catalytic site. The better approach would be to transfer three different peptides onto a single chemical handle creating a 3D environment similar to that of catalytic site. This approach would require a chemical handle onto which three peptides from three different arrays can be transferred sequentially from the synthesis surface and immobilized.

The synthesis of a suitable chemical handle is currently being pursued as a new PhD project. As a partial part of this PhD work preliminary experiments related to the transfer of peptide array form synthesis surface to a recipient surface were carried out.

Transfer of peptide arrays to a target surface

In order to transfer a peptide array to a target surface, the peptides must be cleaved from the synthesis surface so that they can bind to a target surface. During the transfer, the peptide array can be simultaneously purified by introducing a key sequence in the last synthesis cycle so that only fully synthesized peptides are transferred to the receptor surface. The principal concept of peptide array purification was initially reported by Schirwitz *et al.*[35, 106] In the reported method, a peptide array was synthesized on a surface with TFA cleavable rink amid linker (RAM linker). At the end of the peptide synthesis a cysteine (with trityl protecting group) was added. Only full-length peptides obtain this N-terminal cysteine. As a target surface, a gold coated PVDF membrane (wetted with a mixture of TFA (v/v) in toluene) was used. During the transfer only full length peptides were able to bind to the gold receptor surface via the thiol group of cysteine.

However, further modification of this purification concept was necessary because the final goal is to transfer peptides onto a solid support rather than a flexible one. With a flexible support positing of the array during the transfers might cause problems, moreover, flexible supports such as PVDF membranes tend to be fragile. For the transfer experiments HA and FLAG epitope peptides were synthesized on a 100% PEGMA surface in an array format. No special cleavable linker (e.g. RAM linker) was introduced between the surface and peptides. The first amino acid of the peptides form an ester bond with the -OH groups on the polymer surface. The peptides were released from the synthesis surface by cleaving the ester bond using ammonia vapor.

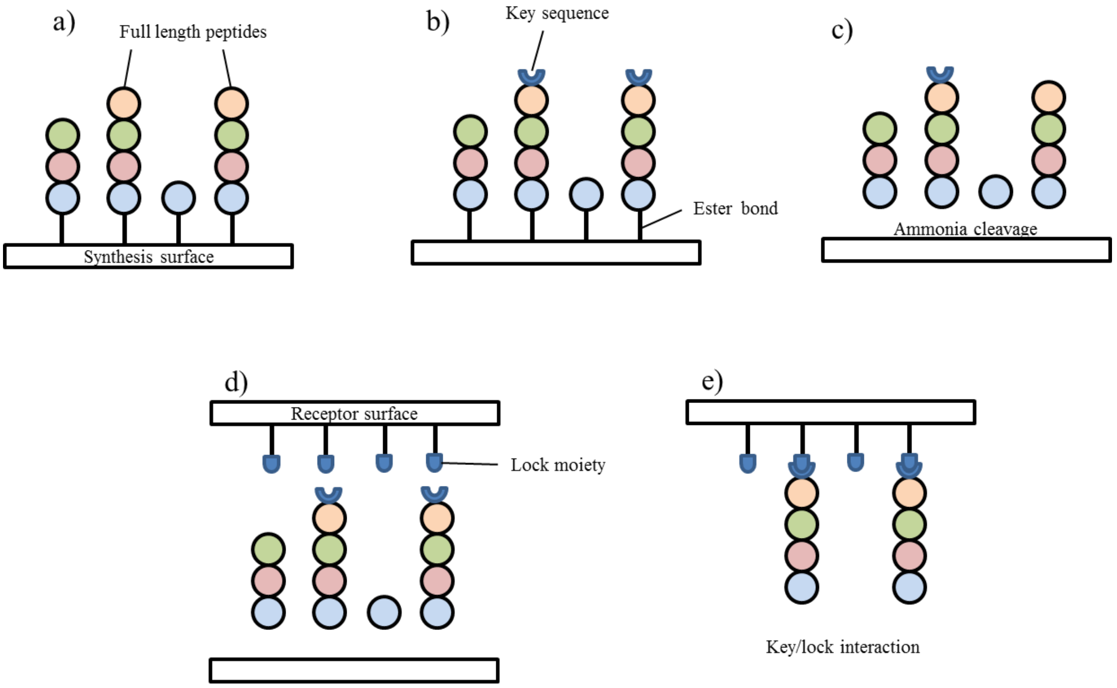
a)
Full length peptides
Synthesis surface
b)
Key sequence
Ester bond
c)
Ammonia cleavage
d)
Receptor surface
Lock moiety
e)
Key/lock interaction

Figure III.53. Concept of a peptide array transfer to a recipient surface. During the transfer the peptide array is simultaneously purified. a) The peptide array is synthesized on a 100% PEGMA surface and the peptides are bound to the surface via an ester bond. b) In the last synthesis cycle only full length peptides obtain key sequence. c) The peptides are cleaved from the synthesis surface with ammonia. d) The synthesis surface is brought in contact with the receptor surface with a lock moiety. e) Only peptides with key sequence bind to the lock moiety on the receptor surface, the rest of the fragments are washed away.

Two key-lock set ups were tested for the transfer and purification experiments

On peptide (key moiety)	On receptor surface (lock moiety)
-SH	alkene (click chemistry)
-SH	Maleimide

Thiol-ene click chemistry

Thiol-ene click chemistry is versatile and is used for preparation of cross-linked polymer networks, hydrogels, lithographic applications etc.[107-112] An attempt was made to use thiol-ene click chemistry for the transfer of peptide arrays. One concern with the transfer of peptide arrays is lateral diffusion of the spots. Presence of excess amount of solvent during the transfer leads to the diffusion of the spots. In order to avoid presence of excess liquid during the transfer, a receptor surface which consists of a thick polymer layer (25 µm) was used. The thick polymer on the surface absorbs the solvent like a sponge. These surfaces were provided by Dr. Pavel Levkin. The surfaces were further modified so that alkene groups were available on the surface (see section V.3.20). The receptor surface was immersed in the solvent, 0.001 mM 2,2-dimethoxy-2-phenylacetophenone (DMPAP) in THF, for 5 min before the transfer. During this 5 min the polymer film on the receptor surface swelled by absorbing the solvent. A peptide array with an *N*-terminal cysteine was used for the transfer. The array was incubated in ammonia vapor for 24 hours (see section V.3.19) and the transfer was done for 30 min in the presence of UV light – 365 nm. After the transfer, the array was stained using fluorescently labelled HA antibody (see section V.3.21). The slide was scanned using Odyssey LICOR scanner.

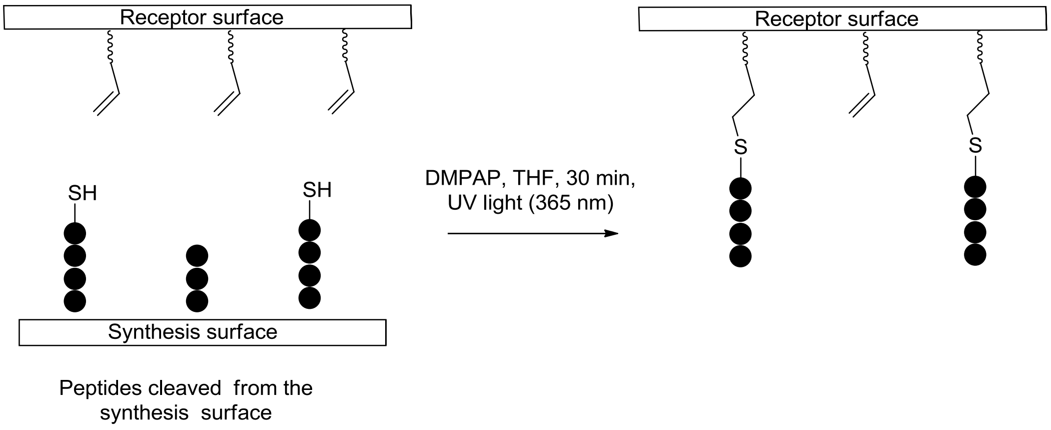
Receptor surface
SH
SH
Synthesis surface
Peptides cleaved from the synthesis surface
DMPAP, THF, 30 min, UV light (365 nm)
Receptor surface
S
S

Figure III.54. Schematic representation of peptide array purification via transfer. Peptides with N-terminal cysteine (-SH) group bind to alkene groups on the recipient surface by radical mechanism.

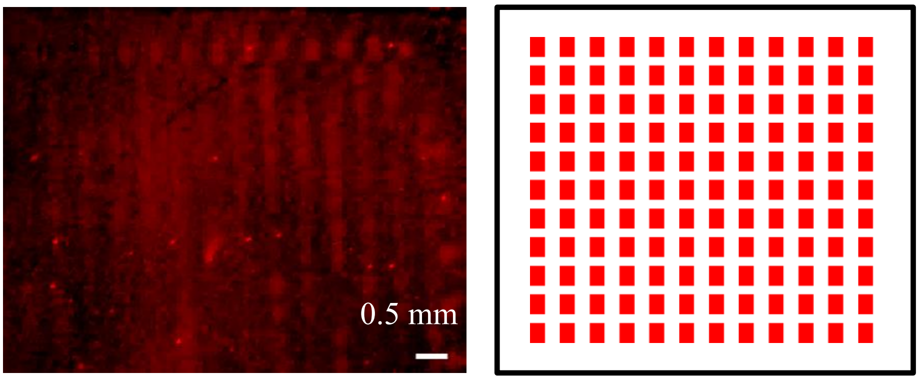

Figure III.55. Fluorescence scan of the receptor surface after the transfer of peptide array via thiol-ene click chemistry. The slide was stained with anti-HA-Dylight 680 after the transfer. The image was acquired using Odyssey Infrared imager at 700 nm excitation wavelength.

From the Figure III.55 it can be noted that even though the peptides were transferred from the synthesis surface to the recipient surface, significant later diffusion was observed. This result suggests that application of pressure during the transfer of array is necessary to prevent later diffusion. However, proper equipment with both UV light source and pressure applying system was not available during the time of these experiments. Therefore, the ene-thiol click chemistry was not pursued any further for the peptide array transfers.

Thiol-maleimide

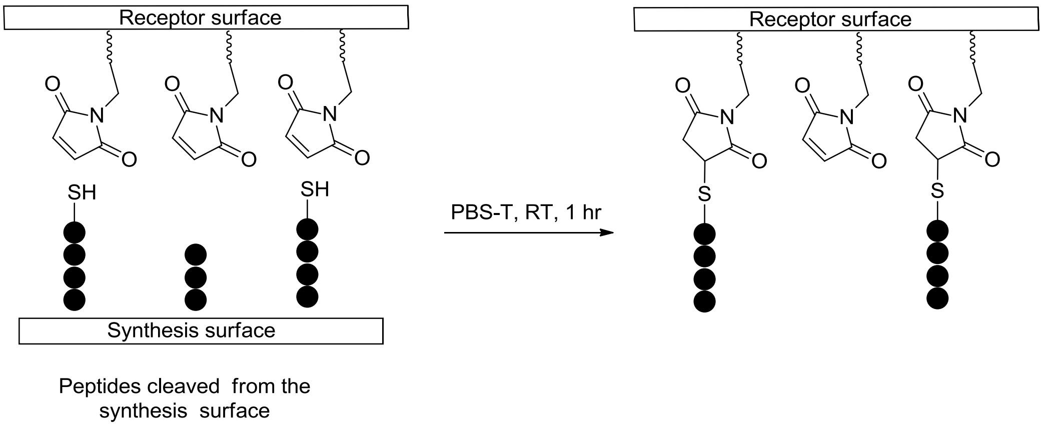

Figure III.56. Schematic representation of peptide array purification via transfer. Peptides with *N*-terminal cysteine (-SH) group bind to maleimide groups on the recipient surface.

A peptide array with an N-terminal cysteine was transferred to a maleimide coated glass slide. The side chains of the peptides were deprotected before the transfer. The array was incubated in ammonia vapor for 24 hours (see section V.3.19) and the transfer was done to using the stamping machine. To avoid later diffusion of peptide spots 2 bar pressure was applied during the transfer. PBS was used as solvent medium for the transfer. The set up was left for one hour following which the slides were separated. The receptor slide was washed thoroughly to remove any buffer salts and the HA peptides were stained using fluorescently labelled HA antibodies (see section V.3.21). The slide was scanned using Odyssey LICOR scanner.

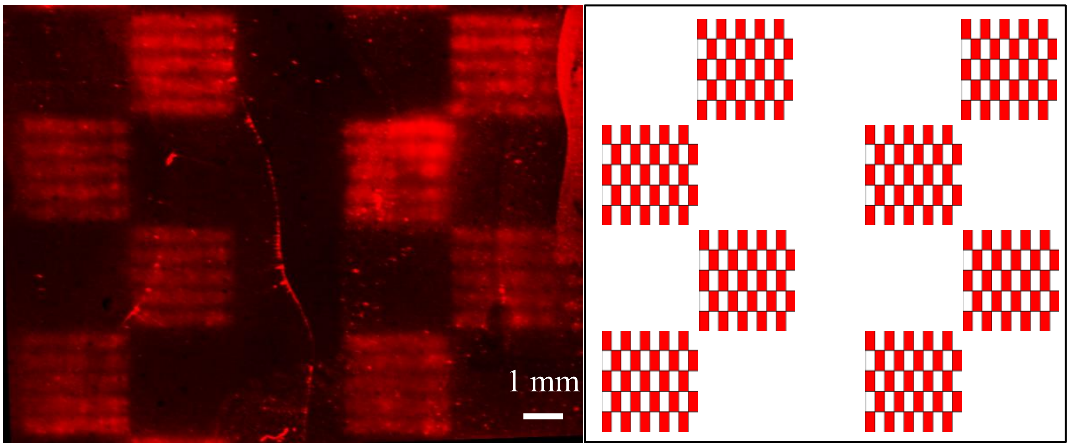

Figure III.57. Fluorescence scan of the maleimide-receptor slide after the transfer of peptide array. Left side: Recipient slide was stained with anti-HA-Dylight 680 after the transfer. (solvent used as transfer medium : PBS). Right side: Lay out of how the array should look after staining with anti-HA-Dylight 680).

From the Figure III.57 it can be noted that the transfer was successful. However, the control peptides which do not have cysteine at the end of the sequence also got transferred. This might be due to unspecific adsorption of peptides to the surface.

In order to verify if the peptides were getting adsorbed to the surface without the involvement of maleimide and thiol bonds, a transfer experiment was conducted with a recipient slide on which the maleimide groups were blocked using 2-mercaptoethanol. After the blocking no free maleimide groups should be available for the transfer. The transfer conditions were kept similar to the previous experiment.

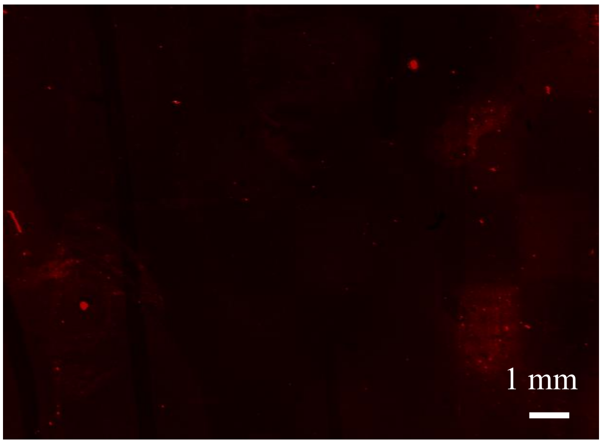

Figure III.58. Fluorescence scan of the blocked maleimide-receptor surface after the transfer of peptide array. The slide was stained with anti-HA-Dylight 680 after the transfer.

From the Figure III.58 it can be noted that peptide array was not transferred to the blocked maleimide receptor surface. This result suggests that there is no significant unspecific adsorption of peptides to the receptor surface. During the peptide array synthesis using laser printer, traces of amino acid (cysteine) dust particles might have contaminated the control spots resulting in cysteine at the end of all peptide sequences.

From Figure III.57 it is evident that the fluorescence intensity of the spots is not even throughout the surface suggesting that the number of peptides transferred were not even throughout the surface. One reason for this might be the poor solubility of the peptides in PBS and also poor wetting of the recipient surface. A transfer experiment was conducted in order to study if adding a surfactant (Tween 20) to the solvent used during the transfer increases the quality of the transfer. A peptide array cleaved with ammonia was transferred to a maleimide receptor surface using PBS-T as the solvent during the transfer. The ‘T’ in the PBS-T stands for Tween 20, a surfactant which is used to increase the wettability of surfaces.

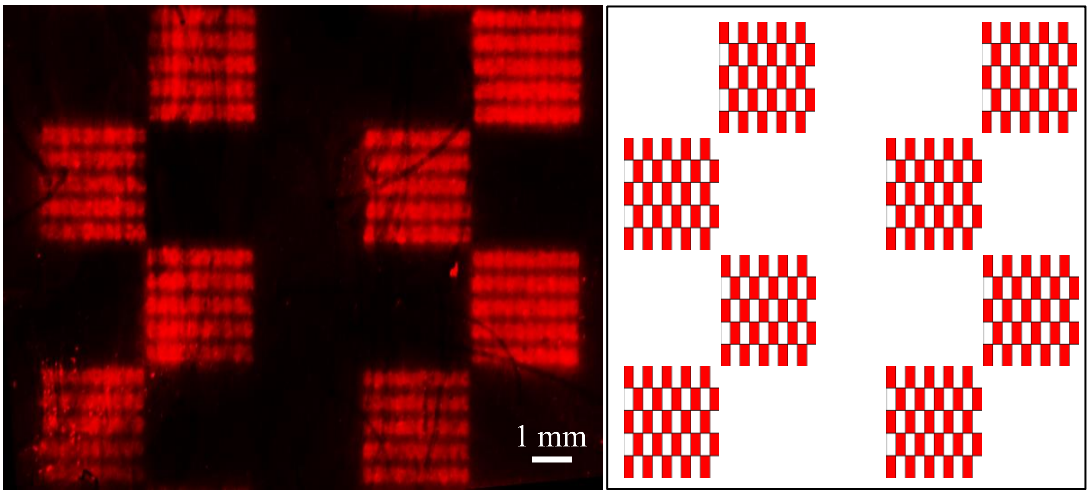

Figure III.59. Fluorescence scan of the maleimide-receptor surface after the transfer of peptide array. Left side: Recipient slide was stained with anti-HA-Dylight 680 after the transfer (solvent used as transfer medium: PBS-T). Right side: Lay out of how the array should look after staining with anti-HA-Dylight 680).

From the Figure III.59 it is evident that the peptide array transfer worked better when PBS-T was used as solvent during the transfer. This suggests that wetting of the surface and the solubility of the peptides during the transfer plays significant role in determining the quality of the transfer.

In summary, two systems (thiol-ene click chemistry and thiol-maleimide) employed for the immobilization of peptides on the recipient surface. Of the two, thiol-maleimide chemistry proved to be optimal for the transfers. Application of pressure during the peptide array transfer proved to be crucial to prevent lateral diffusion. These preliminary peptide array transfer results prove that it is possible to transfer peptides from the synthesis surface to a recipient surface.

IV. Conclusion and outlook

In this work, two assays to detect peptides with proteolytic activity in the array format were developed. The initial approach was to label peptide arrays with a fluorescent label and tracking the rate of loss of fluorescence over time on incubation in buffer solution. Peptides with proteolytic activity should be able to cleave each other resulting in the loss of fluorescence. However, during the study many drawbacks of this approach were noticed. Quenching of fluorescent dye was one of the main concerns. Tryptophan quenched the fluorescent dye intermoleculary by photoinduced electron transfer (PET). Due to all these concerns, tracking of loss of fluorescence was considered to be not an ideal approach for the assay.

An alternative assay was developed where no modifications were made to the peptide array. In this assay, an independent reporter surface which can gain fluorescence on detection of proteolytic activity was developed. The reporter surface is an AEG_3-SAM slide covered with a reporter peptide. The reporter peptide was designed based on the FRET principle, it consists of a fluorophore at the *C*-terminus, quencher at the *N*-terminus and a protease cleavage site in the middle of the sequence. The fluorophore of the FRET peptide is quenched by the quencher. When the reporter surface is brought in contact with a protease, the quencher is cleaved away from the FRET peptide leaving behind the fluorophore resulting in the increase of fluorescence signal. Thus, the gain of fluorescence by the reporter surface serves as a signal for proteolytic activity. Using trypsin as a model protease enzyme, the sensitivity of the reporter surface was determined. The reporter surface showed 20% increase in fluorescence on detection of 429 pmol of protease per cm^2. A peptide array synthesized on a 100% PEGMA surface has a peptide density of (1-4) nmol per cm^2. As the reporter surface should be able to detect concentrations below this amount, it should be suitable for detection of peptides with proteolytic activity in peptide arrays.

To further optimize the screening, there is a need for an automation to bring the reporter surface and the peptide array together, without shifting the two supports wile pressed together. A precise positioning system is necessary to identify which peptide spot in the array is resulting in the gain of fluorescence on the reporter surface. The peptides (in an array) can be cleaved from the solid support with dry ammonia so that they can reach the reporter surface and interact with reporter peptides. When a peptide with proteolytic activity comes in contact with the reporter surface, this will result in a fluorescence signal at a particular peptide spot.

The reporter surface can be used to detect both, peptides with robust proteolytic activity and peptides with weak proteolytic activity. The cleavage of peptides from the surface with dry ammonia is a slow process. When in need to detect peptides with weak proteolytic activity, the peptide array can be placed under ammonia vapor for multiple days until all the peptides are cleaved from the surface. This allows for high concentration of peptides per spot that can interact with reporter surface, thus enabling to detect peptides with weak proteolytic activity. When in need to detect peptides with robust proteolytic activity, the array can be cleaved with ammonia for short period of time before the screen.

It should also be noted that, a simple peptide alone might not be able to possess a robust proteolytic activity. In metalloproteases, a metal ion plays key role in the proteolysis. The established screening process with the reporter surface can be improved by introducing metal ions in the assay. The reporter surface can be covered with a buffer loaded with different metal ions before incubating it with the peptide array to study the effect metal ions have on the characteristic features of peptides.

With the advances in the purification and transfer of peptide arrays, three different peptides can be transferred onto a single chemical handle, which can be a better mimic of a protease by creating a 3D environment similar to that of catalytic site. As a partial part of this PhD work, ground work was carried out to prove that the peptide arrays can be transferred from a synthesis surface to a recipient surface thus paving way for future development of this assay.

Identification of peptides with specific proteolytic activity will pave the way for novel therapeutic agents. For example, in Alzheimer’s disease, β-amyloid peptide plaques are deposited in brain.[113-115] A novel therapeutic molecule can be created by combining a proteolytic peptide with a peptide which can bind specifically to the amyloid deposits. On reaching the target, the peptide binder binds to the amyloid deposits and the proteolytic peptide breaks down the amyloid peptides. This new therapeutic principle is based not only on binding but also destruction of the target.

V. Materials and Methods

V.1. Materials

KOH (p.a.) and isopropanol (p.a), DABCO for synthesis (p.a), DATT (≥ 98 %), MMA (≥ 99 %), PMDETA (≥ 98 %), TEGMME (≥ 97 %), DMSO (≥ 99.8 %), were purchased from Merck chemicals (Darmstadt,Germany).

To obtain anhydrous DMF for capping, Fmoc-removal and washing steps the DMF was dried over molecular sieve (4 Ǻ) purchased from Merck (Germany).

Si (100) wafers were obtained from Georg-Albert PVD GmbH (Silz/Germany).

Fmoc-β-alanine was purchased from Iris Biotech GmbH (Marktredwitz ,Germany).

Durapore filters (0.1 µm pore size, 90 mm in diameter) and Immobilon-P membranes (0.45 µm pore size) were purchased from Millipore Corporation (Merck KGaA, Germany).

Acetic anhydride (≥99 %), and toluene (≥99.5 %) were purchased from *VWR* (Darmstadt, Germany).

(3-Aminopropyl)triethoxy silane (≥ 98 %), 3-GPS (≥ 98 %), acetone (p.a.), β-mercaptoethanol (≥ 99 %), CuCl (≥ 99 %), CuBr (99.99 %), DCM (p.a.), DIC (99 %), DIPEA (≥ 98 %), EG_7-SH (≥ 95 %), Fmoc-pentafluoro-L-phenylalanine, tetrahydrofuran Triisobutylsilane, EtOH (p.a.), MeOH (p.a), NMI (>99 %), PEGMA (Mn≈360 g/mol), TFA (99.9 %), piperidine (99 %), TWEEN 20, and α-bromoisobutyryl bromide (98 %) were obtained from Sigma-Aldrich GmbH (Steinheim, Germany). All chemicals and solvents were used without further purification.

Phosphate buffered saline powder packets were purchased from Sigma-Aldrich GmbH (Germany).

2,2‘-Bipyridine was purchased from Alfa Aesar (Karlsruhe, Germany).

TAMR-NHS ester, DyLight 680 NHS ester and DyLight 800 NHS ester were purchased from Thermo Scientific.

Fmoc-Lys(5/6-TAMRA)-OH and SMCC linker were purchased from Biomol GmbH (Hamburg, Germany).

All the microscope glass slides used were of Nexterion® Glass B uncleaned (EU) type and were purchased from SCHOTT (Jena, Germany).

The maleimide coated glass slides which were used as recipient surfaces for the transfer experiments (thiol-maleimide chemistry) were purchased from *PolyAn GmbH,* Berlin.

A handheld UV lamp was used as the light source for the thiol-ene click reaction. The lamp was purchased from UVP Inc.

The glass slides used for the thiol-ene click chemistry were provided by Dr. Pavel Levkin.[116] The slides were received with free –OH on the surface. 5-hexenoic acid was coupled to these surfaces to have alkene groups on the top.

PBS-T buffer

PBST-buffer with 0.05% (v/v) TWEEN 20 was prepared freshly before use. The salt from one Phosphate buffered saline powder packets (purchased from Sigma-Aldrich) was dissolved in one liter of milli-Q water. The pH of the solution was adjusted to 7.4 using HCl and NaOH. 500 µL TWEEN 20 was added under constant stirring.

Rockland buffer

Rockland Blocking Buffer for Fluorescent Western-Blotting (Rockland buffer) was obtained from Rockland Immunochemicals Inc. (Gilbertsville, PA/USA) and used as received.

Milli-Q water

The water used for washing steps and for preparing various solutions and buffers was obtained from a Milli-Q system which was purchased from water (Millipore Corporation, Merck KGaA, Darmstadt/Germany, resistivity ~18.2 MΩcm)

Pre-synthesized peptides

All pre-synthesized peptides were supplied by Dr. Anette Jacob from Peps4LS GmbH, Heidelberg.

Peptide arrays

All peptide arrays used were ordered from the company *PEPperPRINT GmbH* (Heidelberg, Germany). 100% PEGMA and 10:90 PEGMA-co-PMMA are the polymer films on which the arrays were synthesized. The arrays used were constructed as follows

Array 1: This array format was used for the transfer experiments related to thiol-ene clcik chemistry

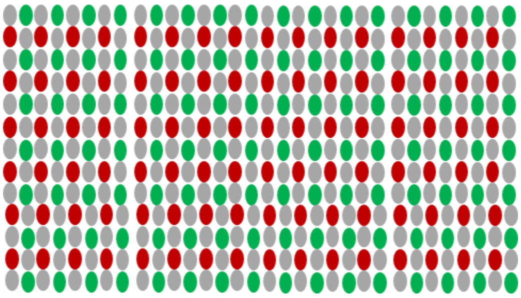

Figure V.1. Green ellipses the FLAG epitope and red ellipses the HA epitope; in the respective fields, the control spots are (shortened in the synthesis and thus N-terminally acetylated) grayed out.

Array 2: This array format was used for the transfer experiments done to maleimide slides.

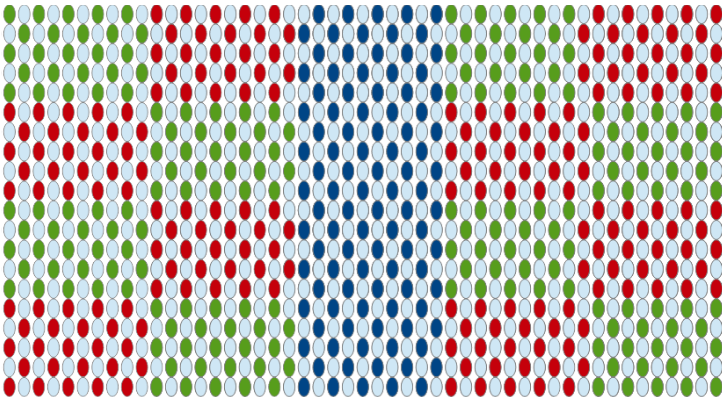

Figure V.2. Blue ellipses correspond to the MYC epitope, green ellipses the FLAG epitope and red ellipses the HA epitope; in the respective fields, the control spots are (shortened in the synthesis and thus N-terminally acetylated) grayed out

V.2. Devices and measuring parameters

V.2.1. Fluorescence scans

Fluorescence scans were obtained either from the *Odyssey Infrared Imager* (*LICOR Biosciences*, Lincoln, NE/USA) or the *GenePix 4000B microarray scanner* (*Molecular Devices*, Sunnyvale, CA/USA).

Odyssey Infrared Imager

Two solid state lasers which can provide excitations at 685 nm and 785 nm are present in the Odyssey Infrared Imager. All the images were taken at 21 µm resolution and detector intensity of 3.0. The brightness and contrast of the images were adjusted using the odyssey software.

GenePix 4000B Microarray Scanner

Two solid state lasers which can provide excitations at 532m and 635 nm are present in the GenePix 4000B scanner. All the scans were at 20 µm resolution, 33 % scan power. The PMT (photo multiplier tube) values of 400-600 were chosen depending on the fluorescence intensity in the preview scan. The focus offset was always set at zero.

XPS measurements

XPS measurements were performed using a K-Alpha XPS spectrometer (ThermoFisher Scientific, East Grinstead, UK). Data acquisition and processing using the Thermo Avantage software is described elsewhere.[117] All samples were analyzed using a microfocused, monochromated Al Kα X-ray source (400 µm spot size). The K-Alpha charge compensation system was employed during analysis, using electrons of 8 eV energy, and low-energy argon ions to prevent any localized charge build-up. The spectra were fitted with one or more Voigt profiles (BE uncertainty: $\underline{+}0.2$eV) and Scofield sensitivity factors were applied for quantification.[118] All spectra were referenced to the C 1s peak at 285.0 eV binding energy (C-C, C-H) controlled by means of the well-known photoelectron peaks of metallic Cu, Ag, and Au, respectively.

ToF-SIMS measurements

The measurements were performed in an ultrahigh vacuum ($p < 5 \times 10^{-9}$ mbar) at a ToF-SIMS device with reflectron ToF analyzer (ION-TOF GmbH, Münster, Germany). For the spatially resolved measurements, a Bi-cluster Liquid Metal Ion Gun in the high current bunched mode was used (pulse duration: 1.10 to 1.30 ns). Bi^{3+} primary ion pulses are generated at a voltage of 25 keV, the lateral resolution was about 4 microns. The primary ion dose is maintained below the static limit of 10^{11} ions per cm². For depth profiles, C_{60} ions with a voltage of 20 keV were used as a sputtering source. Charge compensation was performed when necessary with an electron gun at 21 eV and the ion reflectron was readjusted accordingly**.**

V.3. Methods

V.3.1. Labelling of a peptide array with N-succinimidyl ester derivatives of dyes

N-succinimidyl ester derivatives of dyes, 5/6-carboxytetramethylrhodamine (10 µg, 1.89 µM) DyLight-680 (10 µg, 1.21 µM) and DyLight-800 (10 µg, 0.95 µM), were used for labelling of peptide arrays. The required dye was dissolved in 10 ml PBS-T. The glass slide with the peptide array was placed in a petri dish and the respective dye solution was poured over so that the slide was totally immersed in the solution for one hour. After the specified time, the slide was washed five times for 5 min each with PBS-T, three times for 5 min each with distilled water and rinsed with acetone. The slide was dried under the stream of compressed air and was stored at 4 ^{o}C under argon until further use.

V.3.2. Coupling of Fmoc-Lys(5/6-TAMRA)-OH

Fmoc-Lys(5/6-TAMRA)-OH (7.81 mg, 0.01M, 1 equiv) in 1 ml anhydrous DMF was prepared in an argon flask. DIC (0.02 ml, 15.14 mg, 0.12 M, 1.2 equiv) was added and the solution was stirred for 5 min under argon. Subsequently, NMI (0.02 ml, 16.42 mg, 0.20 M, 2 equiv) was added. The solution was directly added to the samples placed in petri dishes. The petri dishes were placed in a desiccator and were brought to argon atmosphere. The surfaces were left to react overnight. Afterwards the surfaces were washed three times for 5 min each with DMF, two times for 3 min each with MeOH, rinsed with acetone, and were dried in a stream of compressed air.

V.3.3. Deprotection of peptide side chain protecting groups

The samples were incubated in DCM for 15 min to pre-swell the polymer coating. Following, the samples were immersed in a mixture of 51% (v/v) TFA, 44% (v/v) DCM, 3% (TIBS) and 2% (v/v) milli-Q water and were rocked continuously using a rocker. The mixture was replaced every 30 min with a fresh mixture of the same. In total the samples were left in the deprotection mixture for 90 min followed by washing two times for 5 min each with DCM followed by one time for 5 min each with DMF. The samples were immersed in a solution of 5% (v/v) DIPEA in DMF for 30 min followed by washing three times for 5 min each with DMF followed by two times for 3 min each with MeOH and were dried in a stream of compressed air.

V.3.4. Digestion of PW and RP peptides in black 96-well plate

All the 96-wells were filled with respective peptide solutions (5 µg of peptide per well in 100 µL PBS-T solution). 100 µL solution of trypsin in PBS-T (0.05 µg/ml) was added to 80 of the wells and PBS-T was added to 16 of the wells as control. The well plate was placed in the Tecan infinite 200 microplate reader and a fluorescent reading was recorded every 10 min.

V.3.5. Digestion of PW and RP peptides in maleimide coated black 96-well plate

All the 96-wells were filled with respective peptide solutions (1 µg of peptide per well in 100 µL PBS-T solution). The well plate was rocked at 4 ^{o}C overnight to ensure the binding of the peptides to the maleimide groups on the plate. Following that, the peptide solutions were taken out of the wells and the wells were washed with PBS-T three times, 5 min each. Cysteine.HCl (0.002 gm, 0.001 M) in 10 ml PBS-T was added to the wells to block the free maleimide groups. The blocking was done for 1 hour at RT followed by washing of the wells with PBS-T three times, 5 min each. 100 µL solution of trypsin in PBS-T (0.05 µg/ml) was added to 80 of the wells and PBS-T was added to 16 of the wells as control. The well plate was placed in the Tecan infinite 200 microplate reader and a fluorescent reading was recorded every 10 min.

V.3.6. Cleaning and activation of glass slides

Glass slides were cleaned and activated by overnight treatment with 1 M KOH in 2-propanol. The surfaces were intensively washed with water, rinsed with acetone, and then dried under a stream of air.

V.3.7. Cleaning and activation of silicon wafers

Silicon wafers were cleaned and activated by overnight treatment with 3 M KOH + 2 M 2-propanol. The surfaces were intensively washed with water, rinsed with acetone and were dried under stream of argon.

V.3.8. Silanization of glass slides and silicon wafers

The cleaned and activated glass slides and silicon wafers were incubated in a solution of APTES (29.00 ml, 27.43 gm, 1.24 M, 1 equiv) , milli-Q water (2.40 ml, 2.40 gm, 1.33 M, 1.1 equiv) and 94.70 ml of absolute ethanol overnight. The surfaces were then intensively washed with absolute ethanol making sure that the surfaces were not dried during the washing. To achieve the full condensation of the silane on the surface, the surfaces were heated at 110 ^{o}C for 2 hours in oven under argon atmosphere. After cooling to room temperature the surfaces were stored under argon at 4 ^{o}C until the next step.

V.3.9. Immobilization of the initiator for siATRP

A round-bottom flask was filled with 30 ml dry DCM and was cooled down to 0 ^{o}C by placing it in an ice batch. The flask was evacuated and was brought under argon atmosphere. To the now cold DCM, DIPEA (0.74 ml, 0.55 g, 0.141 M, 2.4 equiv) was added under argon with constant stirring. To this solution BIBB (0.21 ml, 0.40 gm, 0.06 M, 1 equiv) was added under argon with constant stirring. The flask was evacuated filled with argon three times successively to remove any moisture in the environment. The surfaces were placed in petri dishes, in a desiccator, which was evacuated and filled with argon. The above solution was added and the desiccator was again evacuated and flooded with argon three times. The surfaces stayed in the reaction mixture overnight. The slides were taken out the following morning and were thoroughly rinsed three times for 5 min each with DCM, two times for 3 min each with MeOH, and were dried in a stream of compressed air. The surfaces were stored under argon at 4^{o}C until the next step

V.3.10.Synthesis of 100% PEGMA films by siATRP

10 ml PEGMA, 10 ml distilled water and 10 ml MeOH were taken in a nitrogen flask and the flask was evacuated and flooded with nitrogen. To this mixture under the stream of argon Bipyridyl (0.23 gm, 49.09 mM, 0.07 equiv) was added and stirred until dissolved. CuBr (0.13 gm, 30.21 mM, 0.04 equiv) was added in this mixture followed by evacuating the flask and flooding it with argon. The mixture was stirred for 5-10 min for dissolution and then it is poured over the surfaces with the Br initiator which were placed in a dessicator under the stream of argon. After covering the slides with the polymer solution the desiccator was evacuated followed by flooding it with argon three times. The polymerization set up was left undisturbed for 24 hours at RT. After the specified time, the surfaces were washed with distilled water three times for 5 min each, five times for 3 min

with MeOH followed by drying of the surfaces under the stream of argon. The surfaces were stored at 4 ^{o}C under argon until further use.

V.3.11.Synthesis of 10:90-PEGMA-co-PMMA films by siATRP

PEGMA (2.88 ml, 3.17 gm, 8.75 mmol, 1 equiv), MMA (8.38 ml, 7.89 gm, 78.85 mmol, 9.01 equiv), 91 µL PMDETA (76.00 mg, 0.44 mmol, 0.05 equiv) and TEGMMA (620 µL, 650 mg, 3.96 mmol, 0.45 equiv) were dissolved and mixed in 37 ml DMSO in a flask. The solution was degassed by evacuating the flask and filling it with argon three times. CuCl (44 mg, 0.44 mmol, 0.05 equiv) was added under the counter stream of argon. The solution was stirred until the copper was dissolved. The surfaces with the Br initiator were kept in a desiccator and were brought under inert gas atmosphere; the polymer solution was then added quickly to the surfaces. The desiccator was evacuated and flooded with argon three times. The polymerization was left undisturbed for 24 hours at RT. After that the surfaces were washed five times for 5 min each with DMSO, two times for 5 min each with MeOH and two times for 10 min each with water. After rinsing with acetone, the surfaces were blown dry under stream of argon followed by storage of the surfaces at 4 ^{o}C under argon until further use.

V.3.12.Coupling of Fmoc-β-alanine-OH

Fmoc-β-alanine was coupled to 10:90-PEGMA-co-PMMA-OH coatings and 100% PEGMA coatings so that there will be free NH_2 groups available for further reactions. 0.1 M Fmoc-β-alanine (0.31 gm, 0.1 M, 1 equiv) was dissolved in 10 ml of anhydrous DMF in an argon flask. DIC (0.19 ml, 151.44 mg, 0.12 M, 1.2 equiv) was added and the solution was stirred for 5 min under argon. Subsequently, NMI (0.16 ml, 164.20 mg, 0.2 M, 2 equiv) was added. The solution was stirred for 1 min and was added to the surfaces placed in petri dishes. The petri dishes were placed in a desiccator and brought to argon atmosphere. The surfaces were left to react overnight. Afterwards the surfaces were washed three times for 5 min each with DMF. To cap residual hydroxyl groups, the slides were directly immersed in a solution of 10 % (v/v) acetic anhydride, 20 % (v/v) DIPEA, and 70 % (v/v) DMF overnight. After washing five times for 5 min each with DMF and two times for 2 min each with MeOH the surfaces were dried in a stream of compressed air. The surfaces were stored under argon at 4^{o}C until the next step.

V.3.13.Cleaving Fmoc-protection group

To remove the Fmoc-protecting groups, the samples were incubated in a solution of 20% (v/v) piperidine in DMF for 20 min. Subsequently the samples were washed three times for 5 min each with DMF followed by two times for 3 min each with MeOH and were dried in a stream of compressed air.

V.3.14.Preparation of AEG_3 surfaces

3-GPS (0.33 ml, 354.51 mg, 30 mM) in 50 ml anhydrous DCM was prepared and added to the activated dry surfaces. The surfaces were left to react overnight in a desiccator under argon atmosphere. After the specified time, the surfaces were washed three times for 2 min each with DCM. A solution of DATT (20.00 ml, 20.20 gm 0.92 mM) in 80 ml anhydrous DMF was directly added to the surfaces without drying. The surfaces were allowed to react overnight. Then, the samples were washed five times for 5 min each with DMF, two times for 3 min each with MeOH, rinsed with acetone, and were dried in a stream of compressed air. The surfaces were stored at 4 °C under argon atmosphere.

V.3.15.Coupling of SMCC linker before spotting of peptides

A solution of SMCC (334.32 mg, 0.1 M, 1 equiv) in 10 ml anhydrous DMF was prepared. Slides with free NH_2 groups were placed in a petri dish, brought to argon atmosphere in a desiccator, and were directly covered with 1 mL of the SMCC solution each. After incubating them under argon atmosphere for 3 hours the surfaces were washed three times for 5 min each with DMF, two times for 2 min each with MeOH, 2 times for 5 min each with acetone and were then dried in a stream of compressed air. The slides were either stored at 4 °C under argon atmosphere.

V.3.16. Spotting of reporter peptides

The four reporter peptides (100 µg/ml in PBS-T) were spotted on different surfaces using Nanoplotter NP2.1 (GeSiM GmbH, Großerkmannsdorf, Germany). The nanoplotter is equipped with 8 piezo tips. All the spots were spotted with a drop volume of 0.5 nL of peptide solution.

V.3.17. Blocking the surfaces after spotting peptides

After the peptide spotting, the slides were left untouched without disturbing for additional 30 min and were then rocked for 30 min in a solution of β-mercaptoethanol (0.28 ml, 305.22 mg, 50 mM, 1 equiv) in PBS-T (pH-7.4). The slides were washed three times for 5 min each in PBS-T, two times for 5 min each in Milli-Q water, two times for 5 min each in EtOH, and were then dried in a stream of compressed air.

V.3.18. Coupling of Fmoc-pentafluoro-L-Phenylalanine-OH

Fmoc-pentafluoro-L-Phenylalanine (47.74 mg, 0.1 M, 1 equiv) in anhydrous 1 ml DMF was prepared in an argon flask. DIC (0.02 ml, 15.14 mg, 0.12 M, 1.2 equiv) was added and the solution was stirred for 5 min under argon. Subsequently, NMI (0.02 ml, 16.42 mg, 0.20 M, 2 equiv) was added. The solution was directly added to the samples placed in petri dishes. The petri dishes were placed in a desiccator and were brought to argon atmosphere. The surfaces were left to react overnight. Afterwards the surfaces were washed three times for 5 min each with DMF, two times for 3 min each with MeOH, rinsed with acetone, and were dried in a stream of compressed air.

V.3.19. Incubation of peptide array under dry ammonia vapor

The array was placed in a desiccator which was attached to a balloon. The balloon and the desiccator were evacuated before filling them with ammonia gas. The set up was left for the required amount of time without disturbing.

V.3.20. Coupling of 5-hexenoic acid

The slides used for the transfer of peptide arrays via click chemistry were provided by Dr. Pavel Levkin. The polymer layer on the slide was made of mixture of 2-hydroxyethyl methacrylate and ethylene dimethacrylate, thus providing free -OH groups on the surface for further modification. 5-hexenoic acid (11.41 mg, 0.1 M, 1 equiv) in anhydrous 1 ml DMF was prepared in an argon flask. DIC (0.02 ml, 15.14 mg, 0.12 M, 1.2 equiv) was added and the solution was stirred for 5 min under argon. Subsequently, NMI (0.02 ml, 16.42 mg, 0.20 M, 2 equiv) was added. The solution was directly added to the samples placed in petri dishes. The petri dishes were placed in a desiccator and were brought to argon atmosphere. The surfaces were left to react overnight. Afterwards the surfaces were washed three times for 5 min each with DMF, two times for 3 min each with MeOH, rinsed with acetone, and were dried in a stream of compressed air.

V.3.21. Immunostaining of peptide array after transfer

After the transfer the recipient surface was immersed in Rockland buffer for 60 min, washed in PBS-T for 5 min and was immersed directly in staining solution. A 1:1000 dilution of ATTO 680-anti-HA in 5 ml PBS-T with additional 0.1 % (v/v) rockland buffer was prepared freshly before the immunostaining. The surface was rocked in this solution for 60 min, washed five times for 5 min each with PBS-T and two times for 2 min each with milli-Q water. The surface was dried under a stream of compressed air before scanning.

VI. Abbreviations

% (n/n)	mole fraction
%(v/v)	volume fraction
AEG_3-SAM	amino-terminated SAM with an intramolecular EG3 spacer
ATRP	atom transfer radical polymerization
Boc	*tert*butoxycarbonyl moiety
BIBB	α-Bromoisobutyryl bromide
DATT	1,13-diamino-4,7,10-trioxatridecane
DCM	dichloromethane
DIC	N,N’-diisopropylcarbodiimide
DIPEA	N,N-diisopropylethylamine
DMF	N,N-dimethylformamide
DMPAP	2,2-Dimethoxy-2-phenylacetophenone
DMSO	dimethyl sulfoxide
DNA	deoxyribonucleic acid
e.g.	[latin] *exempli gratia*, for example
EG7-SH	O-(2-mercaptoethyl)-O′-methylhexaethyleneglycol
equiv	equivalent(s)
EtOH	ethanol
Fmoc	9-fluorenylmethoxycarbonyl (protecting group)

gm	grams
3-GPS	3-(glycidyl)oxypropyl trimethosysilane
HATU	2-(7-Aza-1H-benzotriazole-1-yl)-1,1,3,3-tetramethyluronium hexafluorophosphate
HBTU	2-(1H-Benzotriazole-1-yl)-1,1,3,3-tetramethyluronium hexafluorophosphate
HOBt	1-hydroxybenzotriazole
HPLC	high pressure liquid chromatography
λem	emission wavelength
λex	excitation wavelength
LED	Light emitting diode
M	Mole
MeOH	methanol
min	minutes
ml	milliliters
mmol	millimole
MMA	methylmethacrylate
nmol	nanomole
NMI	N-methylimidazole
OPfp	orthopentafluorophenyl
p.a.	per analysis (quality grade for chemicals and solvents)
PBS-T	phosphate buffer saline with additional
pmol	picomole

TWEEN20	polyoxyethylensorbitan monolaurate (surfactant)
PEG	poly(ethylene glycol)
PEGMA	poly(ethylene glycol) methacrylate
10:90-PEGMA-co-PMMA	graft copolymer film consisting of 10 % (n/n) PEGMA and 90 % (n/n) PMMA
PVDF	polyvinylidenefluoride
RT	room temperature
SAM	self-assembled monolayer
SIMS	secondary ion mass spectrometry
SMCC	succinimidyl-trans-4-(N-maleimidylmethyl)cyclohexane-1-carboxylate
SPPS	solid phase peptide synthesis
TEGMME	tri(ethylene glycol) monomethyl ether
TAMRA	5(6)-carboxytetramethyl rhodamine
TFA	trifluoroaceticacid
THF	tetrahydrofuran
TIBS	triisobutyl silane
TWEEN 20	polyoxyethylensorbitan monolaurate(surfactant)
UV	ultra-violet
XPS	X-ray photoelectron spectroscopy

Three letter and one letter notations of amino acids

Ala	A	Alanine	Leu	L	Leucine
Arg	R	Arginine	Lys	K	Lysine
Asn	N	Asparagine	Met	M	Methionine
Asp	D	Aspartic acid	Phe	F	Phenylalanine
Cys	C	Cysteine	Pro	P	Proline
Gln	Q	Glutamine	Ser	S	Serine
Glu	E	Glutamic acid	Thr	T	Threonine
Gly	G	Glycine	Trp	W	Tryptophan
His	H	Histidine	Tyr	Y	Tyrosine
Ile	I	Isoleucine	Val	V	Valine

VII. Bibliography

[1] E. Fischer, E. Fourneau, *Berichte der deutschen chemischen Gesellschaft* **1901**, *34*, 2868-2879.

[2] M. Bergmann, L. Zervas, *Berichte der Deutschen Chemischen Gesellschaft* **1932**, *65*, 1192-1201.

[3] S. B. H. Kent, *Annual Review of Biochemistry* **1988**, *57*, 957-989.

[4] V. du Vigneaud, C. Ressler, J. M. Swan, C. W. Roberts, P. G. Katsoyannis, *Journal of American Chemical Society* **1954**, *76*, 3115-3121.

[5] R. B. Merrifield, *Journal of American Chemical Society* **1963**, *85*, 2149-2154.

[6] L. A. Carpino, G. Y. Han, *Journal of Organic Chemistry* **1972**, *37*, 3404-3409.

[7] M. Amblard, J. A. Fehrentz, J. Martinez, G. Subra, *Mol Biotechnol* **2006**, *33*, 239-254.

[8] E. Kaiser, R. L. Colescott, C. D. Bossinger, P. I. Cook, *Analytical biochemistry* **1970**, *34*, 595-598.

[9] A. Isidro-Llobet, M. Alvarez, F. Albericio, *Chemical Reviews* **2009**, *109*, 2455-2504.

[10] K. B. Højlys-Larsen, K. J. Jensen, in *Peptide Synthesis and Applications, Vol. 1047*, Humana Press, **2013**, pp. 191-199.

[11] K. D. Kopple, *Journal of Pharmaceutical Sciences* **1972**, *61*, 1345-1356.

[12] T. J. Attard, N. O'Brien-Simpson, E. C. Reynolds, *International Journal of Peptide Research and Therapeutics* **2007**, *13*, 447-468.

[13] W. C. Chan, P. D. White, *Oxford University Press* **2000**.

[14] W. C. Merrick, *Microbiology and molecular biology reviews* **1992**, *56*, 291-315.

[15] P. A. Carr, G. M. Chruch, *Nature Biotechnology* **2009**, *27*, 1151-1162.

[16] S. B. Kent, *Chemical Society reviews* **2009**, *38*, 338-351.

[17] P. Dawson, T. Muir, I. Clark-Lewis, S. Kent, *Science* **1994**, *266*, 776-779.

[18] P. E. Dawson, S. B. H. Kent, *Annual review of Biochemistry* **2000**, *69*, 923-960.

[19] R. P. Ekins, *Journal of Pharmaceutical and Biomedical Analysis* **1989**, *7*, 155-168.

[20] T. W. Chang, *Journal of lmmunological Methods* **1983**, *65*, 217-223.

[21] U. Maskos, E. M. Southern, *Nucleic Acids Research* **1992**, *20*, 1679-1684.

[22] M. Schena, D. Shalon, R. W. Davis, P. Brownt, *Science* **1995**, *270*, 467-470.

[23] J. D. Hoheisel, *Nature reviews. Genetics* **2006**, *7*, 200-210.

[24] J. A. Hong, D. V. Neel, D. Wassaf, F. Caballero, A. N. Koehler, *Current Opinion in Chemical Biology* **2014**, *18*, 21-28.

[25] A. Nesterov, E. Dörsam, Y. C. Cheng, C. Schirwitz, F. Märkle, F. Löffler, K. König, V. Stadler, R. Bischoff, F. Breitling, in *Methods in Molecular Biology, Vol. 669*, Humana Press, New York, **2010**, pp. 109-124.

[26] R. Frank, *Tetrahedron* **1992**, *48*, 9217-9232.

[27] R. Frank, *Journal of Immunological Methods* **2002**, *267*, 13-26.

[28] U. Reineke, *Current opinion in Biotechnology* **2001**, *12*, 59-64.

[29] K. Hilpert, D. F. Winkler, R. E. Hancock, *Nature protocols* **2007**, *2*, 1333-1349.

[30] R. Volkmer, V. Tapia, C. Landgraf, *FEBS letters* **2012**, *586*, 2780-2786.

[31] S. P. A. Fodor, J. L. Read, M. C. Pirrung, L. Stryer, A. T. Lu, D. Solas, *Science* **1991**, *251*, 767-773.

[32] R. J. Lipshutz, S. P. A. Fodor, T. R. Gingeras, D. J. Lockhart, *Nature Genetics supplement* **1999**, *21*, 20-24.

[33] V. Stadler, T. Felgenhauer, M. Beyer, S. Fernandez, K. Leibe, S. Guttler, M. Groning, K. Konig, G. Torralba, M. Hausmann, V. Lindenstruth, A. Nesterov, I. Block, R. Pipkorn, A. Poustka, F. R. Bischoff, F. Breitling, *Angewandte Chemie* **2008**, *47*, 7132-7135.

[34] M. Beyer, A. Nesterov, I. Block, K. König, T. Felgenhauer, S. Fernandez, K. Leibe, G. Torralba, M. Hausmann, U. Trunk, V. Lindenstruth, F. R. Bischoff, V. Stadler, F. Breitling, *Science* **2007**, *318*, 1888.

[35] C. Schirwitz, *PhD thesis - University of Heidelberg (Germany)* **2012**.

[36] G. Fischer, *Chemical Society reviews* **2000**, *29*, 119-127.

[37] N. N. Nemova, L. A. Lysenko, *Paleontological Journal* **2013**, *47*, 1085-1088.

[38] C. Lopez-Otin, J. S. Bond, *The Journal of biological chemistry* **2008**, *283*, 30433-30437.

[39] J. E. Koblinskia, M. Ahrama, B. F. Sloane, *Clinica Chimica Acta* **2000**, *291*, 113-135.

[40] G. Bai, S. L. Pfaff, *Neuron* **2011**, *72*, 9-21.

[41] S. J. de Veer, L. Furio, J. M. Harris, A. Hovnanian, *Trends in molecular medicine* **2014**, *20*, 166-178.

[42] S. Georges, C. Ruiz Velasco, V. Trichet, Y. Fortun, D. Heymann, M. Padrines, *Cytokine & growth factor reviews* **2009**, *20*, 29-41.

[43] D. P. McGregor, *Current opinion in pharmacology* **2008**, *8*, 616-619.

[44] M. A. Phillips, R. J. Fletterick, *Current Opinion in Structural Biology* **1992**, *2*, 713-720.

[45] Q. Li, L. Yi, P. Marek, B. L. Iverson, *FEBS letters* **2013**, *587*, 1155-1163.

[46] A. Anwar, M. Saleemuddin, *Bioresource Technology* **1998**, *64*, 175-183.

[47] L. Feijoo-Siota, T. G. Villa, *Food and Bioprocess Technology* **2010**, *4*, 1066-1088.

[48] K. H. Maurer, *Current Opinion in Biotechnology* **2004**, *15*, 330-334.

[49] M. B. Rao, A. M. Tanksale, M. S. Ghatge, V. V. Deshpande, *Microbiology and molecular biology reviews* **1998**, *62*, 597-635.

[50] A. Goldberg, in *EJB Reviews, Vol. 1992*, Springer Berlin Heidelberg, **1993**, pp. 1-15.

[51] J. Tang, R. N. S. Wong, *Journal of Cellular Biochemistry* **1987**, *33*, 53-63.

[52] D. R. Davies, *Annual Review of Biophysics and Biophysical Chemistry* **1990**, *19*, 189-215.

[53] N. D. Rawlings, A. J. Barrett, in *Methods in Enzymology, Vol. 248*, Academic Press, **1995**, pp. 183-228.

[54] H. Chapman, R. Riese, G. Shi, *Annual review of physiology* **1997**, *59*, 63-88.

[55] J. Kraut, *Annual review of Biochemistry* **1977**, *46*, 331-358.

[56] E. Erez, D. Fass, E. Bibi, *Nature* **2009**, *459*, 371-378.

[57] D. M. Blow, *Accounts of Chemical Research* **1976**, *9*, 145-152.

[58] G. Dodson, A. Wlodawer, *Trends in Biochemical Sciences* **1998**, *23*, 347-352.

[59] R. Huber, D. Kukla, W. Bode, P. Schwager, K. Bartels, J. Deisenhofer, W. Steigemann, *Journal of Molecular Biology* **1974**, *89*, 73-101.

[60] H. C. Watson, D. M. Shotton, J. M. Cox, H. Muirhead, *Nature* **1970**, *225*, 806-811.

[61] J. Kraut, *Annual Review of Biochemistry* **1977**, *46*, 331-358.

[62] B. A, *Annual review of physical chemistry* **1852**, *86*, 78-88.

[63] D. S. Alderdice, G. Collins, R. Foon, *Journal of Chemical Education* **1971**, *48*, 720.

[64] F. J. Watts, J. Wolstenholme, **2003**.

[65] M. P. Seah, W. A. Dench, *Surface and Interface Analysis* **1979**, *1*, 2-11.

[66] A. Benninghoven, *Angewandte Chemie International Edition in English* **1994**, *33*, 1023-1043.

[67] A. Benninghoven, *Surface Science* **1973**, *35*, 427-457.

[68] A. Benninghoven, *Z. Physik* **1970**, *230*, 403-417.

[69] A. M. Belu, D. J. Graham, D. G. Castner, *Biomaterials* **2003**, *24*, 3635-3653.

[70] D. B. J. Vickerman, *IM Publications LLP* **2013**, 1-39.

[71] G. Nagy, P. Lu, A. V. Walker, *Journal of the American Society for Mass Spectrometry* **2008**, *19*, 33-45.

[72] D. Touboul, F. Kollmer, E. Niehuis, A. Brunelle, O. Laprévote, *Journal of the American Society for Mass Spectrometry* **2005**, *16*, 1608-1618.

[73] C. M. Mahoney, S. Roberson, G. Gillen, *Applied Surface Science* **2004**, *231–232*, 174-178.

[74] L. A. McDonnell, R. M. A. Heeren, R. P. J. de Lange, I. W. Fletcher, *Journal of the American Society for Mass Spectrometry* **2006**, *17*, 1195-1202.

[75] T. Stephan, *Planetary and Space Science* **2001**, *49*, 859-906.

[76] Z. Postawa, B. Czerwinski, M. Szewczyk, E. J. Smiley, N. Winograd, B. J. Garrison, *The Journal of Physical Chemistry B* **2004**, *108*, 7831-7838.

[77] J. R. Knowles, *Nature* **1991**, *350*, 121-124.

[78] J. M. Goddard, J. H. Hotchkiss, *Progress in Polymer Science* **2007**, *32*, 698-725.

[79] X. Huang, M. J. Wirth, *Analytical chemistry* **1997**, *69*, 4577-4580.

[80] G. Ivan, Z. Szabadka, R. Ordog, V. Grolmusz, G. Naray-Szabo, *Biochemical and biophysical research communications* **2009**, *383*, 417-420.

[81] L. Polgar, *Cellular and molecular life sciences : CMLS* **2005**, *62*, 2161-2172.

[82] S. Doose, H. Neuweiler, M. Sauer, *Chemphyschem* **2009**, *10*, 1389-1398.

[83] D. W. Piston, G. J. Kremers, *Trends in Biochemical Sciences* **2007**, *32*, 407-414.

[84] T. Foester, *Naturwissenschaften* **1946**, *33*, 166-175.

[85] T. Foester, *Annalen der Physik* **1948**, *2*, 55-75.

[86] M. Nicole, P. K. Jens, S. Markus, W. Jurgen, *Bioconjugate Chemistry* **2003**, *14*, 1133−1139.

[87] N. Marme, J. P. Knemeyer, J. Wolfrum, M. Sauer, *Angewandte Chemie* **2004**, *43*, 3798-3801.

[88] E. D. matayoshi, G. T. Wang, G. A. Krafft, J. Erickson, *Science* **1990**, *247*, 954-958.

[89] V. D. Vladimir, *Biotechniques* **2001**, *31*, 1106–1121.

[90] H. Neuweiler, A. Schulz, A. C. Vaiana, J. C. Smith, S. Kaul, J. Wolfrum, M. Sauer, *Angewandte Chemie International Edition* **2002**, *41*.

[91] D. M. Adams, L. Brus, C. E. D. Chidsey, S. Creager, C. Creutz, *The Journal of Physical Chemistry B* **2003**, *107*, 6668-6697.

[92] A. Hennig, D. Roth, T. Enderle, W. M. Nau, *Chembiochem : a European journal of chemical biology* **2006**, *7*, 733-737.

[93] M. Beyer, T. Felgenhauer, F. Ralf Bischoff, F. Breitling, V. Stadler, *Biomaterials* **2006**, *27*, 3505-3514.

[94] J. Blümmel, N. Perschmann, D. Aydin, J. Drinjakovic, T. Surrey, M. Lopez-Garcia, H. Kessler, J. P. Spatz, *Biomaterials* **2007**, *28*, 4739-4747.

[95] M. Rankl, T. Ruckstuhl, M. Rabe, G. R. J. Artus, A. Walser, S. Seeger, *ChemPhysChem* **2006**, *7*, 837-846.

[96] J. Pyun, T. Kowalewski, K. Matyjaszewski, *Macromolecular Rapid Communications* **2003**, *24*, 1043-1059.

[97] S. Edmondson, V. L. Osborne, W. T. S. Huck, *Chemical Society reviews* **2004**, *33*, 14-22.

[98] R. Barbey, L. Lavanant, D. Paripovic, N. Schüwer, C. Sugnaux, S. Tugulu, H. A. Klok, *Chemical Reviews* **2009**, *109*, 5437-5527.

[99] A. Olivier, F. Meyer, J.-M. Raquez, P. Damman, P. Dubois, *Progress in Polymer Science* **2012**, *37*, 157-181.

[100] M. Ouchi, T. Terashima, M. Sawamoto, *Chemical Reviews* **2009**, *109*, 4963-5050.

[101] A. Ulman, *Chemical Reviews* **1996**, *96*, 1533-1554.

[102] T. P. Sullivan, W. T. S. Huck, *European Journal of Organic Chemistry* **2003**, *2003*, 17-29.

[103] J. C. Love, L. A. Estroff, J. K. Kriebel, R. G. Nuzzo, G. M. Whitesides, *Chemical Reviews* **2005**, *105*, 1103-1170.

[104] K. L. Prime, G. M. Whitesides, *Journal of American Chemical Society* **1993**, *115*, 10714-10721.

[105] T. Ast, N. Heine, L. Germeroth, J. Schneider-Mergener, H. Wenschuh, *Tetrahedron Letters* **1999**, *40*, 4317-4318.

[106] C. Schirwitz, F. F. Loeffler, T. Felgenhauer, V. Stadler, A. Nesterov-Mueller, R. Dahint, F. Breitling, F. R. Bischoff, *Advanced Materials* **2013**, *25*, 1598-1602.

[107] M. T. Gokmen, J. Brassinne, R. A. Prasath, F. E. Du Prez, *Chemical Communications* **2011**, *47*, 4652-4654.

[108] K. L. Killops, L. M. Campos, C. J. Hawker, *Journal of the American Chemical Society* **2008**, *130*, 5062-5064.

[109] A. B. Lowe, *Polymer Chemistry* **2014**.

[110] M. J. Kade, D. J. Burke, C. J. Hawker, *Journal of Polymer Science Part A: Polymer Chemistry* **2010**, *48*, 743-750.

[111] C. E. Hoyle, C. N. Bowman, *Angewandte Chemie International Edition* **2010**, *49*, 1540-1573.

[112] S. Slavin, J. Burns, D. M. Haddleton, C. R. Becer, *European Polymer Journal* **2011**, *47*, 435-446.

[113] T. Silva, J. Reis, J. Teixeira, F. Borges, *Ageing Research Reviews* **2014**, *15*, 116-145.

[114] J. Hardy, D. Allsop, *Trends in Pharmacological Sciences* **1991**, *12*, 383-388.

[115] G. Bartzokis, P. H. Lu, J. Mintz, *Alzheimer's & Dementia* **2007**, *3*, 122-125.

[116] M. Hirtz, M. Lyon, W. Feng, A. E. Holmes, H. Fuchs, P. A. Levkin, *Beilstein Journal of Nanotechnology* **2013**, *4*, 377-384.

[117] K. L. Parry, A. G. Shard, R. D. Short, R. G. White, J. D. Whittle, A. Wright, *Surface and Interface Analysis* **2006**, *38*, 1497-1504.

[118] J. H. Scofield, *Journal of Electron Spectroscopy and Related Phenomena* **1976**, *8*, 129-137.

VIII. Appendix

Acknowledgment

I thank my advisor PD Dr. Frank Breitling for his supervision and constant support during the period of my PhD work. I thank PD Dr. Alexander Nesterov-Müller, Dr. Thomas Felgenhauer and PD Dr. Ralf Bischoff for providing support whenever necessary with peptide arrays and other scientific discussions. I would like to thank Dr. Christopher Schirwitz and Dr. Diego Yepes for helping me with some crucial experiments.

I thank Jakob Striffler for his constant support and for guiding me through my thesis construction and completion. I thank Bastian Muenster and Fanny Liu for the helpful scientific discussions whenever I approached them with a problem. I thank each and every one of my many colleagues who shared their lab space with me and helped me with various tasks whenever I requested.

I thank Bio-interfaces International Graduate School for providing funding for my PhD. I thank the school for the various courses they arranged to help me and other students with inter-disciplinary projects.

I am grateful to my family which has always been my source of strength and motivation. I thank my parents for believing in me. I thank my sisters for always supporting me in all circumstances. For most I thank God for taking care of me through the ups and downs of my life.

Curriculum Vitae

Anitha Golla

Date of Birth	06.11.1987
Place of Birth	Guntur, India.

Educational Qualifications

2/2011 – 5/2014

Pursuing PhD work under the supervision of PD. Dr. Frank Breitling at Karlsruhe Institute of Technology (KIT)

Title of the PhD work: Development of an assay to detect proteolytic activity in peptide arrays

6/2008 – 8/2010

Master of Science – Organic Chemistry

University : Vellore Institute of Technology (VIT), India.

CGPA : 9.63

Project Title : Synthesis of oxazole and thiazole containing peptidomimetics

6/2005 – 6/2008

Bachelor of Science

University : Acharya Nagarjuna University, India.

Score : 89 %

6/2003 – 6/2005

Intermediate

Board of Intermediate education, Andhra Pradesh, India.

Score : 95 %

Erklärung

Hiermit erkläre ich, dass ich die vorliegende Arbeit eigenständig angefertigt und keine anderen als die angegeben Quellen und Hilfsmittel benutzt habe, sowie die wörtlich und inhaltlich übernommenen Stellen als solche kenntlich gemacht habe. Des Weiteren habe ich die Satzung der Universität Karlsruhe zur Sicherung guter wissenschaftlicher Praxis beachtet.

Karlsruhe,

Anitha Golla.